NTNU – Trondheim
Norwegian University of
Science and Technology

Use of Energy Storage in a LVDC Distribution Network for Ships

Ole Christian Nebb

Master of Science in Electric Power Engineering
Submission date: June 2012
Supervisor: Lars Einar Norum, ELKRAFT
Co-supervisor: John Olav Lindtjørn, ABB

Norwegian University of Science and Technology
Department of Electric Power Engineering

Abstract

Demand for offshore support vessels are predicted to increase in the following years, due to new and challenging offshore operations. The environmental rules concerning the vessel emissions are also expected to get stricter in the coming future. As an effort to meet the operational and environmental requirements related to fuel oil consumption and emissions, a DC distribution concept is under development for ships. Energy storage could then easily be added as an environmental friendly power source, and or for assisting the slower responding diesel generators during rapid load variations.

This thesis has focused on the modeling of energy storage technologies such as Li-ion batteries and super capacitors, where they are connected to a DC bus with a bidirectional DC-DC converter. Two different energy storage operation strategies such as peak shaving and load sharing were studied. With a peak shaving strategy, super capacitors and high power Li-ion batteries were tested and compared, for relieving the diesel generators from load variations. With a load sharing strategy, high energy Li-ion batteries in combination with super capacitors were studied, for replacing one diesel generator.

The effect of these energy storage strategies were studied for an operation time equal to one year, in seven different load operation modes. Due to this long time duration, the simulations were carried out in a MATLAB program by using average modeling. The simulation results of interest were; the reduction in fuel oil consumption for different diesel generators operated with variable or fixed speed, the DC-DC converter efficiency, temperature, cooling requirement and size of the energy storage.

From the simulation results and the assumptions made, it was shown possible to reduce the fuel consumption in ships application by applying energy storage. This is however dependent on the system setup, as the reduction in fuel oil consumption showed a dependence between the diesel generators operation mode, vessel's electric load demand and the energy storage operation strategy.

Acknowledgments

I would like to thank the following people:

Lars Norum - *NTNU*: For guidance and support as a supervisor.

Bijan Zahedi - *NTNU*: For great discussions and involving me in publications.

John Olav Lindtjorn - *ABB Marine*: For giving me the opportunity along with inputs

Jan Fredrik Hansen - *ABB Marine*: For giving me the opportunity along with inputs

Frank Wendt - *ABB Marine*: For inputs and discussion on batteries.

Martin Solberg - *ABB Marine*: For MATLAB modeling inputs in my previous work.

Trond Beyer - *Saft* AS: For information and suggestions on Li-ion batteries.

Kenneth, Sivert, Andreas, Jiaying - Office colleagues: For a good working environment.

Abbreviations

AESO: Alternative energy sources

BP: Bollard pull

DG: Diesel generator

DOD: Depth of discharge

DP: Dynamic positioning

EMS: Energy management strategy

EOL: End of life

ES: Energy storage

FDG: Fixed speed diesel generator

FOC: Fuel oil consumption

G: Generator

GPS: Global positioning system

HEB: High energy Li-ion battery

HPB: High power Li-ion battery

LVDC: Low voltage direct current

M: Electrical motors

ME: Mechanical energy

OSV: Offshore support vessel

PMS: Power management strategy

SC: Super Capacitor

sFOC: Specific fuel oil consumption

SOC: State of charge

VDG: Variable speed diesel generator

Table of contents

1- Introduction

The demand for OSV's are predicted to increase in the following years, this is related to an increase in offshore exploration and production on deep waters further away from shore. This would require an vessel with other capabilities versus the older shallow water vessels [1]. Since these operations are further away from shore, a longer vessel operation time is to be expected. At the same time, the future environmental rules concerning emissions are also expected to get stricter along with increased fuel costs.

As an effort to meet these operational and environmental requirements in new vessels, A DC distribution concept is introduced in ships [2]. This concept gives rise to new DG possibilities as they can be operated with a variable speed, and the possibility for an easy connection of AESO and ES on the DC bus. The ASEO main function is to supply the DC bus with power from an environmental friendly energy source, for reliving DG's load power supply. The ES could be used as an environmental friendly power source, but also for assisting the slower responding DG's and ASEO during rapid load changes.

The use of batteries and SC's in a series hybrid system is known from literature such as [3], [4], [5] and [6]. This thesis has a similar area of focus, where the operation and PMS of ES such as Li-ion batteries and SC's in combination with DG's are to be studied. For mapping out the effect and demands of applying Li-ion batteries and SC's over a long time duration, their operations are to be studied for one year.

The thesis outline is as follows; first a description of the motivation, previous work and general description of the concepts with energy storage in a power distribution is done. Then the theory behind the modeling is described for each system component, followed by a component model description used in MATLAB. Each of the component models are then combined in a MATLAB program for simulating different cases. Then the results are discussed and followed by a conclusion I addition to a further work description.

2- A ships LVDC system with energy storage

2.1- Motivation

As a measure for increasing the fuel efficiency in OSV's, ES technologies could be implemented in a vessels electric power distribution. Since LVDC power distribution in ships is emerging on the marked, the DG's could be operated with variable speed. Therefore, the ES are to be tested in combination with VDG's and FDG's for comparison.

The ES technologies such as Li-ion batteries and SC's are to be studied in this context, when operated with PMS's as described in a subchapter below. The operations of the ES technologies in combination with a bidirectional DC-DC converter are to be tested for an OSV's yearly load demand. The areas of interest in this study are as follows; the reduction in FOC for different DG operations, the DC-DC converter efficiency, the ES temperature, the ES cooling requirement and size.

Since the effect of the ES is to be studied for a yearly load demand, simulations should be carried out in a MATLAB program by using average modeling. Some examples of average calculation are shown in Equation 1 and Equation 2 [7],[8].

$$V_d = \frac{1}{T}\int_0^T v_d(t)\,dt = \frac{1}{T}\sum_{n=1}^{T} v_d(n) \qquad [V] \qquad \text{Equation 1}$$

$$V_d = \frac{1}{T}\int_0^T v_d(t)\,dt = \frac{1}{T}\sum_{n=1}^{T} v_d(n) \qquad [V] \qquad \text{Equation 2}$$

The reason for using MATLAB and average modeling is to decrease the simulation time. The program would also need to be constructed in an appropriate manner in order to increase the simulation speed.

2.2- Previous work

In [9], an example of the LVDC system was described where the components were discussed. Figure 1 shows a LVDC distribution where the DG's are shown as a combination of ME and G, AESO e.g. fuel cells, ES e.g. batteries or SC's. These components are connected to the DC bus by power electronics e.g. diode bridge, DC-AC converters or bidirectional DC-DC converters.

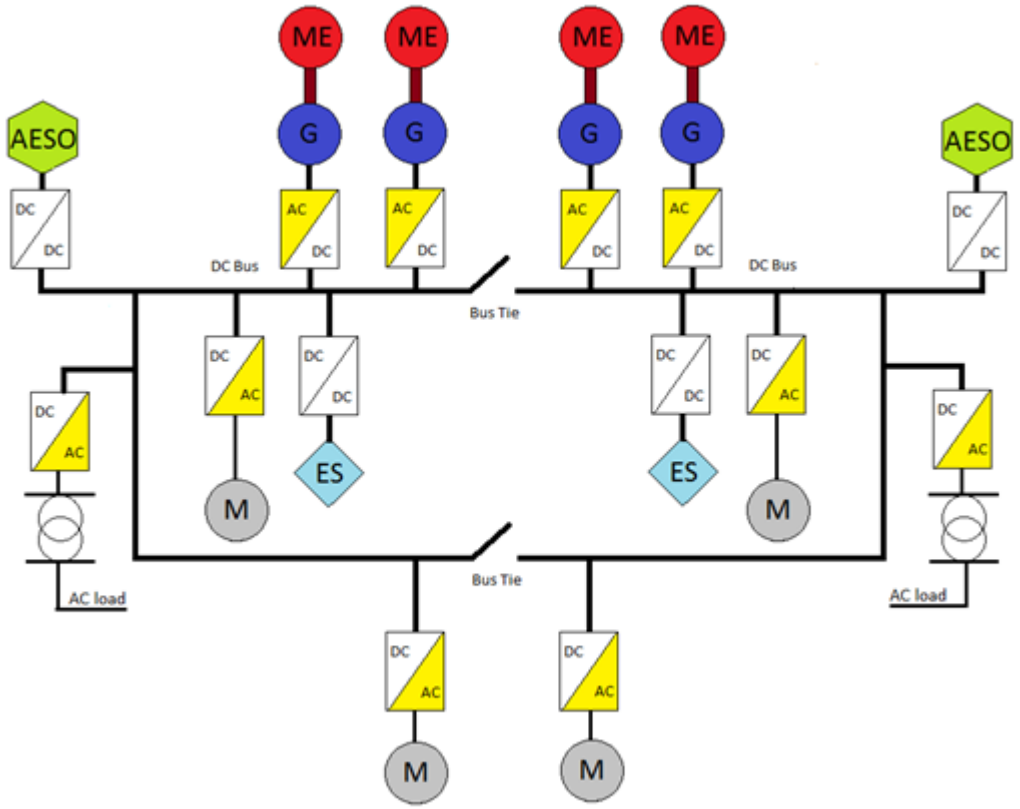

Figure 1: An example of an OSV's LVDC setup with AESO and ES [9]

A Simulink model was created in [9] as an effort to model the transient FOC of the DG's. The results of this model were inconclusive, as the transient FOC model should have been integrated in a complete Simulink model of the LVDC distribution, consisting of DG's, converters and load models.

A MATLAB program was built in [9], where ES was used to improve the fuel consumption of VDG's in an LVDC distribution. The ES technology was simplified and modeled as an energy amount and an efficiency factor. The ES was controlled by the DG's fuel efficiency curve, as

the objective of the ES was to ensure an ideal loading ratio for reduced FOC. This was simulated in three cases with different ES control limits and seven OSV load operation modes. The simulation was done for a vessel operation time equal to one year. The three cases gave varying results, where both an increase and a decrease in FOC were observed depending on the control limit and load operation mode.

In a collaboratively work in [10], the an optimization was added to the MATLAB program in [9]. The optimization found the best control limit which reduced the FOC the most, for each load operation mode. This simulation was done equivalent to an 24 hour load period. The results obtained in [10] gave an small improvement from the results in [9].

For the collaboratively work in [11], different Simulink modeling methods were discussed for an isolated bidirectional converter intended for hybrid ships. Then an average bidirectional DC-DC converter model was derived and validated by using current control.

2.3- Power distribution with Energy storage

How the ES affects the load flow is dependent on the PMS applied to the system, therefor two different PMS strategies are discussed for combining ES with DG's in a LVDC distribution. The firs strategy is shown in Figure 2, where the DG's delivers the average load power and the ES are compensating for the load variations. This PMS is often called peak shaving [8]. The size of the ES would be dependent on the duration and size of load variations. As this strategy would require a fast responding ES and the capability of discharging high powers, HPB's or SC's are used for this application.

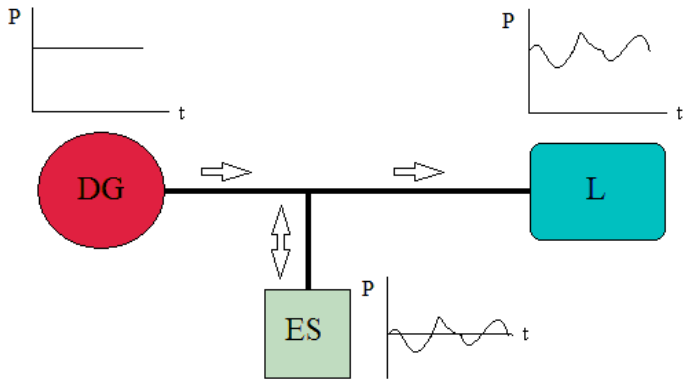

Figure 2: A peak shaving strategy where the ES compensates for the load variations

The second PMS is shown Figure 3, where the DG's delivers a fraction of the load power while the ES delivers the remaining load power. The power delivered from the ES is then a constant average power in combination with a load variation. This strategy is sometimes called load sharing [12]. The size of the ES would be dependent on the duration and size of the load fraction it is supposed to deliver. Since this strategy would require an ES with the capability of supplying high energy and high power, HEB's in combination with power assisting SC's is used.

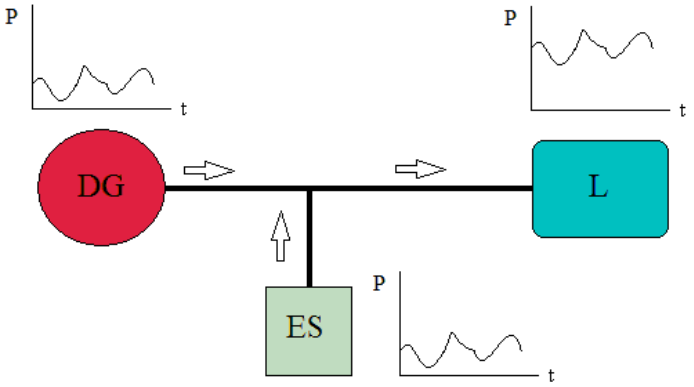

Figure 3: A hybrid strategy where ES is partly compensating for the total DG power

The load distribution for these two PMS's are described by Equation 3, where P_{ES} could be the power from Li-ion batteries, SC's or a combination of them both.

$$P_{load} = P_{ES} + P_{DG} \qquad [W] \qquad \text{Equation 3}$$

3- Ships load power

In an OSV, the largest installed electric load is usually associated with propulsion power. Therefore, the vessels propulsions operational characteristic is important, as I can give an estimate of the load power needed. In this chapter, some theory behind propulsion requirement and operational characteristics are described.

3.1- OSV operation mode

As mentioned in [9], the working conditions for an OSV can be broken down to seven different operation modes. The percent usage of each operation mode is shown in Figure 4.

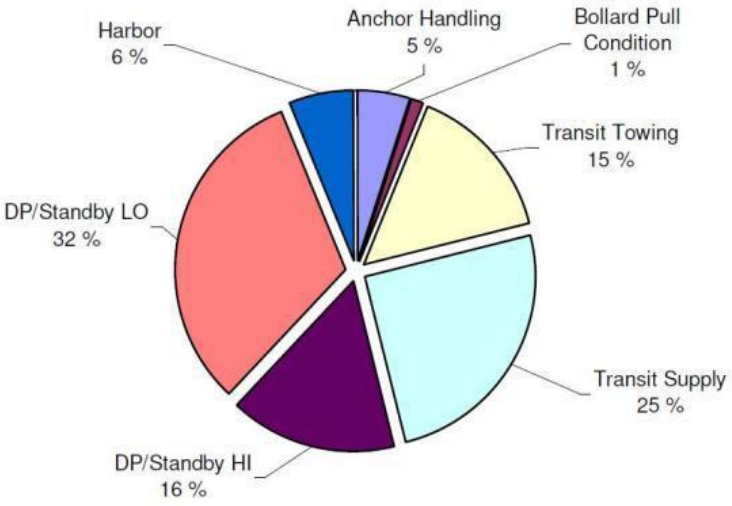

Figure 4: The OSVs different operation modes and their percentage usage for one year [13]

- The DP mode is typical for the vessel during standby operations. The standby operation could either require that the vessel is stationary in a fixed position given by a GPS, or letting the vessel drift within a specific region. This is all dependent on the vessels working conditions.
- Harbor operations usually require power for other electric equipment such as pumps, cranes, light, heat etc...
- BP is a test for measuring the vessels towing capability [14], this would therefore require a high propulsion power.

- Transit towing is an operation where the vessel is towing anchors, fleets or other offshore equipment. This would also require high propulsion power.
- Transit supply is an operation for transporting equipment on the vessel, and therefore it would usually run with moderate propulsion power.

3.2- Estimation of propulsion

As previously mentioned, the majority of electric load in an OSV is governed by the propulsion. Therefore, this subsection describes the theory behind propulsion power estimation and dimensioning. Here, two different methods for estimating propulsion power are shortly explained.

The first method is a theoretical approach, where the amount of required power is dependent of several factors also known commonly as the ships resistance[15]. The resistance is dependent on the ships architecture and design, and can be divided into several subgroups. A frictional resistance is dependent on the friction between the water and the vessels hull. A residual resistance is dependent on the hull design, as there is a pressure on the hull when water is pushed away during motion. Another resistance describes how the relative wind affects the vessel. This is dependent on the ships design, wind speed and direction. The wave resistance is also important to include, and is dependent on the hull structure, waves shape and period. This last resistance may be the most difficult to estimate, as the waves shapes and periods is a complex phenomenon to predict. There are also other resistance factors which could be accounted, such as draught/trim, water depth, temperature and density. These resistances are then calculated with the term $\frac{W}{Speed}$, and the power can be estimated from Equation 4 . Here, η_p is the propeller efficiency, V_{speed} is the vessel speed and R_{Vtot} is the total vessel resistance.

$$P = \frac{V_{speed} \cdot R_{Vtot}}{\eta_p} \qquad [W] \qquad \text{Equation 4}$$

The second method is a more practical way of estimating the propulsion power. This is done by measuring the load requirements, in a relevant vessel, during different operation modes in an extended period of time. The collected load data can be processed into an average value, and or used to make instantaneous propulsion profiles, as done in [8] and [13]. The vessels load power can be expressed as shown in Equation 5, where the $frequency$ is dependent on the load variation, and $sample$ is the time steps used for completing a time duration. The $amplitude$ is the size of the peak load variation while the $offset$ is the average or constant part of the load.

$$P_{load} = offset + amplitude \cdot \sin(2 \cdot \pi \cdot sample \cdot frequency) \quad [W] \qquad \text{Equation 5}$$

3.3- DP propulsion

As Figure 4 shows, DP is the operation mode which has the highest operation time. Therefore, a closer look is taken on the DP load scenarios. A DP operation will require a load proportional to the weather and sea wave conditions. According to [16], the OSV load range could be from $700 - 3500$ kW during calm weather and $500 - 5000$ kW during rough weather. Calm weather would therefore require a low DP mode and rough weather a high DP mode. A typical vessel power load for low DP is shown in Figure 5 with a 30% load variation.

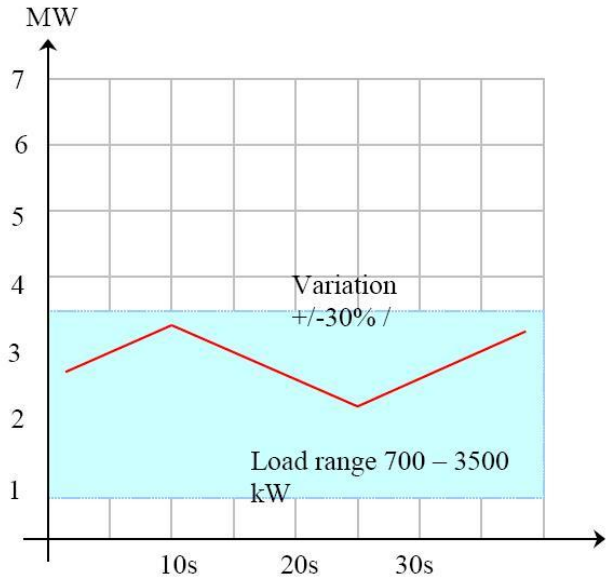

Figure 5: Vessel loading during low DP [16]

In Figure 6, the typical vessel power load for high DP mode is shown. It is seen from the figure that load transients can occur due to rough weather. This is usually caused by the propellers spinning in free air due to large waves. These transients would be dependent on what kind of thruster used, as *Azipods* is usually fully submerged and may be less exposed to this effects.

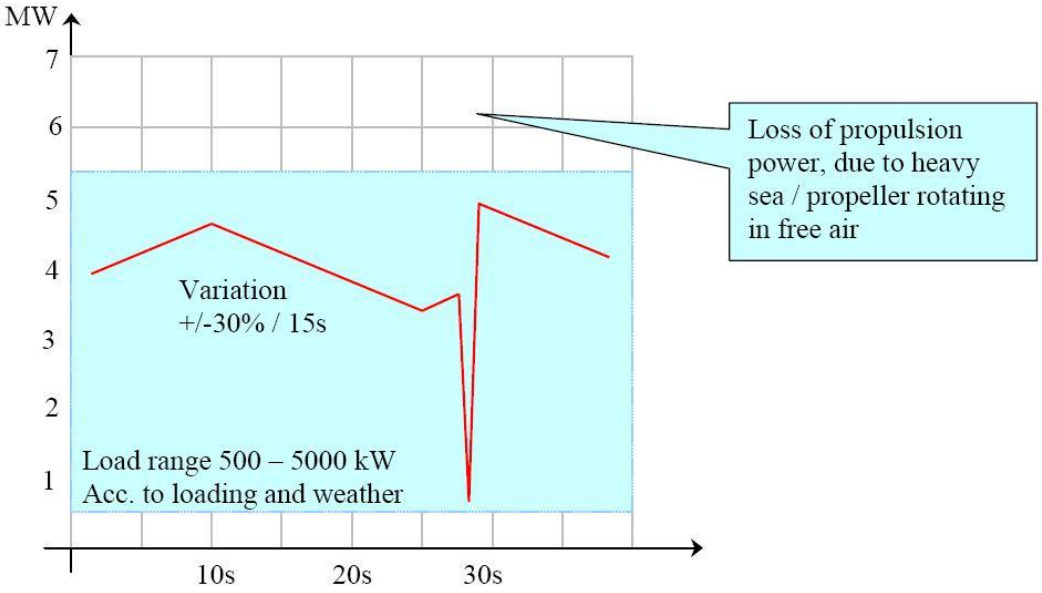

Figure 6: Vessel loading during high DP [16]

Figure 7 shows the vessel power loading during emergency evacuations. This is a typical scenario for the vessel is in DP mode when it is offloading supplies. The loading power is increasing linear until the vessel is in clear of danger, or when the vessel has reached its pre-determined position.

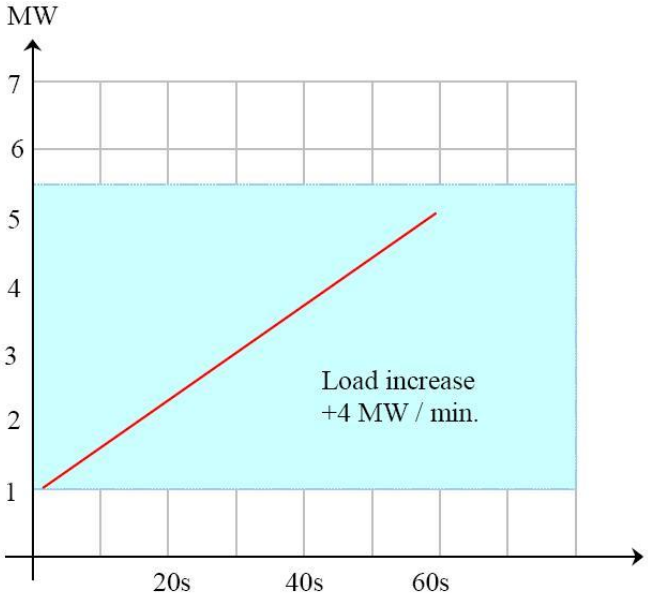

Figure 7: Vessel loading during rapid evacuation [16]

4- Modeling ships electric load

The modeling process, parameters and results of the load power model in MATLAB is described in this chapter.

4.1- The load in MATLAB

The total load for each operation mode is retrieved form an Excel sheet which contains a preset setup. The different loads are then sorted and combined to a single function. The load function shown in Equation 5, is supposed to govern the subroutines and functions in the whole MATLAB program.

Figure 8 shows how the vessel load setup is generated from the information given in an Excel sheet. The variable input ESComb, is a logic value used to change between the two PMS's shown in Figure 2 and Figure 3. If the peak shaving PMS is used i.e. ESComb $= 0$, the loads are combined and a number for DG's may be edited. The number of DG's edited depends on the DG's loading ratio, or DGL-ratio in Figure 8, which is explained in the next chapter. This DGL-ratio would be lower when the DG's are only delivering the average load power. The removal of online DG's is controlled by a loading ratio limit, which compares the DG's loading ratio before and after a removal. This limit is set according to the DG's lower loading limit for protecting the DG's lifetime as described in the next subchapter. The average DG power is shown as $offset$ in Equation 5, where the ES power is shown as $amplitude$ with the sinusoidal variation in Equation 5.

When the load sharing PMS is used i.e. ESComb $= 1$, one DG is removed from the preset setup in the Excel sheet. The power needed to compensate for the removed DG is calculated and assigned as the ES load. The ES load may then contain an $offset$ and a $amplitude$ load power.

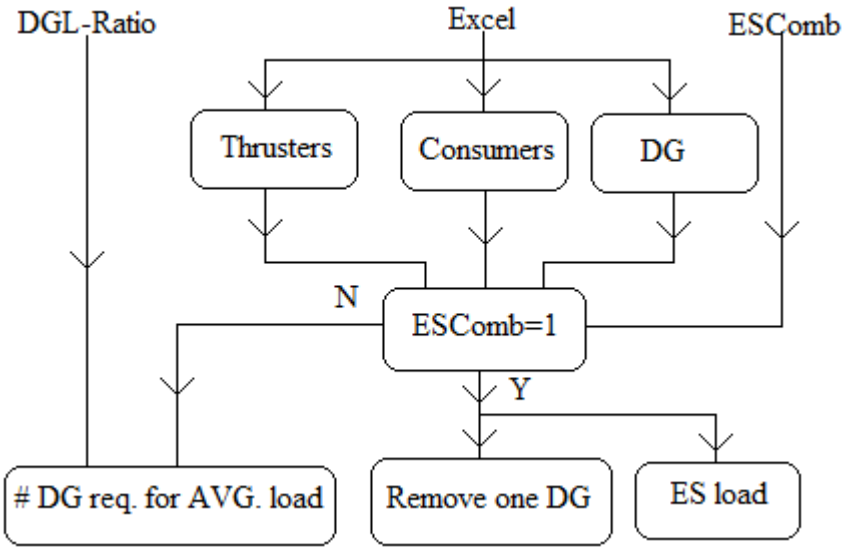

Figure 8: Flowchart for load and DG assembly in MATLAB program

4.2- Load parameters

The load $frequency$ for the DP operations are the same as shown in Figure 5 and Figure 6 i.e. $\frac{1}{30}\ Hz$, while the load $frequency$ is set to $\frac{1}{100}\ Hz$ for some of the other load operation modes. The $sample$ time is set to $0{,}002$ hours for all the simulations. The reason for this sample time is to get a feasible speed of the simulation, as a too low sample time would make the duration of the simulation too long. A too high sample time would come in conflict with the load frequency.

Most of the load and component data has been given by *ABB Marine*, [8] and [16], where the data used in the simulations is shown in Appendix B. The component ratings are taken from a ship by *Myklebusthaug*, which is using an LVDC distribution. A single line diagram of this reference vessel is shown in Appendix D.

4.3- The load model performance

An example of the load shape applied to the DG's is shown in Figure 9, without any ES. This is for a high DP mode with 2 generators online.

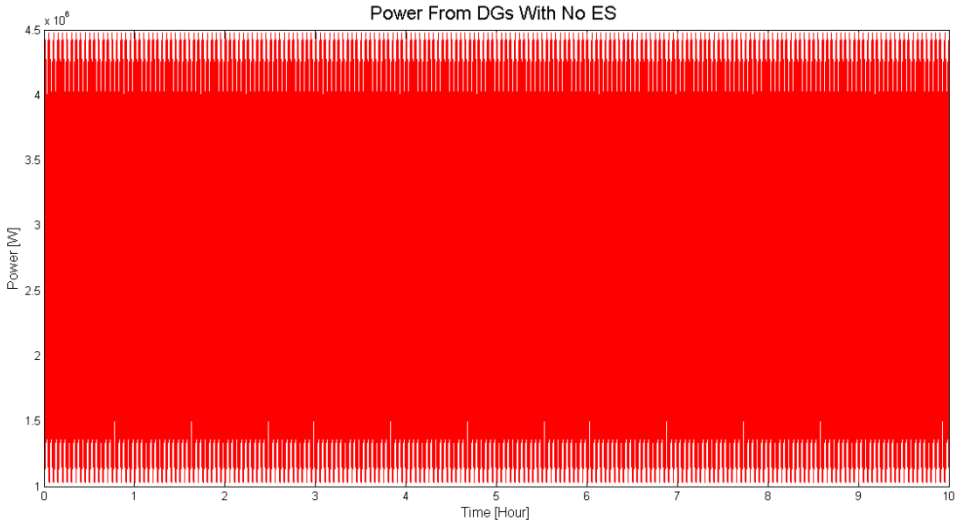

Figure 9: Instantaneous DG load profile for a vessel in high DP mode

There was also an attempt to add some of the DP load scenarios given in the previous section. But because of the simulation speed requirement and sample time used, the load transients shown in Figure 6 were too fast in relation to the sample time. Therefore, this was not added to the program.

ES devices such as Li-ion batteries and SC's will affect the load power supplied by the DG's. Figure 10 and Figure 11 shows an example of the power supplied by the DG's when they are assisted by SC's or HPB's.

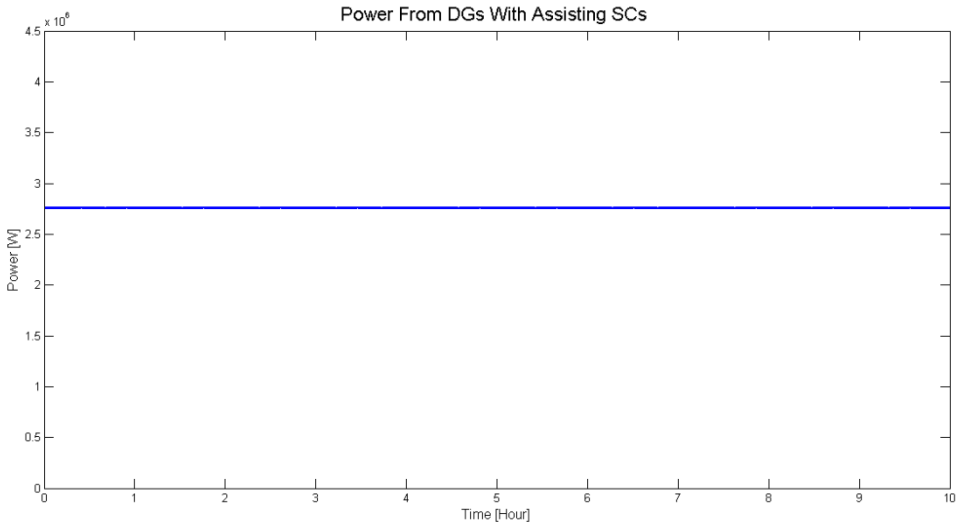

Figure 10: Power delivered by the DG when SC's are used for peak shaving.

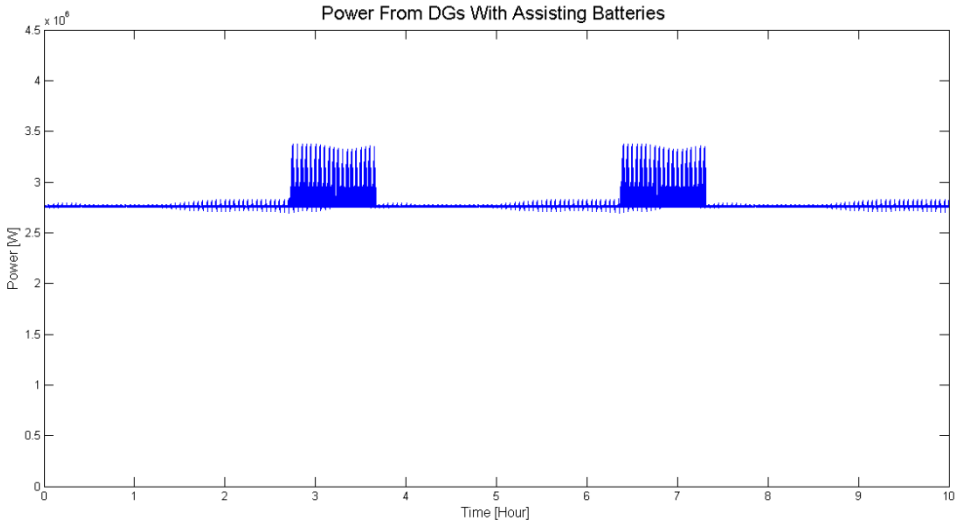

Figure 11: Power delivered by the DG when HPB's are used for peak shaving.

In the example shown in Figure 12, one DG is replaced by a combination of HEB's and SC's. The load power delivered by the remaining DG is shown, where the loading is the same as in Figure 9. The load peak to the right in the figure is caused by depleted HEB's.

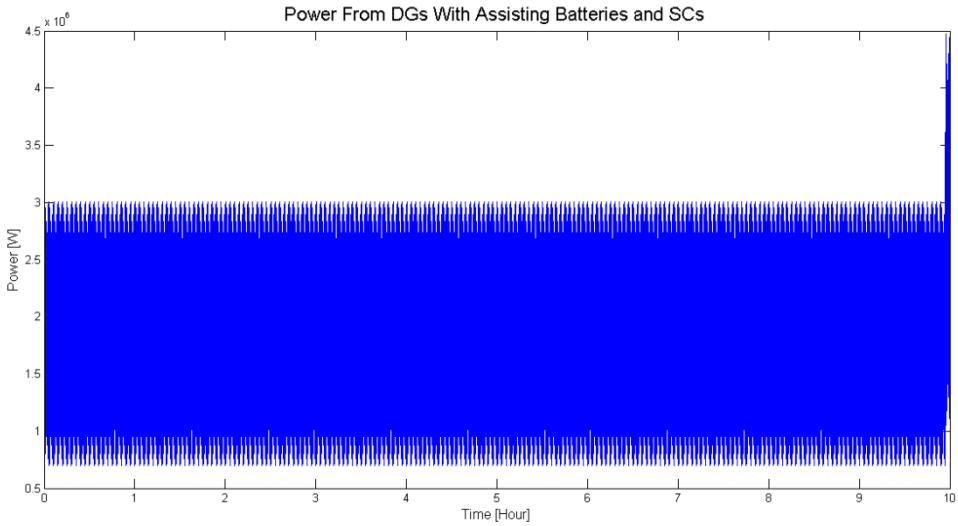

Figure 12: Power delivered by the remaining DG when HEB and SC's are used for load sharing

5- Diesel generators

To improve the DG system, it would be essential to understand some of its working principles. The main focus would be on the fuel consumption for the FDG's and VDG's as this is strongly related to the operation costs and emissions.

5.1- Fuel consumption and operation

In a DG system, the fuel consumption is dependent on the load power applied to the DG's. This fuel consumption is also dependent on how the engine is controlled to respond on the load variations. A DG mechanical load is determined by Equation 6, where τ is the mechanical momentum and ω_{mec} is the mechanical speed of the shaft connecting the ME with the G.

$$P_{DG-mec} = \tau \cdot \omega_{mec} \qquad [W] \qquad \text{Equation 6}$$

In an AC distribution system this power is controlled with fixed shaft speed on the DG's, with a DC distributions system the power could be controlled with variable speed. This gives two different load-dependent fuel characteristics, where the variable speed operated DG would have a more even fuel consumption due to its flexible operation. [9],[8].

The fuel consumption can be calculated using fuel efficiency curves, where $sFOC$ is plotted versus the P_{DGL}. The P_{DGL} is the DG's loading ratio, calculated from the DG's loading relative to the DG rating. The fuel efficiency curves can be expressed by a polynomial, as shown in Equation 7. Where a_f , b_f, c_f and d_f are polynomial constants. The calculation of P_{DGL} is shown in Equation 8, where P_{load} is the load which the DG supplies and $P_{DG-rating}$ is the rated power of the DG.

$$sFOC = a_f + b_f \cdot (P_{DGL}) + c_f \cdot (P_{DGL})^2 + d_f \cdot (P_{DGL})^3 \qquad \left[\frac{gram}{kWh}\right] \qquad \text{Equation 7}$$

$$P_{DGL} = \frac{P_{load}}{P_{gen-rating}} \qquad [Ratio]$$ Equation 8

The FOC can then be calculated as shown in Equation 9, where t is the time in hour.

$$FOC = \left(a_f + b_f \cdot (P_{DGL}) + c_f \cdot (P_{DGL})^2 + d_f \cdot (P_{DGL})^3\right) \ldots \cdot P_{DG-rating} \cdot P_{DGL} \cdot t \qquad [gram]$$ Equation 9

The loading ratio shown in Equation 8 should be operated within an interval of $0.5 - 0.85$. This is because a lower DG loading ratio then described in the interval, may reduce the generators lifetime and give an increased operational cost. A higher loading ratio then the interval will give increase risk of blackout.[17],[8],[9]

5.2- Transient operations

Transients load operations on diesel engines have been known to affect the fuel consumption and emissions. Typical operations which generate transients occur during engine load change, change in throttle position and cold or hot engine startups. The diesel engine transients are usually classified within time durations from seconds to several minutes [18].

During transient operations, the fuel consumption and engine speed is constantly changed by a governor. This will then affect the air supply and cylinder boost pressure. Especially turbocharger systems are affected, as the thermal and fluid dynamic delays influence the air supply in relation to the fuel supply. This leads to unfavorable air-fuel mixtures that affect the torque dynamics, emissions and noise. As understood by [18], the fuel consumption would not be drastically increase during transient operations. Instead, the increase in emissions would be more significant as the optimal air-fuel mixture gets out of balance.

The control schematics for a modern combustion engine are shown in Figure 13. The figure shows the inputs, outputs and sensors for the involved component processes during air-fuel mixture. As seen from the figure, load transients may affect several processes in a diesel engine.

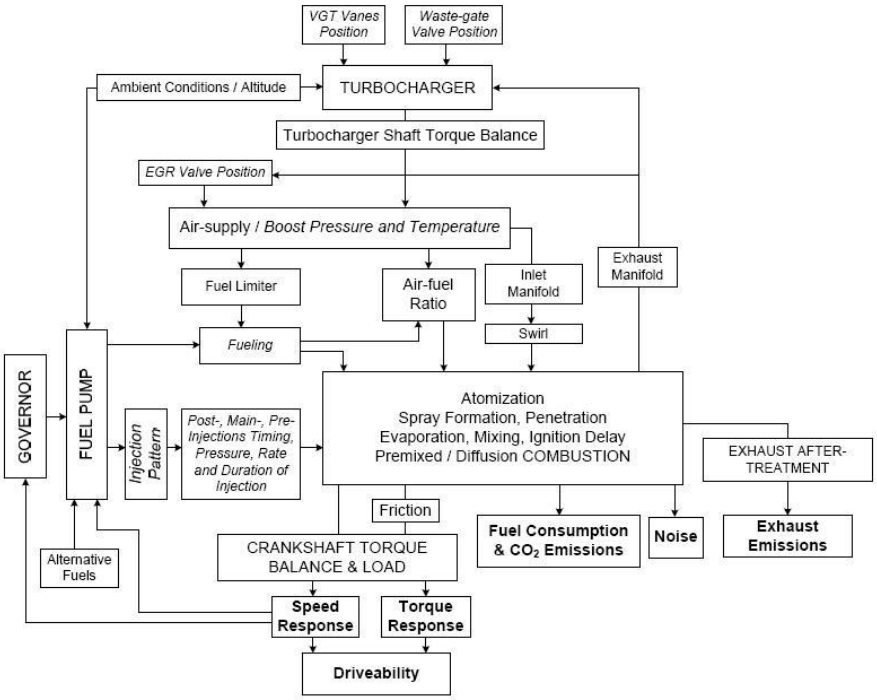

Figure 13: Diesel engine control schematics, including inputs and outputs [18]

In a DG system, the damper windings in the generators would smoothen some of the load transients. But this is dependent on the generator design along with the size and duration of the transient. [19]

6- Modeling diesel generators

The modeling process, parameters and results of the DG model in MATLAB is described in this chapter.

6.1- The diesel generator in MATLAB

The DG's are modeled by their fuel consumption, as described in the previous chapter. A flowchart of the MATLAB calculations is shown in Figure 14. As seen in the flowchart, the fuel is directly calculated by the DG load power, which is the variable input.

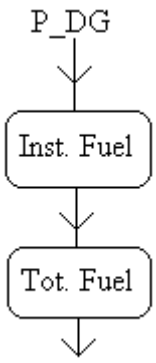

Figure 14: Flowchart for MATLAB DG fuel calculation

Modeling the engine operations during transients can be done by using a quasi-linear model or mean value approach. This approach is often chosen versus a nonlinear model as it involves less complex mathematical expressions. The model consists of steady-state model versions of system elements such as engine cylinders, manifolds, injections etc., with empirical correction constants. The simplified model is therefore dependent on available experimental data. Since the nonlinear dynamics of the system is disregarded in the simplified model, an error of 5-20 % in each of the system element models is expected when compared to a nonlinear model [18].

Since a simplified model of the transient fuel consumption would give a relative large error and requires detailed information on a specific diesel engine, it is not included in this MATLAB model.

6.2- Diesel generator Parameters

Two different DG's where used, one for fixed speed and one for variable speed. It is assumed that all the DG's of both types are equally loaded during operation, as this is an common procedure for vessels with a power management system [8]. The sFOC versus DG loading ratio where given by *ABB Marine*, [9] and [8]. These sFOC values are shown in Table 1.

sFOC FDG	sFOC VDG	%Loading
205.0	180.0	1.0
195.0	173.75	0.75
210.0	173.75	0.5
290.0	186.25	0.25

Table 1: sFOC for VDG and FDG versus loading level

The DG sFOC curves are shown in Figure 15 and Figure 16 for a FDG and VDG. These curves where made by curve fitting polynomials from the values in Table 1.

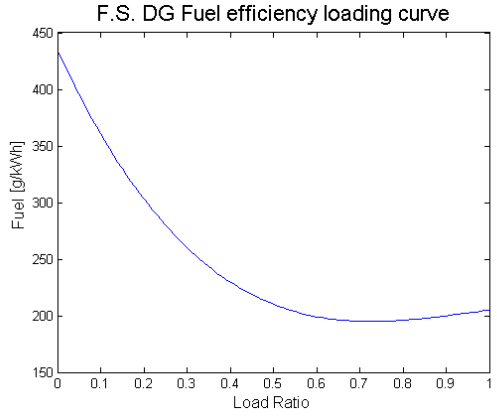

Figure 15: sFOC of fixed speed DG

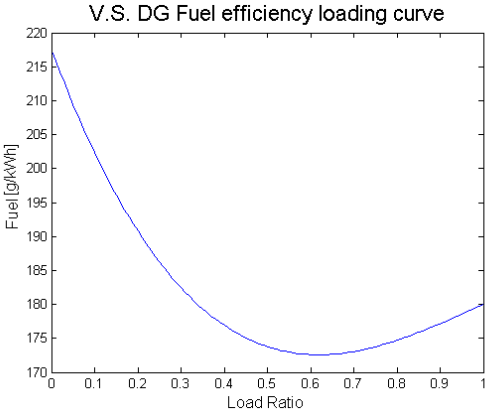

Figure 16: sFOC of variable speed DG

6.3- The Diesel generator model performance

An example of instantaneous fuel consumption is shown in Figure 17 for a variable speed operated DG's. The VDG's fuel is calculated from the load given in Figure 9.

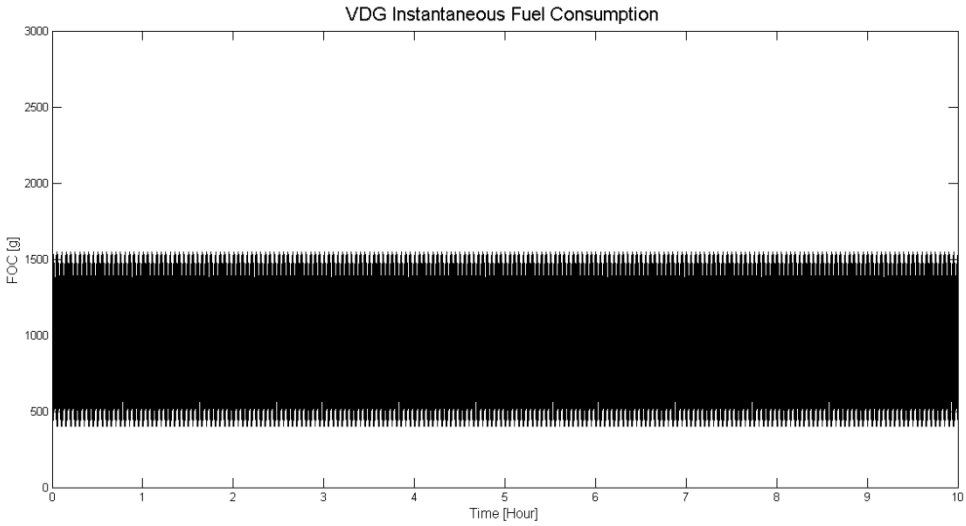

Figure 17: Instantaneous fuel consumption of a variable speed DG

The total fuel consumption of FDG and VDG is shown in Figure 18, with and without the use of Li-ion Batteries or SC's in the peak shaving strategy. The load power used in the total FOC calculation is the same as in Figure 9, Figure 10 and Figure 11. In the figure, the pink line is on top of the green line and may be hard to spot.

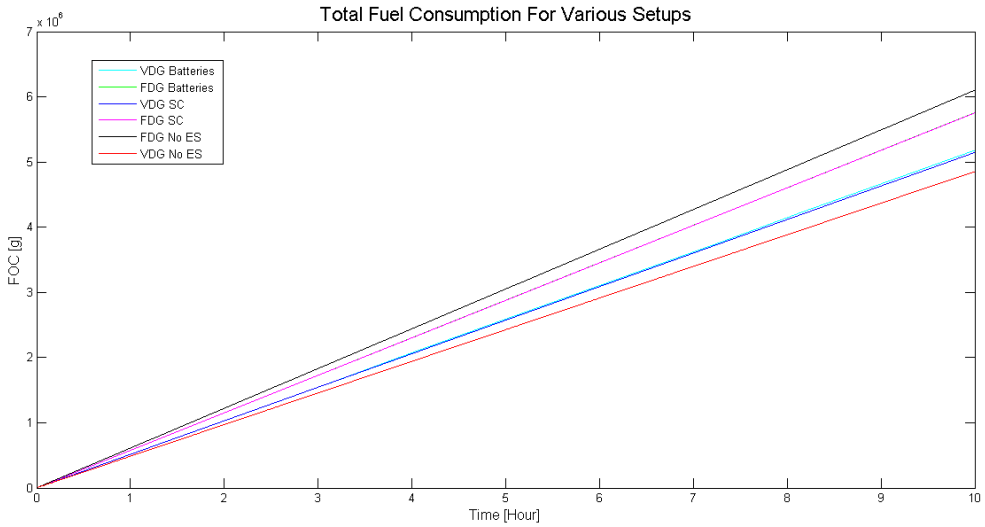

Figure 18: The VDG's and FDG's total fuel consumption with and without Li-ion batteries or SC's

7- The Li-ion Batteries

Figure 19: Cylinder shaped HPB cells from *Saft* manufacture [20]

The first commercial Li-ion battery was made available on the marked in 1991. This was an improved technology of the older lithium metal batteries, which had an instability problem in the cells. Examples of the new cells used in batteries are shown in Figure 19. Since the battery suppliers are now starting to deliver Li-ion battery systems for the marine environment, this technology is to be studied closer.

7.1- Li-ion batteries properties

The basics of a Li-ion battery cells is similar to other battery technologies. It uses an anode and cathode electrode of different oxidation potential. These electrodes have to be combined with an electrolyte so that the Li-ions can be transferred between the electrodes. A simplified drawing of a cell is shown in Figure 20.

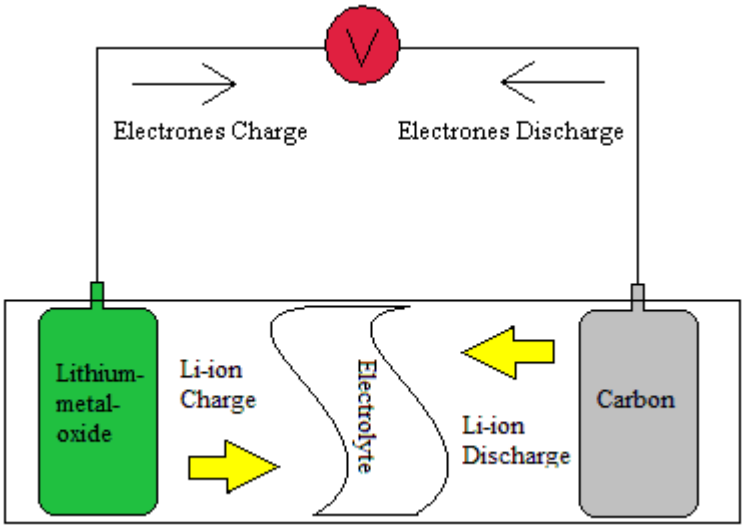

Figure 20: A simplified Cell in a Li-ion battery

According to [21], in newer versions of the Li-ion battery the anode material is made of carbon. The cathode material could either consist of lithium cobalt oxide, lithium manganese oxide, lithium nickel manganese cobalt, lithium nickel cobalt aluminum oxide and lithium iron phosphate. A general chemical reaction equation for a Li-ion battery with a lithium metal oxide is shown in Equation 10 [22]. Here, M represents the different compounds in the lithium cathode.

$$Li_xC + Li_{1-x}M_yO_z \rightleftharpoons C + LiM_yO_z \qquad \text{Equation 10}$$

By mixing cathode and anode materials, different qualities can be enhanced in the Li-ion batteries. But as there is a balance in these qualities, an increase in one may lead to a decrease in another. This especially applies for the load current which is dependent on the batteries capacity. The battery capacity can be calculated using Equation 11 [22], where $i(\vartheta)$ is the current to be integrated from the battery during time t.

$$C_b = \int_0^t i(\vartheta)\, d\vartheta \qquad [Ah] \qquad \text{Equation 11}$$

Li-ion batteries can be divided in HEB's and HPB's depending on how the cathode is constructed and the materials used.

HEB's are used in applications where the load needs long and sustainable energy supply. These batteries are limited by their power rating, as a large current would give a large internal resistance in the battery. This would lead to high temperatures and reduced lifetime. A battery energy rating is determined by Equation 12, where V_{N_b} is the nominal voltage of the battery.

$$E_{battery} = C_b \cdot V_{N\_b} \qquad [J] \qquad \text{Equation 12}$$

HPB's are used for high power operations, as they can deliver large amounts of energy in a small timeframe. This is because they have a low internal resistance during discharge. This high power rating usually comes with a price of lower energy rating. HPB cells also have to be designed smaller than high energy cells for securing sufficient heat dissipation during discharge.

As can be understood by the two Li-ion battery types above, that the internal resistance governs most of the batteries application. This internal resistance is dependent of how the Li-ions separates and combines in the cathode as shown in Equation 10. This process is also dependent on temperature and amount of charges left in the Li-ion battery. As this chemical process depends on several factors which are time dependent, time constants are included in the internal resistance. The internal resistance is therefore referred to as the internal impedance. This internal resistance would also differ, depending on the battery operation mode i.e. charging or discharging.

7.2- Cost of Li-ion batteries

Li-ion batteries are a relative expensive technology compared to other batteries. As found in [23], the costs of Li-ion batteries is dependent on the use of raw material and production complexity. There are cheaper ways of designing the Li-ion battery, but this will usually be counterbalanced by reliability and lifespan. Therefore, most manufactures prefer a robust and more expensive design. The price of Li-ion batteries are estimated to be in the range of $500 - 1000 \frac{\$}{kWh}$. [24]

7.3- Lifetime of Li-ion batteries

The lifetime and ageing of Li-ion batteries are important factors to take into account, as Li-ion battery failure can give increased safety risks and costs. The EOL for batteries is according to [25] characterizes as $20\ \%$ loss in the Li-ion battery capacity C_b. The critical factors for affecting the cell aging are related to the size of discharge/ charge currents, cell temperature, DOD, internal impedance and number of cycles. In addition, there would also be a normal storage aging process in the cells.

The DOD, which is related to the Li-ion battery capacitance, can affect the lifetime as the internal resistance is dependent on the charge level. A fully depleted Li-ion battery can then give permanent damage to the cells. Therefore an operation interval is set to the amount of energy in the Li-ion battery. Dependent on Li-ion battery material, the operation limit is often set between $20\% - 90\%$ SOC which is the opposite of DOD. The Li-ion battery SOC and DOD is derived from the energy used versus energy stored, and can be calculated as shown in Equation 13 [22].

$$SOC_B = \left(1 - \frac{\int_0^t i(\vartheta)\, d\vartheta}{C_b}\right) \cdot 100\% = 100\% - DOD_B \qquad [\%] \qquad \text{Equation 13}$$

The SOC operation limits, now termed t_1 and t_2, can be included in Equation 13 and solved for DOD as shown Equation 14. This is also called the battery stress factor [26], as it can be

used to determine the number of charge and discharge cycles a Li-ion battery can withstand before EOL.

$$\Delta DOD_B = \left(\frac{\int_{t_1}^{t_2} i(\vartheta)\, d\vartheta}{C_b} \right) \cdot 100\% \qquad [\%] \qquad \text{Equation 14}$$

A typical plot of how the stress factor affects the cycles is shown in Figure 21 for variety of batteries.

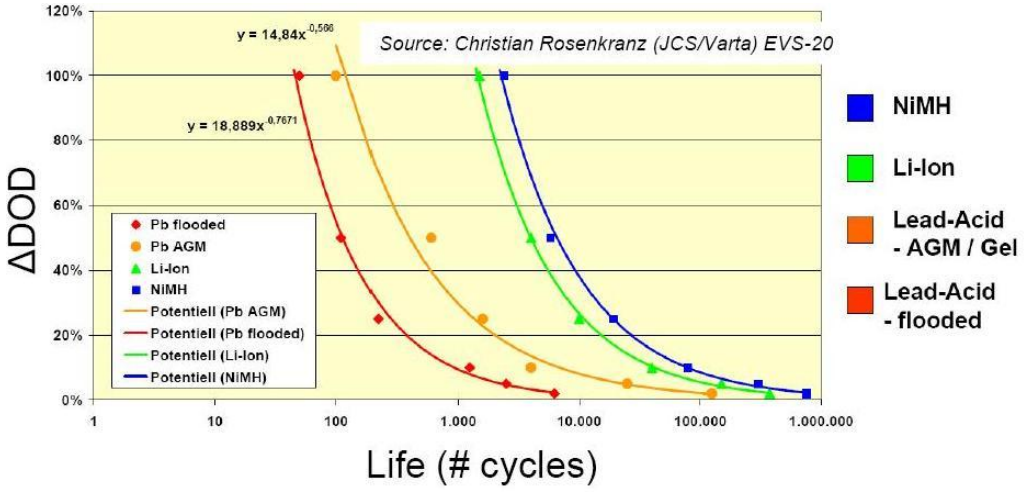

Figure 21: General plots of stress factors cycles versus cycles for different battery technologies [26]

This kind of data is usually hard to obtain from the battery suppliers and manufactures. Therefore Equation 15 can be used to generate a similar figure from the scares information obtained [26]. Cycles_0 and λ are constants obtained by using known data and the procedure shown in Appendix D.

$$Cycles(\Delta DOD_B) = \text{Cycles}_0 \cdot e^{\lambda \cdot \Delta DOD_B} \qquad [\#] \qquad \text{Equation 15}$$

Equation 15 is the most commonly used formula for estimating the number of battery cycles, but there are a also a few other examples mentioned in [26].

The heat dissipated by the Li-ion batteries would also influence the Li-ion batteries lifetime. Figure 22 shows the temperature affects the Li-ion batteries lifetime. The figure shows that the Li-battery has an ideal temperature range of $10 - 60°C$ during operations. This data is somewhat difficult to obtain from the battery manufactures.

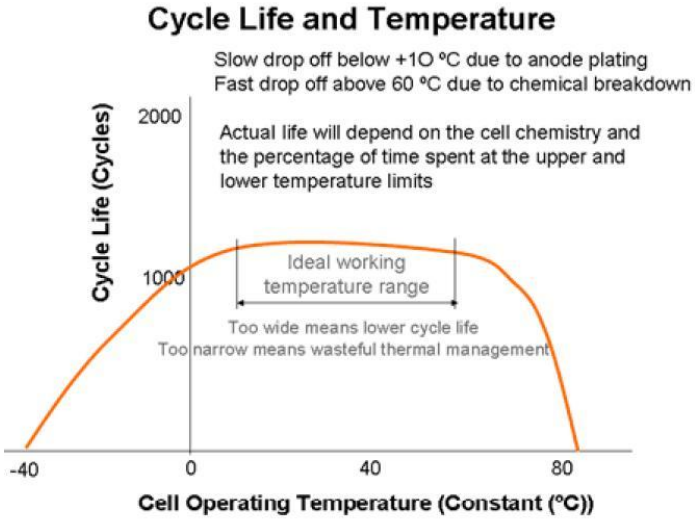

Figure 22: Lifecycle versus cell temperature of a Li-ion battery [27]

The thermal Li-ion battery behavior can be calculated based on the procedures given in [28]. This is a practical method using the lumped capacitance principle. This means that the temperature is calculated for a whole module or cabinet of battery cells.

The heat transferred from the battery cells $q(t)_B$, is determined from the Li-ion batteries internal resistance during charging and discharging as shown in Equation 16, where R_{Bint} is the internal battery resistance, $I_{RMS}(t)$ is a load dependent RMS current to or from the Li-ion battery.

$$q(t)_B = R_{Bint} \cdot I_{RMS}(t)^2 \qquad [W] \qquad \text{Equation 16}$$

The heat removed from normal air convection is calculated using Equation 17, where $T_{air}(t)$ is the ambient air temperature and $T_{Bint}(t)$ is the internal temperature in the Li-ion battery. The sum in the denominator is called the thermal resistance, where A is the area in contact with air, s is the surface, k is the thermal conductivity and h is the convective heat transfer coefficient.

$$q(t)_{air} = \frac{T_{air}(t) - T_{Bint}(t)}{\frac{1}{h \cdot A} + \frac{s}{k \cdot A}} \qquad [W] \qquad \text{Equation 17}$$

The heat removed by additional cooling systems e.g. forced air, can be calculated based on the cooling power required as shown in Equation 18. Here, $P_{cool}(t)$ is the cooling power required to maintain a specific temperature. This could also be described as the Li-ion batteries transferred heat which needs to be removed.

$$q(t)_{cool} = P_{cool}(t) \qquad [W] \qquad \text{Equation 18}$$

The balanced equation for the battery heat system can be written as shown in Equation 19, where Ct_B is the total cell heat capacitance of a whole Li-ion battery module or cabinet.

$$\frac{dT_{Bint}(t)}{dt} = \frac{q(t)_B - q(t)_{cool} - q(t)_{air}}{Ct_B} \qquad [W] \qquad \text{Equation 19}$$

In addition to the internal temperature dissipation, the ambient temperature may also affect the Li-ion battery during storage. A low storage temperature may have negative impact on the Li-ion batteries operation, whereas high storage temperatures may affect the Li-ion batteries lifetime.

7.4- Operation of Li-ion batteries

The discharging of the Li-ion batteries is preformed according to the battery supplier specification, depending on weather it is a high power or high energy technology. But when the Li-ion battery is charging, a coulomb efficiency is added for compensating losses of charges during the chemical charging reaction.

The charging of Li-ion batteries can be done in several ways, either constant current, constant voltage or pulse current charging [22]. The different charging methods can influence the Li-ion batteries lifetime depending on the SOC level. Therefore, a combination of different charging methods in a charging algorithm is preferred. The charging voltages and currents are specified by the battery suppliers. The characteristics of charging parameters is

a considerably lower current then the discharge rating, and a higher voltage then then the nominal battery voltage.

The Li-ion batteries are equipped with a battery management system for surveillance and control of the cells. This is done mainly as a safety measure for preventing cell failure, but also for improving the Li-ion battery lifetime during charging and discharging. Typical measurements by the battery management system would be the cell voltage and temperature. This is also done on the lithium iron phosphate cathode Li-ion batteries, even though they are characterized for being a safe Li-ion battery technology.

7.5- Sizing of Li-ion batteries

Dimensioning the amount of ES is in general difficult for vehicles or vessels, as the amount depends on the load demand and duration. On a large scale, the amounts of ES can be dimensioned according to the number of ES modules or ES cabinets as shown in Figure 23.

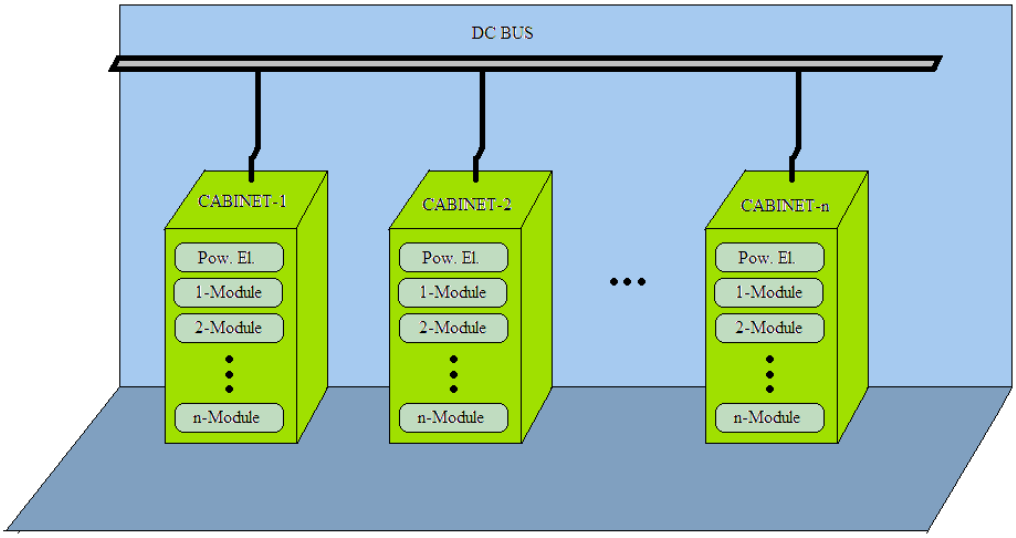

Figure 23: Cabinets and modules dimensioned in a DC bus system

As explained in the previous load chapter, the load demand depends on many factors. The first and simplest step, is usually to determine the number of cells in series [29]. This is calculated based on the DC bus voltage and the battery cell voltage as shown in Equation 20, where U_{bus} is the nominal bus voltage and U_{Bcell} is the nominal cell voltage.

$$N_{B-series} = \frac{U_{bus}}{U_{Bcell}} \quad [\#] \qquad \text{Equation 20}$$

The $N_{B-series}$ may also be determined by the battery suppliers module or cabinet size. The number of module or cabinets in parallel is dependent on the EMS and constrains of the Li-ion battery system. There are three constrains which Li-ion batteries should be dimensioned after, these are as follows:

1. The batteries capability of discharging the maximum power requested by the load.
2. The batteries capability of charging the maximum power delivered by the load.
3. The batteries capability of delivering the maximum energy requested by the load.

For the first constraint, the parallel amount is dimensioned according to Equation 21. Here, $P_{load\_\max\_req}$ is the largest power request from the load, P_{Bcell_Dis} is the nominal power a Li-ion battery cell can deliver. η_{eff_sys} is the efficiency of the ES system i.e. converter loss, battery loss, etc.

$$N_{BP\_Dis-parallel} = \frac{P_{load\_\max\_req}}{N_{B-series} \cdot P_{Bcell\_Dis} \cdot \eta_{eff\_sys}} \quad [\#] \qquad \text{Equation 21}$$

For the second constraint, the parallel amount is dimensioned according to Equation 22, where $P_{load\_\max\_del}$ is the largest regenerative power delivered from the load, P_{Bcell_Cha} is the nominal charging power a Li-ion cell can accept.

$$N_{BP\_Cha-parallel} = \frac{P_{load\_\max\_del}}{N_{B-series} \cdot P_{Bcell\_Cha} \cdot \eta_{eff\_sys}} \quad [\#] \qquad \text{Equation 22}$$

The third constraint requires the parallel number of batteries to be dimensioned according to Equation 23. Here, the $E_{load\_\max\_req}$ is the largest energy requested by the load and E_{Bcell_Dis} is the nominal energy in a battery cell. The ΔDOD_B is added since the SOC limits will affect the available energy in the cells.

$$N_{BE\_Dis-parallel} = \frac{E_{load\_\max\_req}}{N_{B-series} \cdot E_{Bcell\_Dis} \cdot \Delta DOD_B \cdot \eta_{eff\_sys}} \quad [\#] \qquad \text{Equation 23}$$

As mentioned above, the amount of batteries in parallel is also dependent on the EMS. Different EMS's may affect the above mentioned constraints in different ways. Therefore, the constraints have to be evaluated relative to each other. In [29], several examples of EMS's scenarios are presented. One scenario suggests that the battery supplies the whole load demand alone, as shown in Figure 24. This means that the batteries must have the ability to discharge the largest power requested by the load, charge the largest power supplied by the load during regenerative operations, and enough energy for the whole load duration.

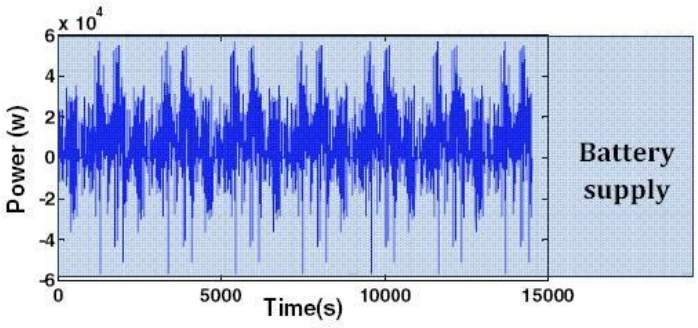

Figure 24: Batteries supplying the whole load demand alone [29]

For dimensioning the number of batteries required in parallel for this EMS, all the constraints have to be taken into account. The required number is then calculated according to Equation 24.

$$N_{B-parallel} = MAX(N_{BE_{Dis}-parallel}, N_{BP_{Cha}-parallel}, N_{BP_{Dis}-parallel}) \quad [\#] \qquad \text{Equation 24}$$

For a second EMS scenario, the batteries are used for delivering maximum power as shown in Figure 25. This strategy would require the batteries to be able to discharge the largest load power demanded. Since the batteries charging power is not prioritized, the battery must contain enough energy for the load duration. This should be done with respect to the given charging abilities.

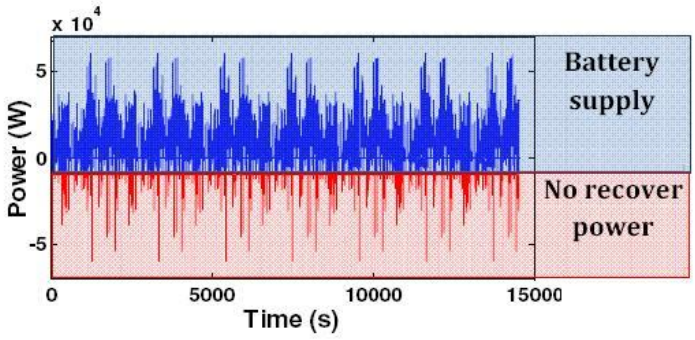

Figure 25: Batteries supplying the whole load demand alone [29]

For this EMS, two constraints have to be taken into account when dimensioning the number. This is shown in Equation 25.

$$N_{B-parallel} = MAX\left(N_{BE_{Dis}-parallel}, N_{BP_{Dis}-parallel}\right) \quad [\#] \qquad \text{Equation 25}$$

In a third EMS scenario, the batteries supplies most of the energy during the whole load duration. The batteries can therefore not discharge or charge the maximum power requested or supplied by the load. For this EMS scenario, the batteries should be assisted by SC's for handling a large load power request and supply. This is shown in Figure 26.

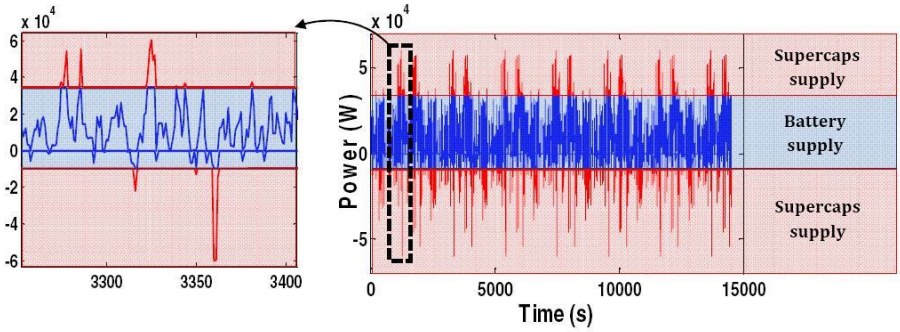

Figure 26: Batteries delivering the whole load assisted by SC's [29]

Since this strategy is only focus on delivering all the energy requested by the load, the number of batteries in parallel is determined by the battery energy limit as shown in Equation 26.

$$N_{B-parallel} = N_{BE_{Dis}-parallel} \quad [\#] \qquad \text{Equation 26}$$

7.6- LiFePO4 cathode batteries

According to *Saft*, the cell cathode material best suited for marine applications would be lithium-iron-phosphate also described as LiFePo4. Some of the main reasons for this choice is the good safety properties, robustness, thermal stability and a long life cycle [30]. It also has a small internal resistance which makes it suiting for high power applications and lower cell temperature rise. The tradeoff is the lower cell voltage of about $3{,}3\ V$ versus almost $3.6\ V$ of other cathode materials. The LiFePo4 battery would also have a lower battery capacitance.

8- Modeling of the Li-ion battery

The modeling process, parameters and results of the Li-ion battery model in MATLAB is described in this chapter.

8.1- The Li-ion battery in MATLAB

The Li-ion battery is modeled according to a simplified circuit diagram as shown in Figure 27, where an internal voltage source with a resistance in series gives the terminal voltage. The voltage drop over the resistance is included in the model as this would accounts for some loss during the Li-ion batteries operation. A coulomb efficiency is also added during charging for compensating the internal losses. The Li-ion battery cell voltage and SOC is modeled as shown in Figure 28, where the cell voltage is modeled as a look up table.

In Figure 28, the voltage of only one cell is modeled, this is based the assumption that all the cells in a cabinet are equally loaded. Therefore, the total cell number in a cabinet is multiplied with the one cell voltage. When the Li-ion batteries SOC has reached the lower limit, the Li-ion battery will go into a charging mode where it charges more current then it discharges. This discharge while charging strategy is used for preventing large load power peaks on the DG's. The Li-ion battery current and the DC-DC converter efficiency is the variable input in the calculations.

The discharge power of the HPB and HEB are dependent on the current requested by the load power and the terminal voltage of the battery cabinets. Only the HPB's are modeled with a charging ability. The charging process is carried out with a constant voltage over the Li-ion batteries, a current in accordance to the regenerative load and the Li-ion battery SOC charging limits.

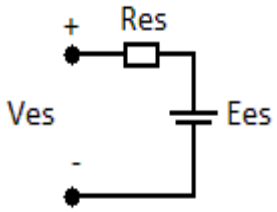

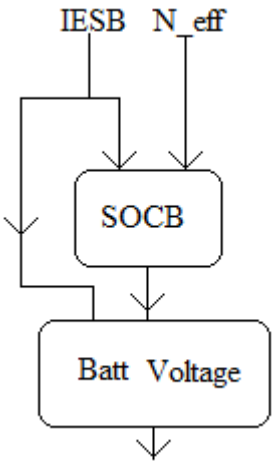

Figure 27: Simplified ES circuit diagram

Figure 28: Battery SOC and voltage flowchart of MATLAB model

The modeling of the Li-ion batteries temperature and cooling is shown in Figure 29. This is modeled by the lump capacitance principle for a cabinet containing Li-ion battery cells. The Li-ion batteries instantaneous temperature starts with an initial value. The new temperature is calculated from the heat dissipated in the Li-ion battery cells, by using the battery current as a variable input along with the air to cabinet convection. If the temperature is high enough, cooling is applied.

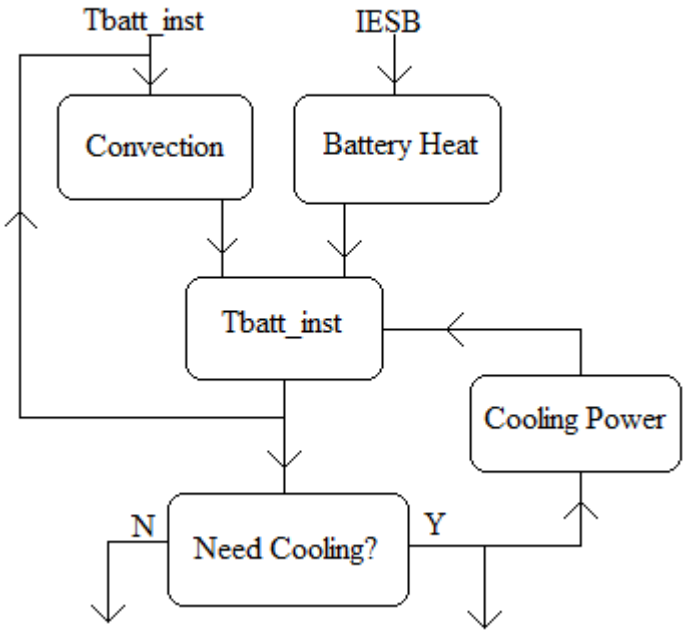

Figure 29: Temperature and cooling flowchart describing MATLAB model of Li-ion batteries cabinet

The Li-ion batteries Lifetime is modeled as shown in Figure 30, where the Li-ion batteries SOC is the variable input used to determine a depletion cycle. When the Li-ion battery SOC level has reached a minimum, the cycle number is decreased and the remaining battery cycles are determined from the batteries change in DOD from a look up table.

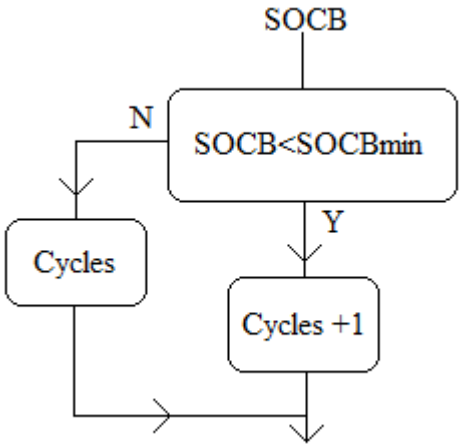

Figure 30: Lifetime flowchart describing the MATLAB model of Li-ion battery cells

Figure 31 shows the dimensioning process of the Li-ion batteries, where the variable input is the Li-ion battery power request and the converter efficiency. The number of Li-ion battery cabinets is calculated by the requested load power relative to the Li-ion battery cabinets nominal discharge power. The Li-ion battery power request is set equal to the $amplitude$ of Equation 5 during peak shaving. This power is set equal to one DG's $offset$ power similar to Equation 5 during load sharing.

The reason for only finding the number of Li-ion battery cabinets in parallel, is because the cells are assumed connected in series in each module, then each module are assumed conceded in series in each cabinet.

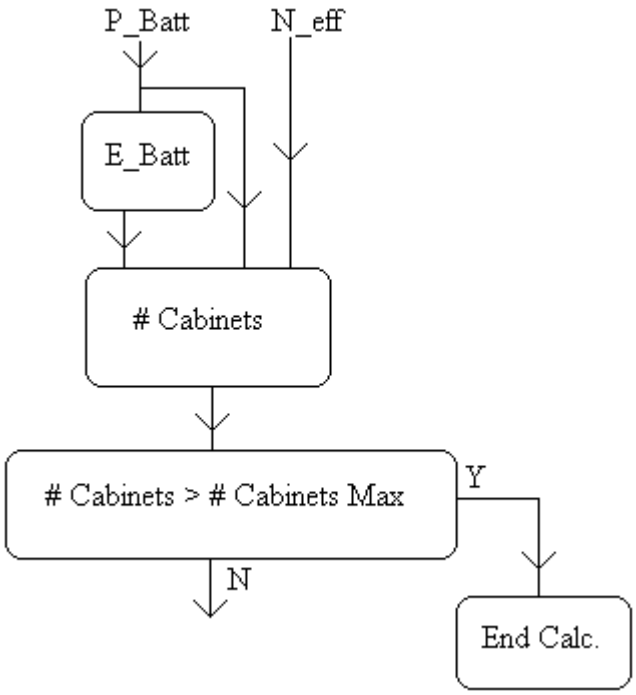

Figure 31: Flowchart for determining number of cabinet in the MATLAB Li-ion battery model

8.2- Li-Ion battery parameters

The Li-ion batteries used in the MATLAB program as reference, is the *Super-Phosphate VL 10 Fe high power battery* and *Super-Phosphate VL 45 high energy battery* from *Saft*. The data sheets of these LiFePo4 batteries and a battery cabinet for marine applications are shown in Appendix A. The Li-ion battery cabinet can hold 13 modules, where each module can hold 12 cells.

The internal resistance of the HPB cells is also used in the HEB cells as this is the only available parameter. Experimental tests values from the internal resistance in LiFePO4 batteries have been compared to the values given in manufacturers datasheet in [31]. It showed that the resistance is only slightly affected by temperature and the cell chemistry level. Therefore, the internal resistance is not compensated for any temperature change. In addition, the Li-ion battery temperature is held constant within a certain limit when cooling is applied in the MATLAB model. The columbic efficiency during charging is set to 98% with the same assumptions as in [32].

The internal cell voltage is modeled from the cell voltage graph shown in the datasheets with a curve fitting polynomials in MATLAB. Since the internal Li-ion battery voltage source value is not available, the cell voltage graph with the lowest discharge current is used. This voltage is the closest alternative to an open circuit voltage value from the available parameters. The values used to make the curve fitting polynomial are shown in Table 2 for HEB cells and Table 3 for HPB cells.

Cell voltage HE vl45p /30 deg. C, 9 A	**% SOC**
4	100,00
3,42	90,00
3,3	80,00
3,26	70,00
3,26	60,00
3,26	50,00
3,26	40,00
3,23	30,00
3,2	20,00
3,15	10,00
1,50	0,00

Table 2: HEB cell voltage versus SOC level

Cell voltage HP vl10p /20 deg. C, 10 A	% SOC
4,00	100,00
3,26	90,00
3,26	80,00
3,26	70,00
3,26	60,00
3,14	50,00
3,14	40,00
3,14	30,00
3,02	20,00
2,96	10,00
1,50	0,00

Table 3: HPB cell voltage versus SOC level

The polynomials created from Table 2 and Table 3 is plotted in Figure 32 and Figure 33.

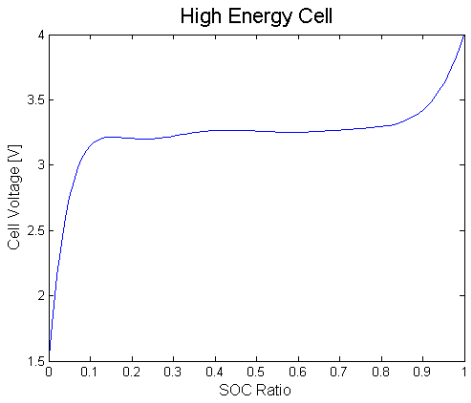

Figure 32: HEB cell voltage

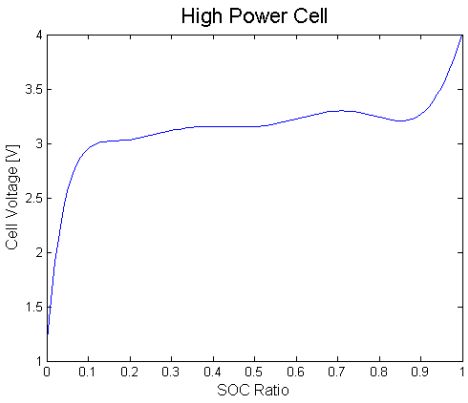

Figure 33: HPB cell voltage

As the specific heat capacitance for LiFePo4 batteries is hard to obtain, a parameter from [33] is used. The heat capacitance used is $795\ \left[\frac{J}{Kg \cdot Celsius}\right]$ and is taken from a $6\ Ah$ high power Li-ion battery cell from *Saft*. Since the specific heat capacitance is mostly determined by component material properties, the specific heat capacitance given in [33] should have a small deviation from a FeLiPo4 battery.

The parameters used for modeling the heat convection are as follows; the Li-ion battery cabinet area in contact with air, ambient air temperature and the convective heat transfer coefficient. The Li-ion battery cabinet area in contact with air is calculated from the setup shown in Figure 23, and the data from the Li-ion battery cabinet datasheet. As the convective heat transfer coefficient was hard to obtain from the battery cabinet, it was set equal to the SC's cabinet value given in Appendix A.

As the maximum ambient temperature in ships is $45\ ^{o}C$, the ambient temperature is chosen to be $35\ ^{o}C$. The maximum Li-ion battery cell temperature is choses to be $40\ ^{o}C$ as this should not affect the Li-ion batteries lifetime according to Figure 22. The thermal resistances are neglected in the model for simplicity and due to lack of data. This simplification should give a small deviation in the calculated internal cell temperature. The cooling power applied is set equal to the heat transferred from the Li-ion battery cells to air.

The Li-ion battery SOC limits are set to $90\ \%$ for the maximum and $30\ \%$ for the minimum. For HPB's, the maximum discharging current is set to $150\ A$ for each Li-ion battery cabinet, and the maximum charging current is also set to $150\ A$ for each cabinet. According to the HPB datasheet, the charging current can be set to $150\ A$ as long as it has the duration of about 6 minuits, which should be applicable when using a load variation as described in electric load modeling section. The discharge current is set to $150\ A$ for getting a similar loss and heat generation as the SC's in the next section. The HPB's charging voltage is set to $3{,}6\ V$.

During a peak shaving strategy when the Li-ion battery is empty and goes into charging mode, The Li-ion batteries are programed to discharg $66{,}67\%$ of the discharging current. The HEB's maximum discharging current is set to $50\ A$, and the maximum charging currents is set to $6{,}3\ A$ according to the datasheet of the HEB.

Due to the lack of parameters for the cycle life time of LiFePo4 batteries, the values given in [34] from *Saft* was used. The parameters are listed Table 4 where an exponential function created by these values is shown in Figure 34.

Cycles	% Delta DOD
3000,00	80,00
1000000,00	3,00

Table 4: Cycles versus % delta DOD for Li-ion batteries

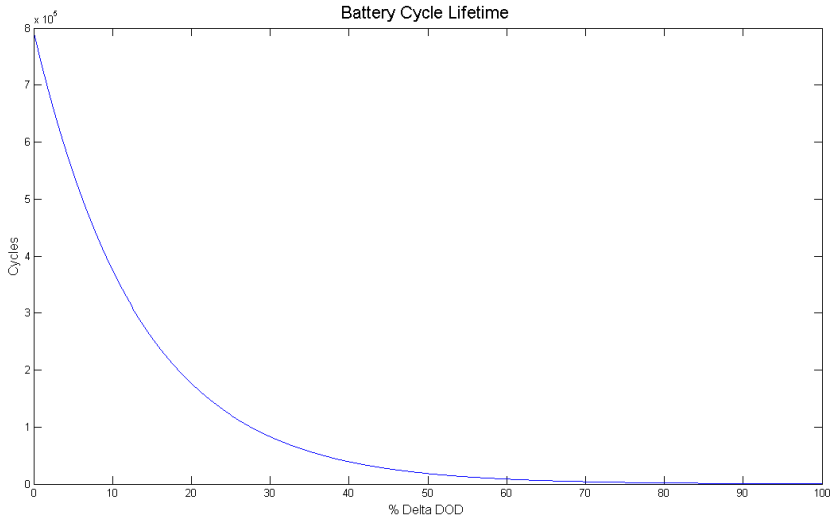

Figure 34: The cycle lifetime versus delta DOD for Li-ion batteries

8.3- The Li-Ion battery model performance

Some examples of the Li-ion battery model are shown here. The load shown in Figure 9 is used to calculate the results in Figure 35 to Figure 39. In Figure 35 the voltage over one Li-ion battery cell is shown, the figure shows how the voltage behaves during charging and discharging.

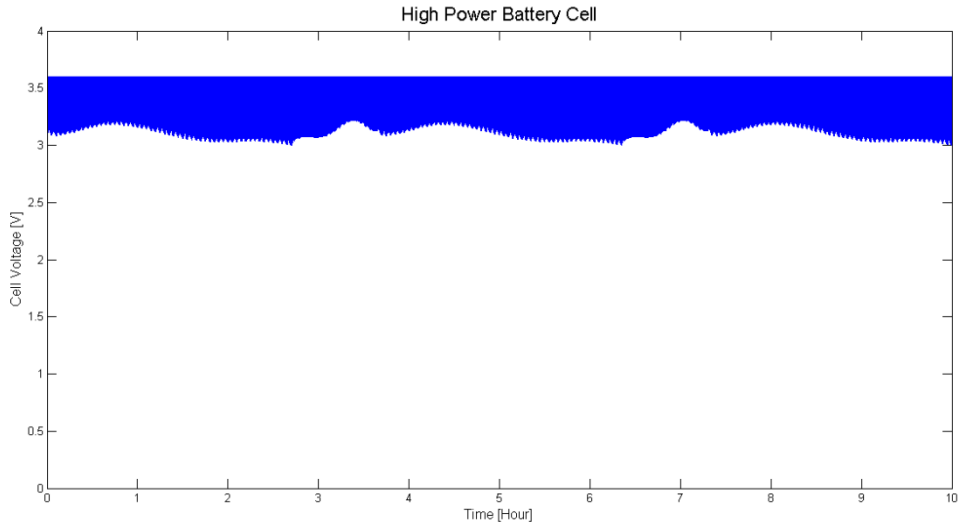

Figure 35: HPB cell voltage during discharge and charge

Figure 36 shows the Li-ion battery SOC level during charge and discharge, where it is kept within its limits. The reason for the Li-ion battery SOC to charge faster than discharge is because the numbers of Li-ion battery cabinets are dimensioned according to the largest charging power, and a lower discharging current is used in the charge mode.

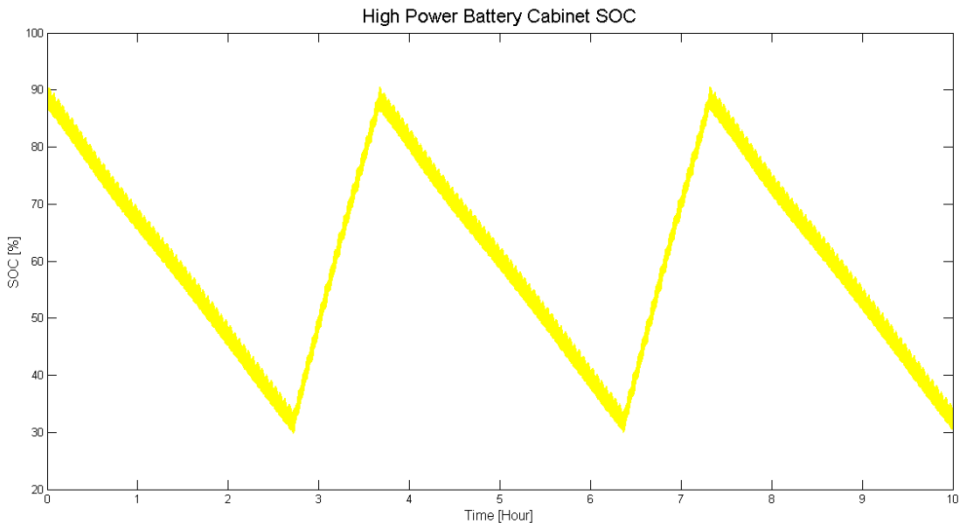

Figure 36: HPB battery SOC level during discharge and charge

An example of the charging and discharging current of a Li-ion battery cell is shown in Figure 37, this shows how the discharge current is reduced when the battery goes into charging mode.

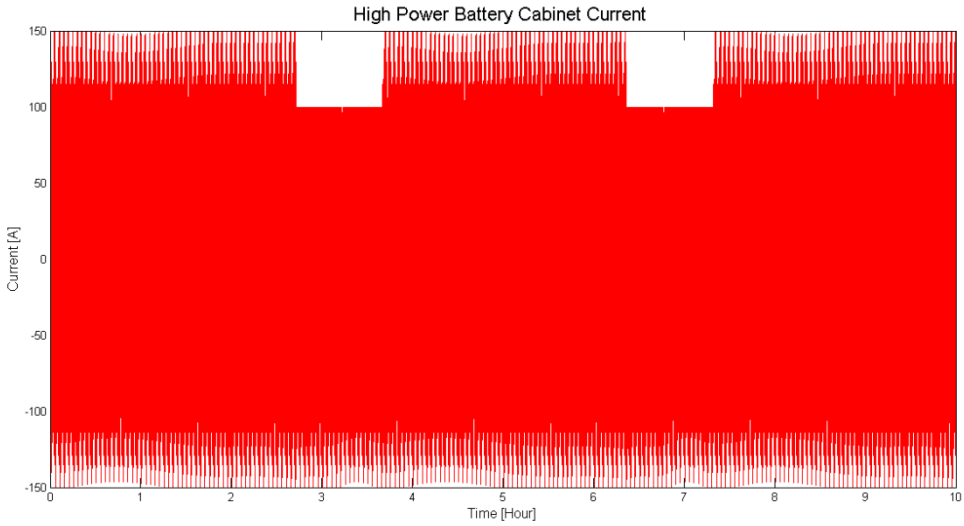

Figure 37: A HPB cabinet discharge and charge currents

Figure 38 shows an example of the Li-ion battery cabinets instantaneous and average temperature, where the internal cabinet temperature is kept around $40\ ^{o}C$. Figure 39 shows the instantaneous and average cooling power needed for keeping the cabinet at $40\ ^{o}C$.

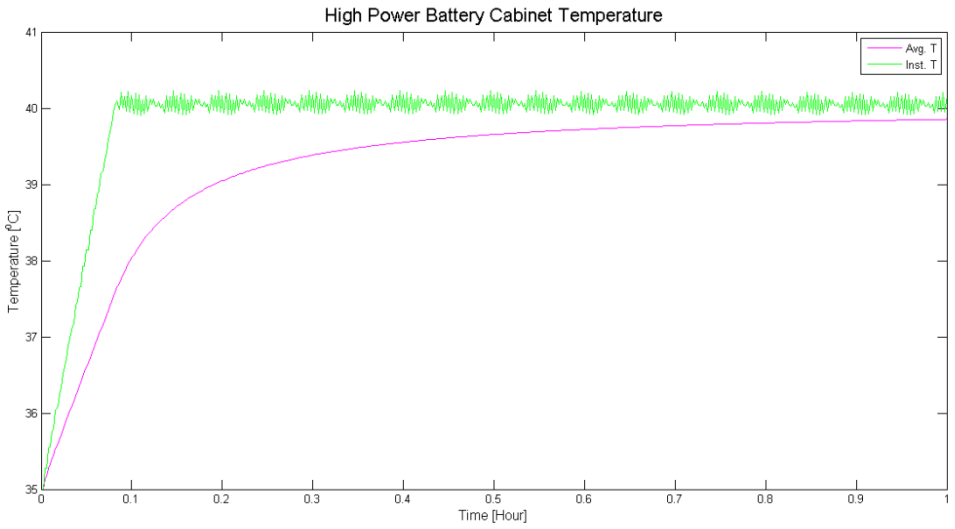

Figure 38: Instantaneous and average HPB cabinet temperature during discharge and charge

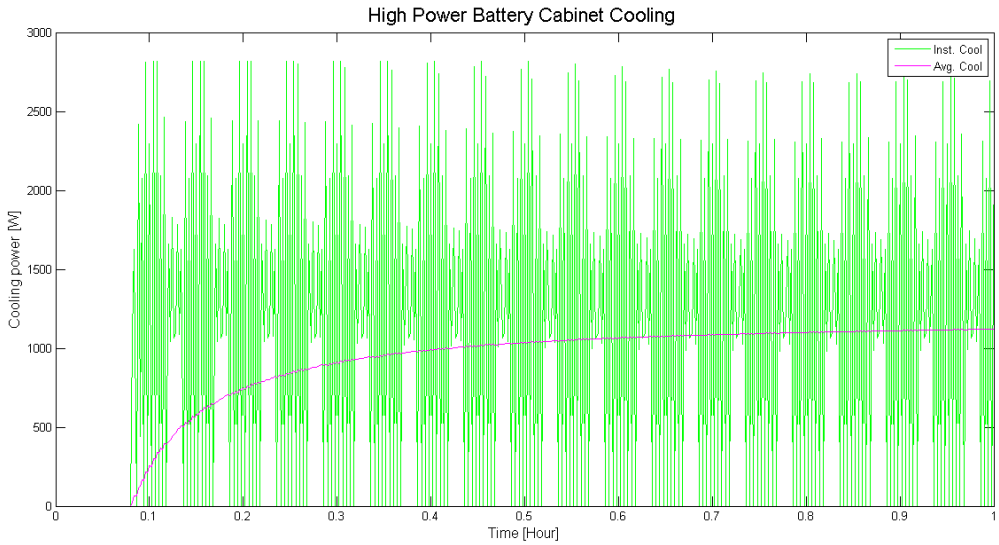

Figure 39: Instantaneous and average HPB cabinet cooling power during discharge and charge

9- The super capacitors

Figure 40: Super capacitor cell and its internal structure [13]

The SC technology was first commercialized in the 1970s, where they started out as computer memory backups. Super capacitors are today characterized for fast charging and discharging power. This makes them suiting for high power applications, especially in electric and hybrid vehicles [35].

9.2- Super capacitors properties

There is a large variety of SC technologies such as, double layer capacitors, metal oxide capacitor, polymer capacitors [36]. A simplified structure of a doubled layer capacitor is shown in Figure 41.

SC consists of two electrodes which are separated by a dielectric material. The electrodes are usually made of active carbon or active carbon fibers for generating a large surface area. Since the electrodes are made of active carbon, an oxidation on the surface would occur and cause a small leakage current in the SC.

The choice of electrode carbon structure is dependent on the electrolyte used, e.g. sulfuric acid or an organic compound. An electrolyte of an organic compound would be preferable as they can achieve a higher cell breakdown voltage.

When an active carbon material is used in a double layered capacitor, a double electric field is generated when a charge is applied to the electrodes [37]. A separator, usually made of a polymer, is used for separating the two layers as shown in Figure 41.

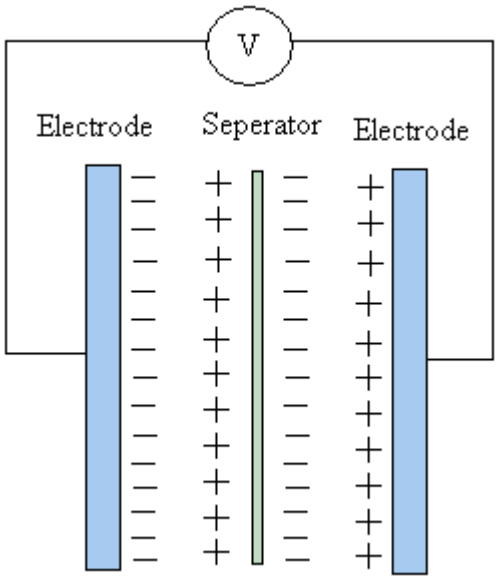

Figure 41: simplified structure of a double layer capacitor

The larger area and a smaller distance between the electrodes is the main difference between a SC and a conventional super capacitor. This difference in design gives the SC a large capacitance C_{sc} according to Equation 27 [22]. Here, ε is the dielectrics permittivity, A is the area of the electrode plates and d is the distance between the electrodes.

$$C_{sc} = \varepsilon \cdot \frac{A}{d} \qquad [\mathrm{F}] \qquad \text{Equation 27}$$

The amount of energy in a SC is usually lower than batteries, and is determined by Equation 28 [22], where V_{SC} is the voltage between the electrodes.

$$E_{sc} = \frac{1}{2} \cdot \ C_{sc} \cdot V_{SC}^2 \qquad [J] \qquad \text{Equation 28}$$

SC's has an internal resistance which gives energy loss and dissipates heat. This resistance is dependent on the SC's electrode and electrolyte material.

9.3- Operation of Super capacitors

In a similar manner as for the Li-ion batteries, the SC's are operated according to the suppliers specifications where SC's can be charged just as fast as a discharged. This property gives the ability for fast power cycling. But as mentioned previously, they do have a leakage current which makes them less suited for long term ES.

The SC cells has a voltage limit of about $2{,}5 - 2{,}7\ V$ [35], therefore they are packet in modules for achieving higher operational voltages. This would in turn require a management system similar to the Li-ion batteries for surveillance. This gives the module a safer operation, and prevents some of SC cells to be exposed by higher voltages than others.

9.4- Lifetime of super capacitors

The lifetime of SC's are mainly dependent of the applied voltage and temperature, as previously explained. SC's are in general expected to last millions of cycles. This is what gives SC's an upper hand versus high power Li-ion batteries. When the SC is discharging and the voltage declines, the current starts to rise. For preventing too high currents, the SC is operated within SOC limits in the same manner as batteries. According to [13], The SC's SOC limit should be set to a minimum value of $50\ \%$ and a maximum value of $100\ \%$, which is equivalent to $50\ \%$ DOD. This should allow the SC's to discharge $75\ \%$ of their energy.

The SC's SOC is based on the energy used versus energy stored derived from Equation 28 [22], The result is shown in Equation 29. Here, ΔV_{SC} is a change in voltage over the SC and V_{SCn} is the nominal voltage over the SC.

$$SOC_{SC} = \frac{V_{SCn} - \Delta V_{SC}}{V_{SCn}} \cdot 100 \qquad [\%] \qquad \text{Equation 29}$$

SC's are known for their long lifetime with respect to charge and discharge cycles, while the SC cells are vulnerable to a large cell voltage over time [35]. The cell voltage expression can be derived from Equation 28 and calculated as shown in Equation 30. Here, i_{sc} is the SC current, t is the time in seconds, V_{sc} is the voltage over the SC when it is operated, V_{sc_start} is the initial or nominal SC voltage and V_{sc_new} is the new voltage over the SC.

$$V_{sc\_new} = V_{sc\_start} - \sqrt{\frac{2 \cdot V_{sc} \cdot i_{sc} \cdot t}{C_{sc}}} \qquad [V] \qquad \text{Equation 30}$$

An SC's course of life with different cell voltages and temperatures is shown in Figure 42.

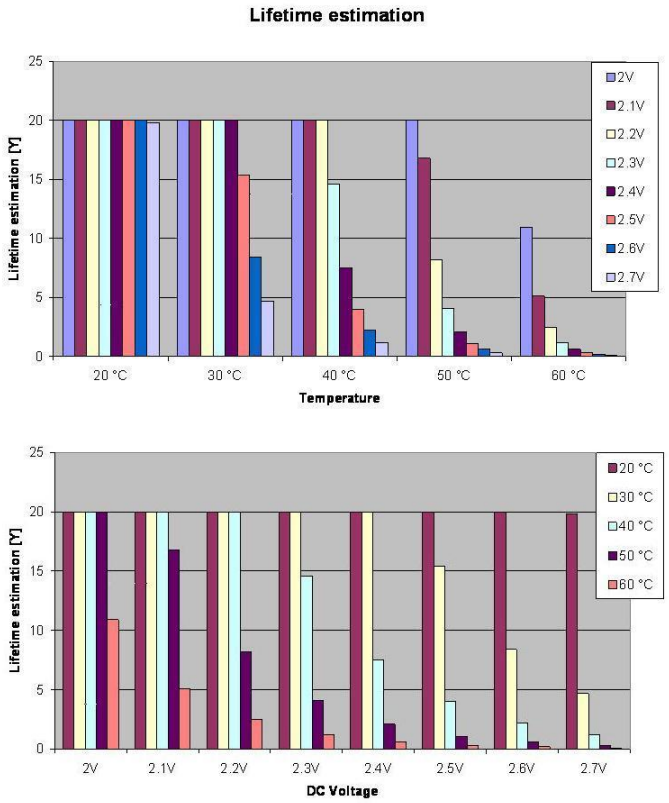

Figure 42: SC lifetime versus Cell voltage and temperature [13]

A lifetime equation similar the Li-ion batteries Equation 16 can be used on the SC's lifetime data. But instead of cycles, the SC's lifetime can be calculated based on years. For a given temperature the SC lifetime equation can be expressed as shown in Equation 31, where $Years_0$ and ρ are constants obtained by using known data and a similar procedure as shown in Appendix C.

$$Years(SOC_{SC}) = Years_0 \cdot e^{\rho \cdot SOC_{SC}} \qquad [years]$$ Equation 31

As seen in Figure 42, the SC's lifetime is dependent on temperature in a similar manner as batteries. Therefore the SC's temperature behavior is calculated using the same lumped capacitance principle as for the Li-ion batteries in Equation 16 - Equation 18. This would give the balanced SC temperature behavior shown in Equation 32, where $T_{SCint}(t)$ is the temperature in the SC module or cabinet, $q(t)_{SC}$ is the heat dissipated by all the SC cells in a module or cabinet and Ct_{SC} is the total heat capacitance of a SC cells in a module or cabinet.

$$\frac{dT_{SCint}(t)}{dt} = \frac{q(t)_{SC} - q(t)_{cool} - q(t)_{air}}{Ct_{SC}} \qquad [W]$$ Equation 32

9.5- Cost of super capacitors

The price of SC's is estimated to be high compared to other ES technologies [35]. The SC's costs are related to the raw material, production and assembly complexity. An estimated price range for SC's is around $2400 - 6000 \ \frac{\$}{kWh}$ [24].

It is important to include lifetime when assessing the profitability of an ES. Therefore, the operational costs should be included in the total costs when evaluating the investments of SC's.

9.6- Sizing of super capacitors

Dimensioning the number of SC's needed for energy storage is commonly done with respect to the energy demand during the largest peak in the load power. This is because SC's are short term energy storage devises and are therefore applied in peak power demand

situations. The procedure for calculating SC's in parallel is shown in Equation 33, where the $E_{load\_\max\_req}$ is the maximum load energy during the largest power request, $N_{SC-series}$ is the number of SC cell in series calculated in a similar manner as Equation 20, U_{SC} is the nominal SC voltage, η_{eff_sys} is the system efficiency and the DOD_{SC} has been added.

$$N_{SCE-parallel} = \frac{8 \cdot E_{load\_\max\_req} \cdot N_{SC-series}}{3 \cdot U_{SC}^2 \cdot C_{sc} \cdot \eta_{eff_{sys}} \cdot DOD_{SC}} \qquad [\#] \qquad \text{Equation 33}$$

For an EMS with Li-ion battery and SC as shown in Figure 26, the number of SC's in parallel are determine by an energy difference according to Equation 34, where $P_{load}(t)$ is the power demand from the load and $P_B(t)$ is the power delivered by the batteries.

$$E_{load\_\max\_req} = \int_0^t P_{load}(t) - P_B(t)\, dt \qquad [J] \qquad \text{Equation 34}$$

As mentioned in [8], the amount of SC's would also be dependent on the maximum discharge power. Therefore, the dimensioning process should also include the SC's capability of discharging the maximum load power. This can be done in a similar manner as shown in Equation 21. This leads to the required number of SC's in parallel determined by Equation 35. Here, the $N_{SCP-parallel}$ is the number of SC's required when dimensioning with respect to maximum power discharge and charge.

$$N_{SC-parallel} = MAX\left(N_{SCE-parallel}, N_{SCP-parallel}\right) \qquad [\#] \qquad \text{Equation 35}$$

10- Modeling of the super capacitors

The modeling process, parameters and results of the SC model in MATLAB is described in this chapter.

10.1- The super capacitor in MATLAB

In MATLAB, the SC is also models according to the simplified circuit diagram shown in Figure 27 . The voltage and SOC of the SC is shown in Figure 43, where the cell voltage is calculated directly from the variable inputs i.e. the SC current and the DC-DC converter efficiency.

As the all the SC cells are assumed equally loaded, the total number of cells in a SC cabinet is multiplied with the SC cell voltage to give the cabinet voltage. The SC's SOC level is directly calculated from the voltage in the SC cell. As with the Li-ion battery model, if the SC's SOC has reached the lower limit, the SC's will go into a charging mode where it charges more current then it discharges.

The discharge power of the SC's are dependent on the current requested by the load and the variable terminal voltage of the SC cabinets. The charging power of the SC's are carried out with a constant voltage over the SC's and a current in accordance to the regenerative load and charging limits.

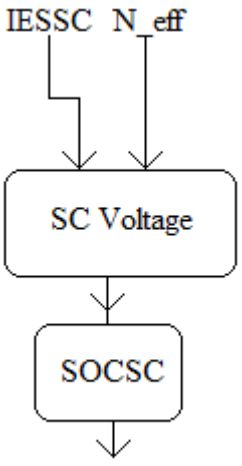

Figure 43: Voltage and SOC flowchart for the MATLAB model of SC

Also in the same manner as described in the Li-ion battery model, the temperature and cooling is modeled for SC cabinets as shown in Figure 44. This model is also based on the lump capacitance principle.

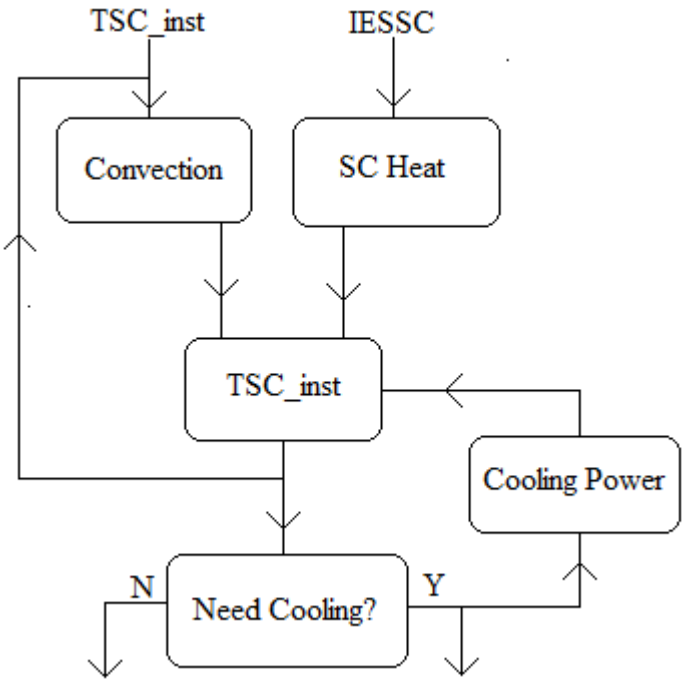

Figure 44: Temperature and cooling flowchart describing MATLAB model of a SC cabinet

The dimensioning model is done in with a similar approach as for the Li-ion battery model. Figure 45 shows the dimensioning process for SC cabinets, where the SC power requested from the load is the variable input. This power is set equal to the $amplitude$ of Equation 5 for peak shaving strategy, but an $amplitude$ is also used for the load sharing strategy.

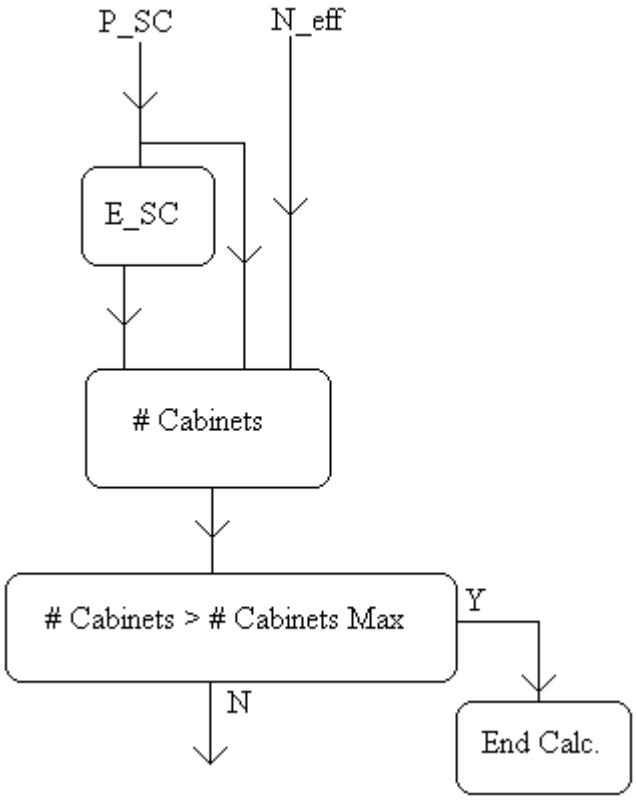

Figure 45: Flowchart for determining number of cabinet in the MATLAB SC model

The SC cell lifetime is modeled as shown in Figure 46, where the variable input is the average SOC value in the SC cabinet. When the average SOC value is below a limit, a new lifetime in years is calculated from a look up table. If the average SOC value in the SC cabinet is above the limit, a predetermined lifetime in years is used.

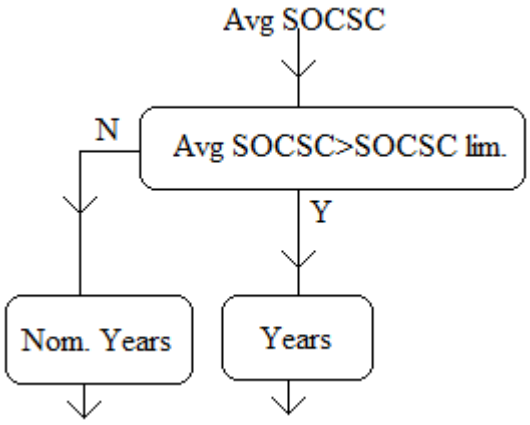

Figure 46: Lifetime flowchart describing the MATLAB model of SC cells

10.2- The Super capacitor parameters

SC module used in the MATLAB program is the *BMOD0063 P125 B04/08*, where the datasheet is shown in the Appendix A. The SC cabinet used is the same as in [8] an is also shown in Appendix A. The SC cabinet has room for 7 modules, where each module can hold 48 SC cells.

The losses from the SC's leakage current are neglected in the program as the SC's are used in an ES application with a short storage time. The internal resistance is not compensated for any temperature increase as cooling is applied.

The heat capacitance and the convective heat transfer coefficient are given in the datasheet for the SC module and the SC cabinet. The cabinet's convection area in contact with air is calculated by using the values in the SC cabinet datasheet, and the cabinet setup shown in Figure 23.

The reference temperature and temperature limits are set similar to the ones described in the parameter subsection of the Li-ion battery modeling chapter. The cooling power is set equal to the heat transferred from the SC cells to the air outside the cabinets. This was then multiplied with a factor. The reason for adding this factor is a result of the low heat capacitance of the SC modules, combined with the size of the sample step used in the simulation. This combination gives a large overshot when trying to maintain an average SC cabinet temperature of $40\ ^{o}C$. Therefore a factor of $1{,}07$ was multiplied with the heat transferred from the SC cells to air. This factor was found by using a trial and error method on the temperature and cooling model in MATLAB.

The SC's SOC limits are set to $100\ \%$ as a maximum value and $50\ \%$ as a minimum value. The maximum SC current limits are set to $150\ A$ for charging and discharging. If the SC's goes into charging mode, the SC's are programed to discharg $33{,}33\ \%$ of the discharge current limit. The voltage over the SC cells is set to $2{,}6\ V$ during charging.

The lifetime of the SC's are modeled from Figure 42, where the cell data at $40\ ^{o}C$ is used. From Figure 42 it can be seen that the SC's lifetime is only affeceted if the average SC's SOC is within the interval of $100 - 81.5\ \%$. If the SC's average SOC is outside this interval, then

the lifetime is set to 20 years. The model was created as an look up tabel from the data given in Table 5 and plottet as an exponential function shown in Figure 47. The reason for using an exponential function is because of the data given in Figure 42 has an exponentila caracteristics.

Years	Avg %SOC
1,66	100
20	81,5

Table 5: Years lifetime versus % SOC for SC's

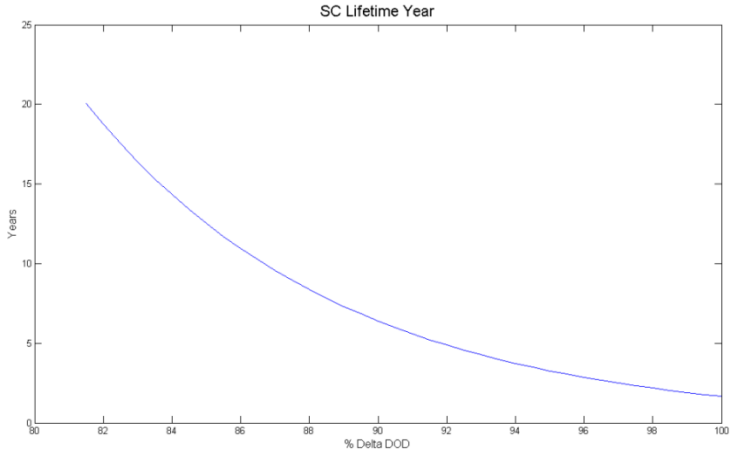

Figure 47: The lifetime in years versus % SOC for SC's

10.3- The super capacitor model performance

Some examples of the SC modeling are show shown here. The load shown in Figure 9 is used as a reference for the calculations. An example of the voltage in a SC cell during charging and discharging is shown in Figure 48, where the cell is operated within its recommended cell voltage limits. Since this figure shows the internal cell voltage, the charging voltage over the SC cell is not shown.

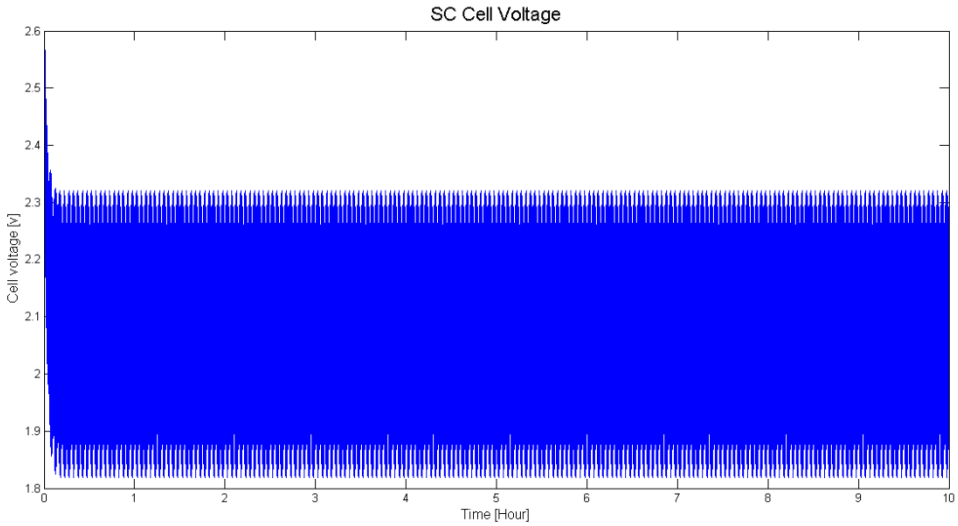

Figure 48: Voltage in a SC cell during charging and discharging

Figure 49 shows a SC cabinet % SOC during charging and discharging. As seen from the figure, the % SOC is operated well within its limits.

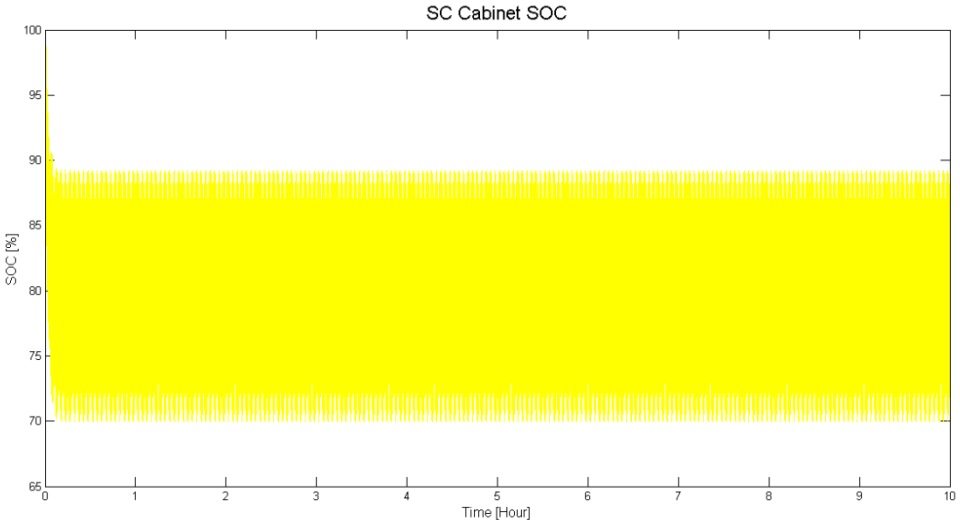

Figure 49: A SC cabinet % SOC during charging and discharging

An example of a cabinet current during charging and discharging is shown in Figure 50. It is seen that it operates well within is current limits, as the number of cabinets decides how much each cabinet is loaded.

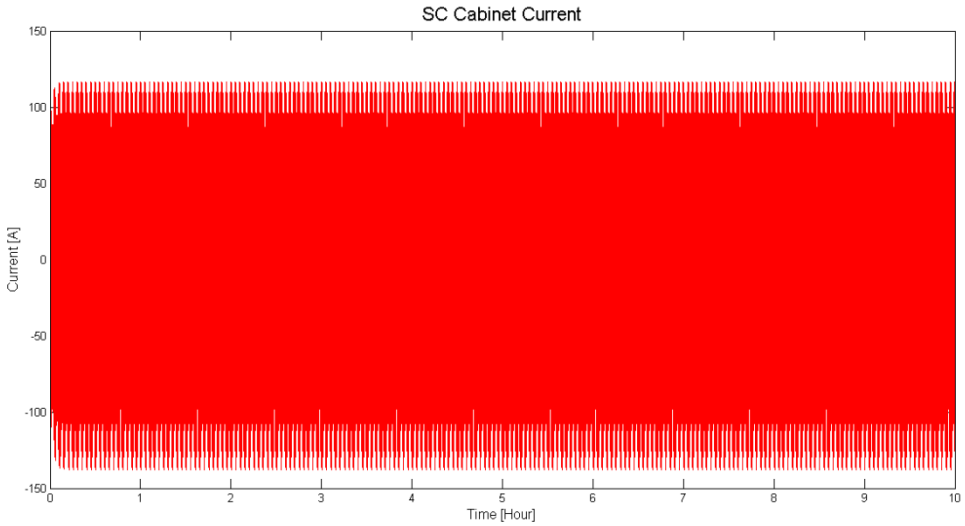

Figure 50: A SC cabinet discharge and charge currents

In Figure 51 and Figure 52 the average and instantaneous SC cabinets cooling and temperature are shown. As seen in Figure 51, the instantaneous SC cabinet temperature has a large variation due to the sampling and heat capacitance problem explained in the parameter subsection.

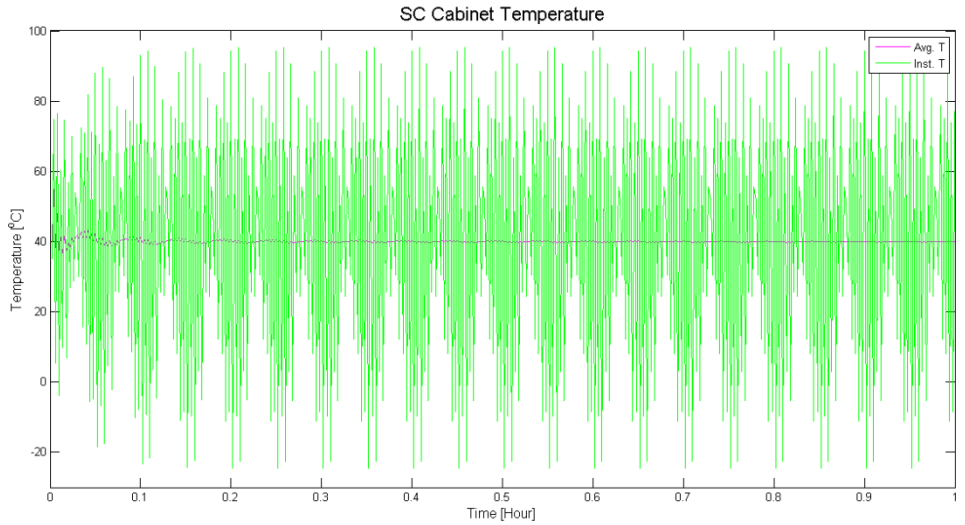

Figure 51: A SC cabinet instantaneous and average temperature

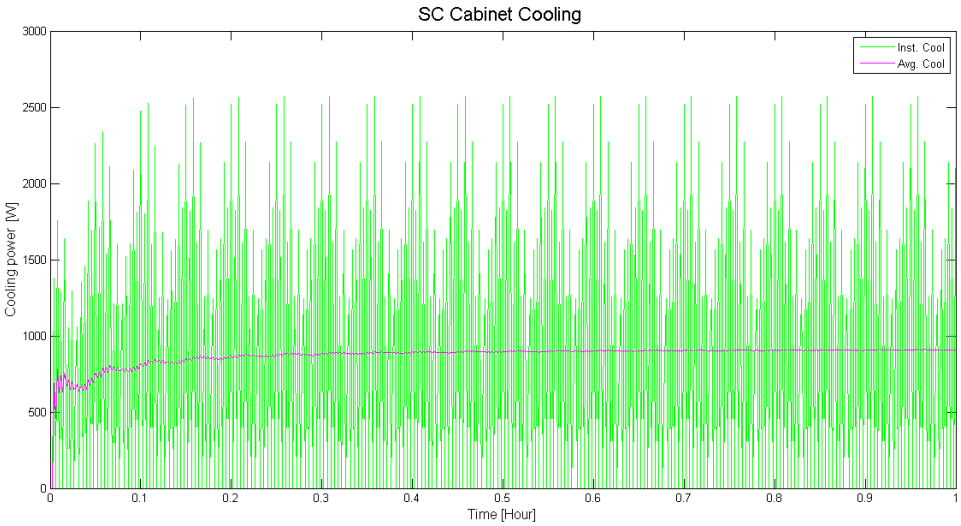

Figure 52: The instantaneous and average cooling power applied to a SC cabinet.

11- The bidirectional DC-DC converter

The converter commonly used for batteries and super capacitors, is the bidirectional two-quadrant DC-DC converter. This is because it has the ability to interchange between boost mode when discharging, and buck mode when charging. For areas where weight and size is of importance, a non-isolated converter is recommended, as an isolated converter would require a large transformer for achieving electric isolation.

For an optimized efficiency in a non-isolated converter, the operation mode should be discontinues. This is for achieving a high power density, lower diode recovery losses and reduced size of the inductor. This would require several interleaved converter phase-legs with a coupled inductor for removing high frequency current ripples. Since a discontinuous mode would lead to higher turn off losses and parasitic ringing, a soft switching operations should be implemented by using a zero-voltage resonant transition technology [38].

11.1- The DC-DC converters components

A circuit diagram of a one phase bidirectional DC-DC converter is shown in Figure 53. In the figure, R_{bus} is the resistance on the bus, R_{es} is the internal resistance of the ES, C_{ES} is the filter capacitance on the ES side, C_{bus} is the filter capacitance on the bus side and L is the inductor. Figure 53 also show two ideal switches with antiparallel diodes, the switches usually consist of IGBT technology.

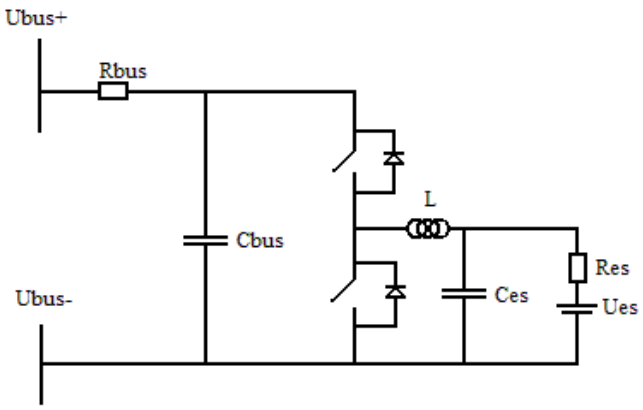

Figure 53: Bidirectional converter for charging and discharging

The size of the inductances can be calculated using Equation 36, where V_{bus} and V_{ES} is the bus voltage and ES voltage, T_s is the switching period, D is the duty cycle and Δi_L is the inductor current ripple.

$$L = \frac{V_{bus} - V_{ES}}{2 \cdot \Delta i_L} \cdot D \cdot T_s \qquad [H] \qquad \text{Equation 36}$$

The duty cycle is set to 0.5 for the inductor calculations as this is a bidirectional converter, and the inductor current ripple is usually chosen to be $10 - 20$ % of the full load current rating.

The voltage ripple out of the converter should be reduced according to the DNV regulations [40], which demands a voltage ripple of less than 10 % on a DC battery system. The size of the output filter capacitance C_{bus} can be calculated in Equation 37 which is accordance to a boost converter from [39]. Here, Δv is the voltage ripple from the converters output.

$$C_{bus} = \frac{V_{bus} \cdot D \cdot T_s}{2 \cdot \mathrm{R_{bus}} \cdot \Delta v} \qquad [F] \qquad \text{Equation 37}$$

The capacitance on the ES side can according to [39] be sized according to a buck converter. The capacitance C_{ES} is calculated from Equation 38.

$$C_{ES} = \frac{\Delta i_L \cdot T_s}{8 \cdot \Delta v} \qquad [F]$$ Equation 38

The IGBT switches are dimensioned according to the systems voltage and current capabilities. For high power applications, the IGBT's are connected in parallel or series in modules to meet the voltage and current requirements.

11.2- The DC-DC converters operations and simplifications

The bidirectional DC-DC converter shown in Figure 53 can be simplified by assuming V_{bus} to be threaded as a constant voltage source. And as the V_{bus} would be larger then V_{ES}, the capacitance C_{bus} and resistance R_{bus} can be neglected. If V_{ES} is treated as a strong voltage source, C_{ES} can also be neglected [38].

The duty cycle for the bidirectional converter is shown in Equation 39 for buck operation mode [13]. The current path in the DC-DC converter for on and off buck switching operations is shown in Figure 54 and Figure 55, where the simplifications described above is included.

$$D_{bu} = \frac{V_{ES}}{V_{bus}} \qquad [Ratio]$$ Equation 39

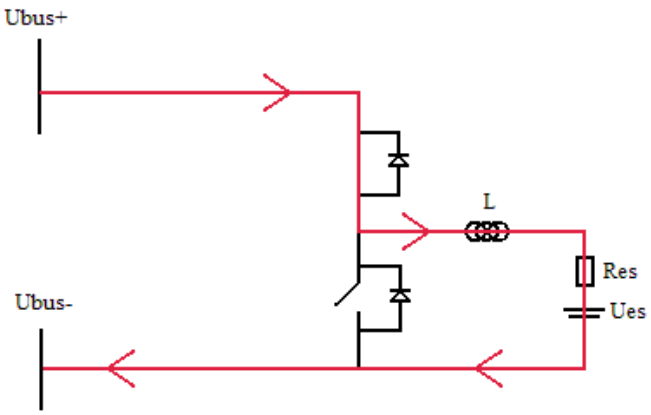

Figure 54: Buck charging operation when the switch is on

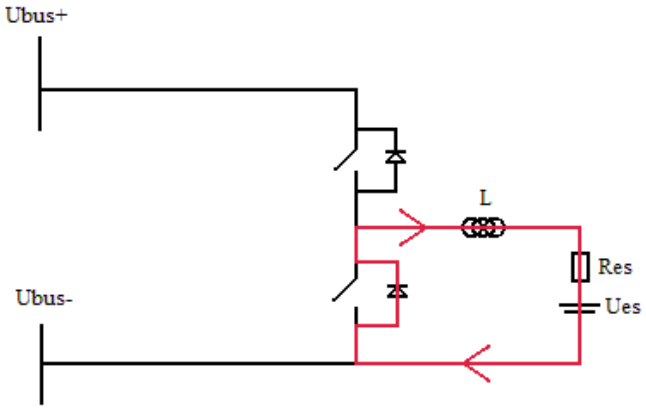

Figure 55: Buck charging operation when the switch is off

The balanced DC voltage equation for buck operation mode with respect to the inductor is given in Equation 40 [39]. The expression to the left of the + sign is the DC voltage during on operations, and the expression to the right of the + sign is the DC voltage during off operations. Here, V_L is the voltage drop in the inductor, V_{on} is the on voltage drop in the switch, V_D is the on voltage drop in the diode, V_{Res} is the internal resistance voltage drop of the ES and $D_{bu}{}'$ is the buck duty cycle for off operation mode defined by Equation 41.

$$D_{bu} \cdot (V_{Res} + V_L + V_{on} - V_{Bus}) + D_{bu}{}' \cdot (V_{Res} + V_L + V_{on}) = 0 \qquad \text{Equation 40}$$

$$D_{bu}{}' = 1 - D_{bu} \qquad [Ratio] \qquad \text{Equation 41}$$

For boost operations of the bidirectional converter, the duty cycle is opposite to the one shown in Equation 39. The boost duty cycle is shown Equation 42 for on operations. The current path in the converter for boost during off and on operations is shown in Figure 56 and Figure 57 with the above described simplifications.

$$D_{bo} = 1 - \frac{V_{ES}}{V_{bus}} \qquad [Ratio] \qquad \text{Equation 42}$$

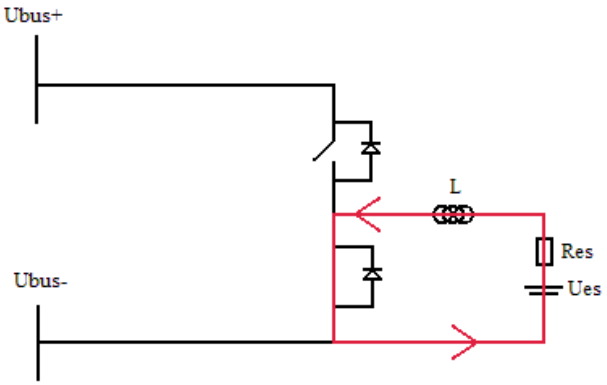

Figure 56: Boost discharge operation when the switch is on

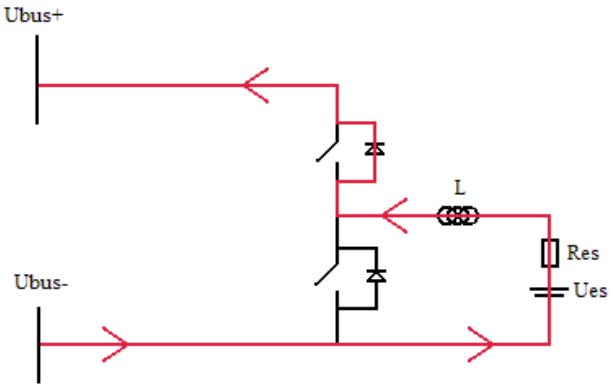

Figure 57: Boost discharge operation when the switch is off

As with the buck mode, the balanced DC voltage equation for boost operation mode with respect to the inductor is given in Equation 43. The expression to the left of the $+$ sign is the DC voltage during on operations, and the expression to the right of the $+$ sign is the DC voltage during off operations. $D_{bo}{}'$ is the buck duty cycle for off operation mode defined by Equation 44. [39]

$$D_{bo} \cdot (V_{Res} - V_L - V_{on}) + D_{bo}{}' \cdot (V_{ERes} - V_L - V_D - V_{Bus}) = 0 \qquad \text{Equation 43}$$

$$D_{bo}{}' = 1 - D_{bo} \qquad [Ratio] \qquad \text{Equation 44}$$

11.3- Efficiency of the DC-DC converter system

When the bidirectional DC-DC converter is operated, it is either in a buck mode or in a boost mode. Therefore, the losses are calculates according to these two states.

The RMS current is used for calculating losses, as there is an inductor in the circuit which generates a current ripple. The RMS current can be calculated according to Equation 45, where the derivation is shown in [38]. Here, i_{load} is the current during charging or discharging of the ES terminal.

$$I_{RMS} = \sqrt{i_{load}^2 + \frac{\Delta {i_L}^2}{3}} \qquad [A] \qquad \text{Equation 45}$$

Equation 45 is used to calculate losses and heat in the internal resistances of the ES.

For calculating the semiconductors conduction and switching losses in the DC-DC convert, the upper and lower ripple value has to be adjusted. This is because the maximum and minimum value of the inductor ripple would depend on the load current and duty cycle. The RMS currents which passes the IGBT switches I_{RMS-on} and diodes I_{RMS-d}, is corrected for its variable duty cycle. The basis for the calculations is the inductor current i_L which also is dependent on the operation mode of the converter.

- i_L is equal to the current from the ES terminal, i.e. i_{ES}, during discharging boost mode.
- i_L is equal to the bus current , i.e. i_{buss}, into the converter during charging buck mode.[41]

The calculations of the IGBT and diode ripple currents can be done from Equation 46 - Equation 49 [38]. Here, i_{L-max} is the upper inductor current ripple for either boost or buck operations, i_{L-min} is the lower inductor ripple for boost or buck operations and D is the duty cycle for either bucks or boost operation mode.

$$I_{on\_max} = i_{L-max} \cdot \sqrt{\frac{D}{3}} \qquad [A] \qquad \text{Equation 46}$$

$$I_{on\_min} = i_{L-min} \cdot \sqrt{\frac{D'}{3}} \qquad [A]$$ Equation 47

$$I_{d\_max} = i_{L-min} \cdot \sqrt{\frac{D'}{3}} \qquad [A]$$ Equation 48

$$I_{d\_min} = i_{L-max} \cdot \sqrt{\frac{D}{3}} \qquad [A]$$ Equation 49

The RMS currents through the conducting IGBT's are then calculated according to Equation 50 and the diodes according to Equation 51 [38].

$$I_{RMS-on} = I_{on\_max} + I_{on\_min} \qquad [A]$$ Equation 50

$$I_{RMS-d} = I_{d\_max} + I_{d\_min} \qquad [A]$$ Equation 51

Losses in the IGBT's and diodes are determined by the on-state voltage drop in the components and the conducting current. There will also be a loss when the IGBT's or diodes are not conduction, but this is of a negligible size compared to the on-state. Therefore it is common to neglect the off-state losses [41].

The on-state power loss of an IGBT can be calculated by Equation 52 [38], where $v(I_{RMS-on})_{IGBT}$ is the current dependent on-state voltage drop of the IGBT. As a voltage drop versus current curve is often given in IGBT datasheets, $v(I_{RMS-on})_{IGBT}$ can be expressed as a linear function as shown in Equation 53 [38], where v_a and v_b are constants.

$$P_{on\_IGBT-loss} = I_{RMS-on} \cdot v(I_{RMS-on})_{IGBT} \qquad [W]$$ Equation 52

$$v(I_{RMS-on})_{IGBT} = v_a + v_b \cdot I_{RMS-on} \qquad [V]$$ Equation 53

A similar approach can be done for the diodes, where the power loss is calculated according to Equation 54. $v(I_{RMS-d})_{diode}$ is an linear current dependent function of the diodes on-state voltage drop as shown in Equation 55.

$$P_{D-loss} = I_{RMS-d} \cdot v(I_{RMS-d})_{diode} \qquad [W]$$ Equation 54

$$v(I_{RMS-d})_{diode} = v_a + v_b \cdot I_{RMS-d} \qquad [V]$$ Equation 55

For calculating the switching losses of the IGBT's, the on-state, off-state and the reverse diode recovery losses are accounted for. The diode recovery loss is caused by excess charge carriers in the diode, during the transition to a reversed bias state. This makes the diode conductive and generates losses. The calculations of these switching losses are done according to energy loss curves shown in Equation 56 [38], [41]. In this case, f_{sw} is the switching frequency of the IGBT's, $E(I_{RMS-on})_{sw_{on}}$ is a current dependent on-state energy loss curves, $E(I_{RMS-on})_{sw_{off}}$ is a current dependent off-state energy loss curve, $E(I_{RMS-d})_{rr(on)}$ is a current dependent diode reverse recovery energy loss curve. V_{test} is the test voltage used by the manufactures whens specifying the energy loss curves in the datasheet.

$$P_{sw_{IGBT}-loss} = f_{sw} \cdot \left(E(I_{RMS-on})_{sw_{on}} + E(I_{RMS-on})_{sw_{off}} + E(I_{RMS-d})_{rr(on)}\right) \cdot \frac{V_{bus}}{V_{test}} \qquad [W]$$ Equation 56

The inductance would also contribute to a power loss in the DC-DC converter. This loss is mainly determined by the hysteresis, eddy currents, skin effects and chopper losses [39]. Equation 57 shows how the hysteresis loss in a magnetic core is calculated by integrating an H-field over a B-field. Here, A_c is the area of the core and l_m is the length of the core.

$$P_{H-loss} = f_{sw} \cdot A_c \cdot l_m \cdot \int H \, dB \qquad [W]$$ Equation 57

The chopper loss is typical expressed as a resistive loss shown Equation 58, where R_{cu} is the total chopper winding resistance.

$$P_{cu-loss} = I_{RMS}^2 \cdot R_{cu} \qquad [W]$$ Equation 58

As the DC-DC converter was simplified in the previous subsection, the filter capacitor losses are neglected. The loss in the bus resistance is also neglected as the DC-DC converter and ES system is the main area of focus.

The total efficiency for the DC-DC converter can be expressed as shown Equation 59. The loss in the internal resistance of the ES is not added to calculations. This is because the internal resistance loss is included as a voltage drop in the ES terminal voltage V_{ES}.

$$\eta_{tot} = \frac{i_{bus} \cdot V_{bus}}{P_{cu-loss} + P_{H-loss} + P_{sw\_IGBT-loss}} \cdot \ldots \\ \frac{1}{(i_{ES} \cdot V_{ES}) + P_{D-loss} + P_{on\_IGBT-loss}} \cdot 100 \quad [\%]$$

Equation 59

12- Modeling the bidirectional DC-DC converter

The modeling process, parameters and results of the bidirectional DC-DC converter model in MATLAB is described in the following sections.

12.1- The bidirectional DC-DC converter in MATLAB

Each SC cabinet or Li-ion battery cabinet is assumed to be equipped with a bidirectional DC-DC converter when they are used in peak shaving or load sharing strategy. The DC-DC converter is shown as $Pow.EL.$ in Figure 23. Figure 58 shows a flowchart of the converters operation in MATLAB. The total requested ES bus current is calculated from the total ES power which is a variable input. The total requested ES bus current is divided by each ES cabinet which is a variable input. The duty cycle is calculated from a cabinet's voltage and the bus voltage. The cabinet's voltage is modeled as a variable input, whereas the bus voltage is assumed constant. The duty cycle is added to a cabinet's bus current request, and the ES discharge current is calculated. The charging and discharging operations are of the Li-ion battery and SC cabinets, are explained in the previous Li-ion battery and SC modeling chapters.

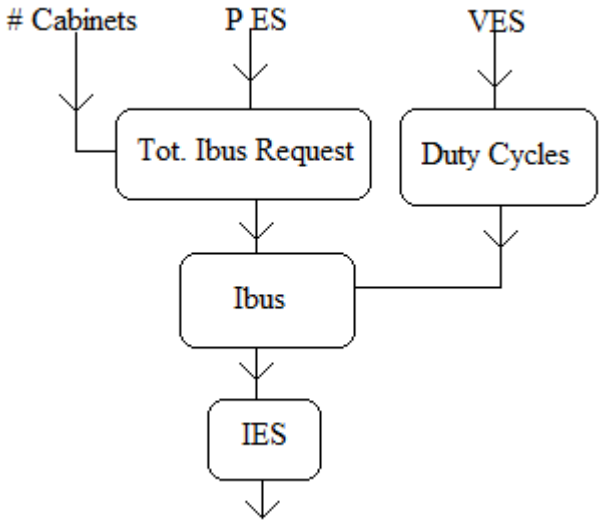

Figure 58: The Bidirectional DC-DC converters operation flowchart in the MATLAB model

A flowchart of the DC-DC converters loss model is shown in Figure 59 where the variable inputs are ES cabinet voltage, ES cabinet current and ES cabinet bus current. These currents are then used to calculate the currents flowing in the diode and the IGBT. When all the currents have been calculated, the power losses in each component are calculated. The conductive and switching power loss in the IGBT's and diodes are calculated from look up tables, whereas the inductor losses are simplified and calculated as a percentage of the DC-DC converters bus power. The reason for simplifying the inductor losses is related to the inductor dimensioning process, which requires and optimization of different core designs, material and wire cross section [7]. The converters efficiency is then calculated by using the ES cabinet's voltage. In the bidirectional DC-DC converter model, thermal and cooling calculations are neglected along with IGBT gate drive losses.

When the ES cabinets are discharging, the converters efficiency factor is added to the ES cabinet's output power. When the ES cabinets are charging, the efficiency factor is added to the SOC calculations of the ES.

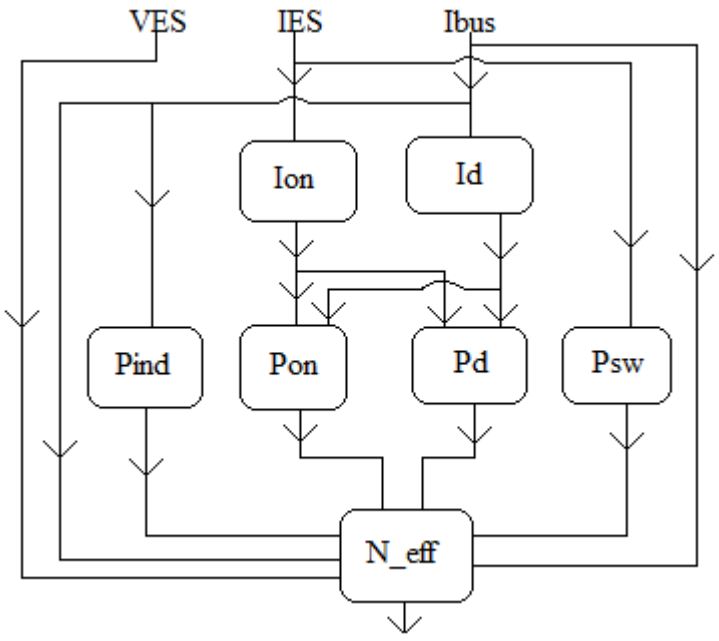

Figure 59: Flowchart for the bidirectional DC-DC converter losses in the MATLAB model

12.2- Bidirectional DC-DC converter parameters

For this application, the converter consists of two high power IGBT modules with freewheeling diodes. The IGBT modules used in the calculations are *CM300DU-24NFH* from *Powerex inc*. where the datasheet is shown in Appendix A. These modules are designed for high power operations with the operational ratings of $1200\ \mathrm{V}$ and $300\ \mathrm{A}$. The IGBT switching frequency is set to $2\ \mathrm{kHz}$ as done for similar work as in [13] and [8]. The peak to peak current ripple from the inductor is assumed to be $10\ \%$ in the calculations. When the bus voltage is required in calculations such as duty cycles and efficiency, it is set to a constant value of $1000\ V$.

As mentioned in the previous section, the conduction and switching losses where modeled as look up tables. For the switching losses, curve fitting polynomials where made from the energy loss versus current diagrams for on, off and diode reverses recovery switching. The values used for making these polynomials are shown in Table 6 and is taken from the datasheet.

Amper	Esw on	Esw off	Err on
30	0,003	0,003	0,0101
60	0,004	0,004	0,0101
80	0,005	0,0045	0,0104
200	0,009	0,0075	0,025
300	0,0105	0,0095	0,03

Table 6: Current versus on, off and diode recovery switching energy loss

The conductive on-state losses for the IGBT and the diode are modeled as linear functions created by the current versus on-state voltage drop diagrams in the datasheet. The constants used for the linear function described in Equation 53 and Equation 55, is shown in Table 7. Where the datasheet showed two different voltage drops with two different temperatures, an average value was used.

	v_a	v_b
IGBT on :	1	0.01167
Diode on :	1	0.004827

Table 7: Constants for the linear on state conductive voltage drop in the IGBT and diode

Plots of the polynomials created from Table 6 is shown in Figure 60 for the IGBT's on switching loss, Figure 61 for the IGBT's off switching loss and Figure 62 for the revered diode recovery switching loss.

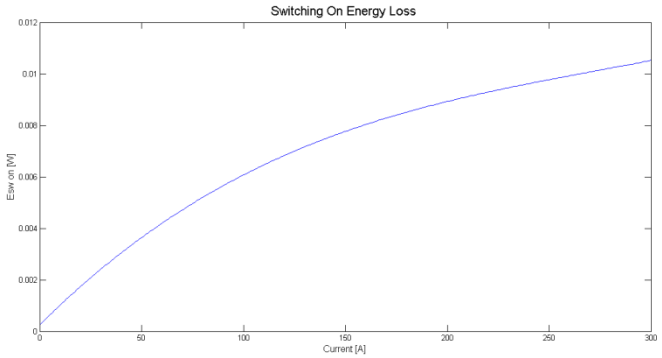

Figure 60: IGBT switch on energy loss versus current through the IGBT

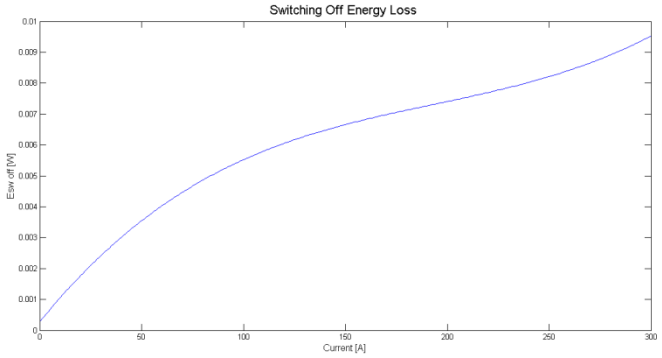

Figure 61: IGBT switch off energy loss versus current through the IGBT

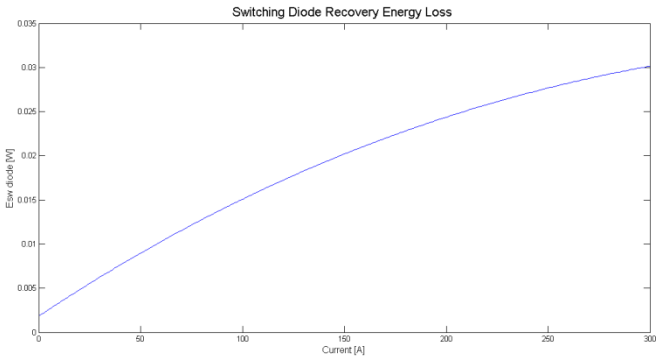

Figure 62: Diode reverse recovery switch energy loss versus current through the diode

Plot of the on-state conductive voltage drop of the IGBT's are shown in Figure 63, whereas the on-state conductive voltage drop of the diodes are shown in Figure 64.

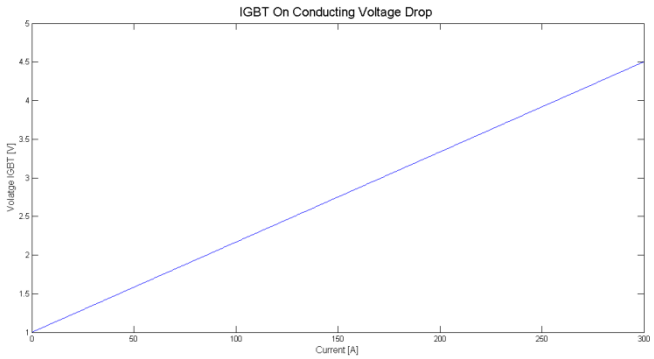

Figure 63: On state conductive voltage drop of the IGBT versus current through the IGBT

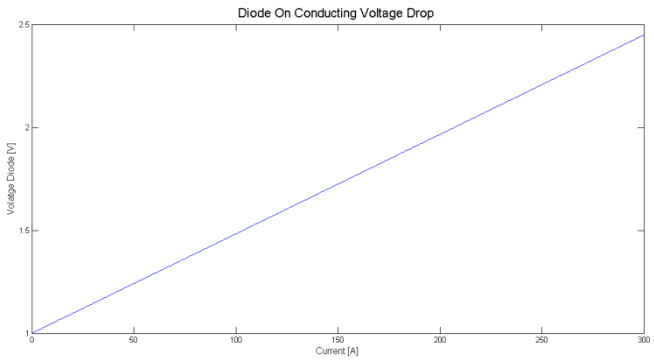

Figure 64: On state conductive voltage drop of the diodes versus current through the diodes

The inductor loss of the DC-DC bidirectional converter is assumed to be 1 % of the power flowing on the bus side of the DC-DC converter, during charging and discharging. The assumed loss percentage is based on assumptions made in [42] for the total inductor losses in an buck-boost converter.

12.3- The bidirectional DC-DC converter model performance

Some examples of the converter model are shown in this subsection where the load shown in Figure 9 is used as a reference for the calculations. Figure 65 shows how the duty cycle of the DC-DC converter operates during charging and discharging of a HPB or SC cabinet.

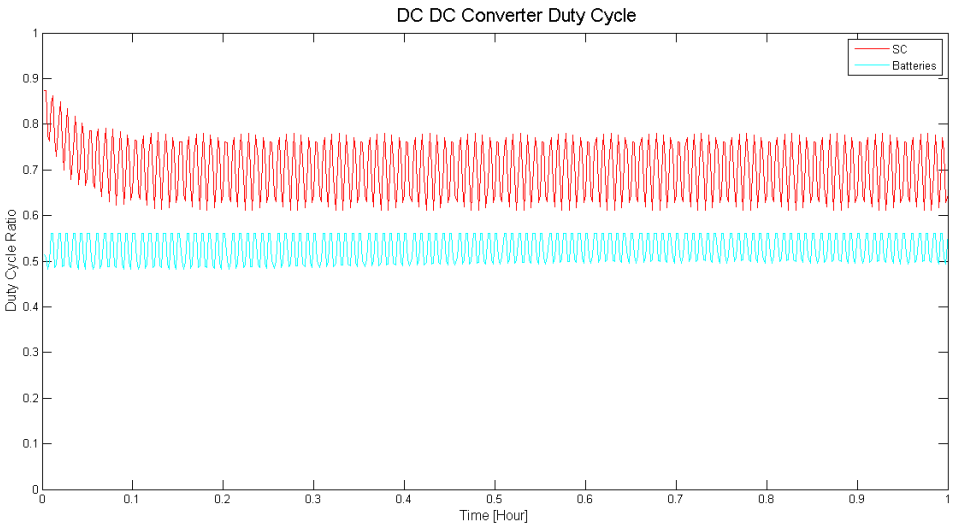

Figure 65: Duty cycles of the converter when a SC and a HPB cabinet is connected

The bus current from a HPB cabinet is shown in Figure 66 when it is charging and discharging.

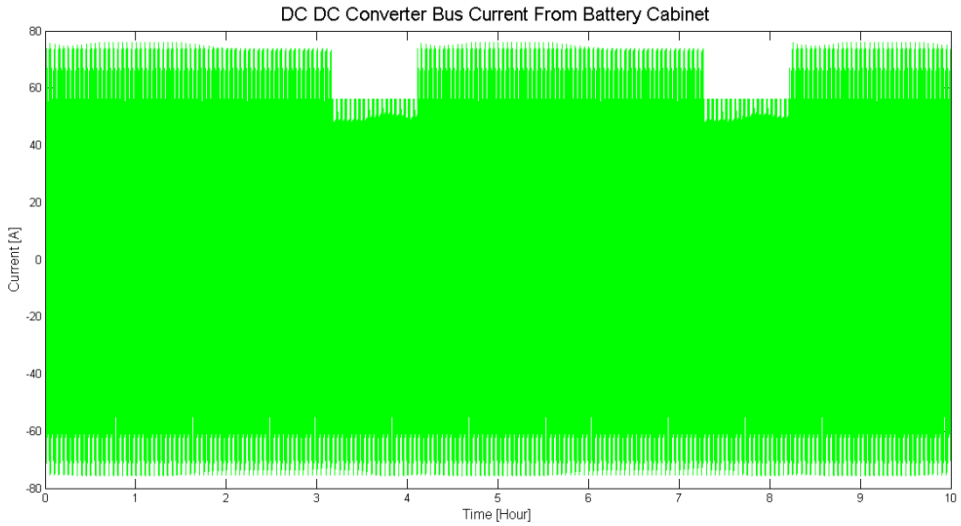

Figure 66: A HPB cabinet's current on the converter bus side, during charging and discharging

The bus current from a SC cabinet is shown in Figure 67 when it is charging and discharging.

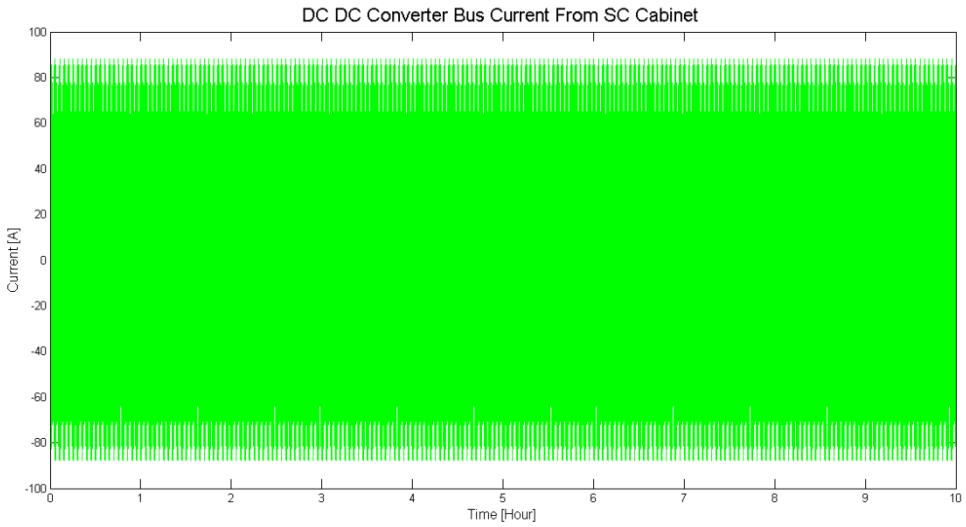

Figure 67: A SC cabinet's current on the converter bus side, during charging and discharging

The converters average and instantaneous efficiency is shown in Figure 68 when a SC and a HPB cabinet are connected. It is seen that the average efficiency lies between $98.7 - 98.5$ %. This is not an too unrealistic value since the high power bidirectional converter described in [38] had an efficiency of about 98 %.

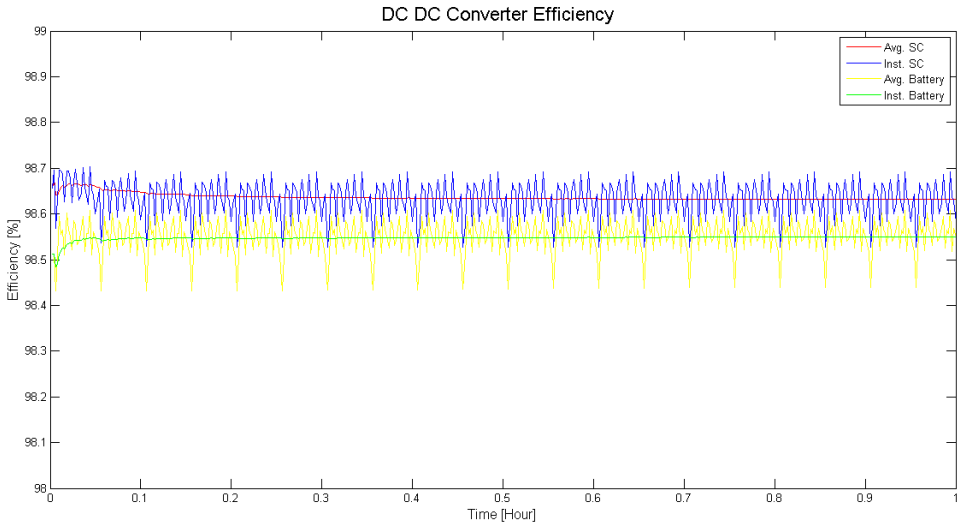

Figure 68: The DC-DC converters average and instantaneous efficiency for SC and HPB operation

13- The MATALB program

This chapter discusses the combined MATLAB program which is shown in Appendix E. Then two load cases which are used as inputs for MATLAB simulations are also discussed.

13.1- The combined models in MATLAB

The combined MATLAB program created from the models described in previous chapters is shown in Figure 69. The program is assembled with respect to simulation speed, therefore a minimum of subroutines are used, especially in loops with many repeats.

The first outer loop is changing between the seven OSV load operation modes, where each load operation modes activates two subroutines. In the first subroutine, the program retrieves its load setup according to Figure 8. The next subroutine determines the number of ES cabinet's needed. Since this process is dependent on the efficiency, the ES SOC and voltage models shown in Figure 43, Figure 28 and the converter model shown in Figure 58, Figure 59 are added in this subroutine. If the number of cabinets should exceed any maximum cabinet limit, a logic value will be activated.

The next inner loop is running the load function for each operation mode, which is measured in hours. Then the required current for each ES cabinet is calculated as shown in Figure 58, and the duty cycle and ES current is calculated. The DC-DC converters efficiency is then calculated as shown in Figure 59, where the average value is stored in the result. Then the ES SOC and voltage as shown in Figure 43, Figure 28 is calculated followed by the ES cooling and temperature as shown in Figure 29, Figure 44. The average value of the required cooling power and cabinet temperature is stored in the results. Then the ES lifetime is calculated as shown in Figure 30, Figure 46, where the average values are sent to the results. Then the power distribution between the ES and the DG's are calculated, and the DG's power is used to calculate the fuel consumption for FDG's and VDG's according to Figure 14. The fuel consumption without any ES is also calculated, this is for finding the percent difference in

fuel consumption with and without ES. When all of the load operation modes have been simulated, the results are written to the Excel sheet.

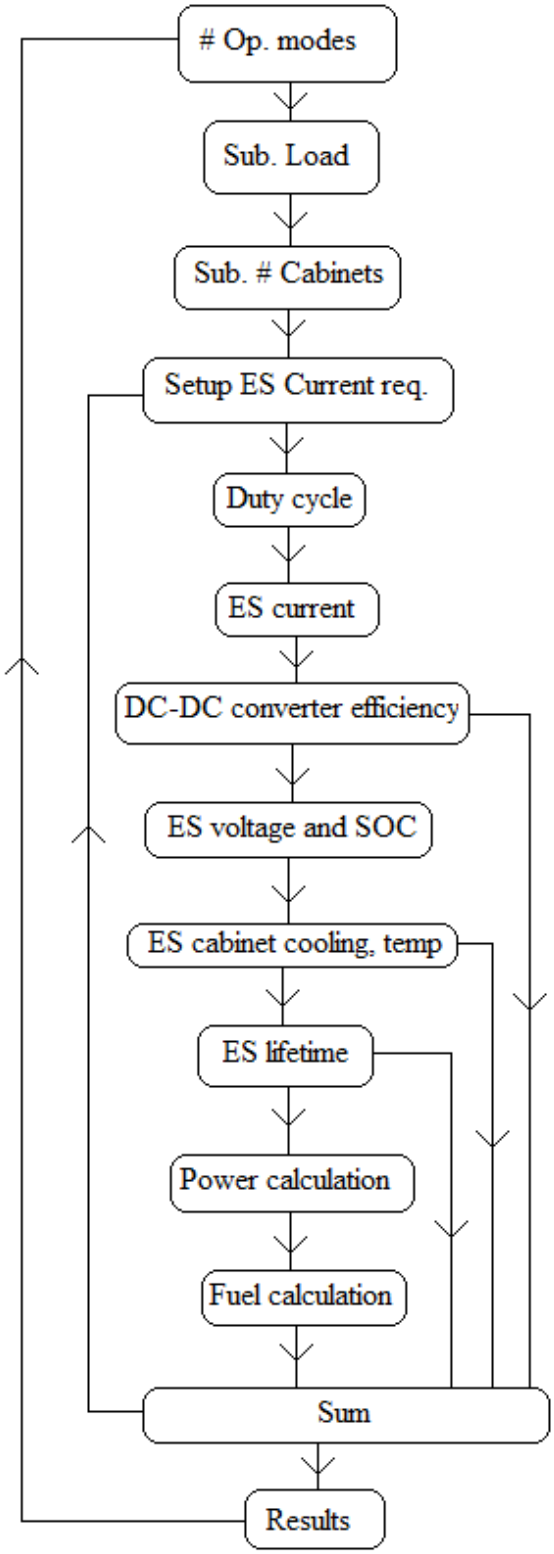

Figure 69: Flowchart for the MATLAB simulation program

13.2- Simulation cases

Two different cases are created for simulating the peak shaving and load sharing strategy. The first objective of these simulation cases is to compare the SC and HPB for a peak shaving strategy. The second objective is to study the possibilities of replacing one DG with ES, where the ES consists of HEB's assisted by SC's in a load sharing strategy.

The Excel load input data for the two cases is shown in Appendix B, where the initial DG loading ratio in the Excel sheet is set as close as possible to $0{,}8$ for each case. This is for preventing an overload on the DG's and for achieving an FOC favorable DG loading ratio. The DG's lower loading ratio for the peak shaving strategy is set to $0{,}5$. This is for preventing under loading of the DG's. The case load data is as mentioned previously created from information by *ABB Marine* in [8] and [16], where the efficiency factors for the DG's, thrusters and consumers are assumed.

The parameters for the DC-DC converter, SC and Li-ion battery model is the same as described in each respective section. The SC and Li-ion battery model parameter is chosen to be as similar as possible for making it easier to compare the two different technologies.

Besides from different case loading data, case 1 has no maximum limits on the number of ES cabinets. In case 2 however, the maximum limit of ES cabinets is set to 50. This limit is an assumption as the maximum number of ES cabinets would depend on the vessel size and application. The reason for carrying out a simulation without any ES cabinet limits is for making it easier to compare the number of SC and HPB cabinets required.

For each load operation mode simulated the values and variables start from an initial state, except for the HPB cycle lifetime as this is counting for the whole year.

14- Results and discussion

The simulation time for each case and strategy, was around 40 minuites. When starting the simulation at 0 hours as an initial value, several errors and *NaN* values appeared in the results for unknown reasons. The initial starting time was therefore set to 0.0001 hours.

The results of the peak shaving strategy for case 1 are shown in Table 8 for SC's and Table 9 for HPB. For case 2, the results of the peak shaving strategy are shown in Table 10 for SC's and Table 11 for HPB. The results for the load sharing strategy are shown in Table 12 for case 1 and Table 13 for case 2. The results from both strategies show the change in FOC for both VDG's and FDG's, number of ES cabinets, a logic value if the number of cabinets tries to exceed the ES cabinet limit, average cabinet temperature, average cooling power required and the ES lifetime. In the results given by the peak shaving strategy, the total DG power needed with and without ES is also shown. The DG's efficiency factor is included in these DG power results.

In Table 8 and Table 9, the SC's and HPB gives an FOC reduction with both FDG's and VDG's, during a DP high, DP low and anchor handling operation mode. The results show a relative large deviation in fuel consumption for FDG's FOC and VDG's FOC. This is as expected since the VDG's power can be operated with more flexibility for minimizing the FOC versus an FDG. It is however seen that the reduction in FOC is less when using HPB versus SC's. One possible cause is the HPB's need for charging when they have reached a minimum SOC level, this is shown in Figure 11. The simulation in case 1 did not contain any limit for the maximum number of ES cabinets. Therefore, the results in Table 8 and Table 9 shows that the load shaving strategy requires less SC cabinets then HPB cabinets. The converter efficiency is about the same for SC's as for HPB's. The cooling power required in a HPB cabinet is slightly higher than the required cooling in the SC cabinet. The reason for this may be in the Li-ion batteries heat capacitance which is larger than the one used for the SC's. This would require a longer duration of the cooling process on the Li-ion batteries for lowering the temperature. The lifetime of the SC's during DP high, DP low and anchor handling operation mode are kept at the maximum value of 20 years. The HPB's cycle lifetime is reduced during each of these mentioned operation modes. The peak shaving strategy results

in case 1 also shows that one DG is removed during the DP high and DP low operation mode for both SC's and HPB's.

As seen from the input load data for case 1 in Appendix B, harbor, BP, transit towing and transit supply operation modes only contain constant load data. Therefore, these operation modes do not give any meaningful results in Table 8 , Table 9 and are therefore neglected. The number of ES cabinets required are shown as 1 during these operation modes since it is an initial value used in the MATLAB calculations.

Op. Mode:	DP High	DP Low	Anchor Handling	Harbor	BP	Transit Towing	Transit Supply
Peak Shaving with SC							
FFOC without SC [gram]	845721027,445	1272110870,090	539387651,276	14935901,618	128731355,617	1309149139,420	1601463420,410
FFOC with SC [gram]	768142687,602	1126433247,439	534813803,765	14935901,618	128731355,617	1309149139,420	1601463420,410
%FFOC difference.	9,173	11,452	0,848	0,000	0,000	0,000	0,000
VFOC without SC [gram]	688664797,550	1015016366,360	477197419,549	8228537,383	114448295,428	1167289372,333	1423793522,086
VFOC with SC [gram]	675326752,361	995305913,381	475903347,942	8228537,383	114448295,428	1167289372,333	1423793522,086
% VFOC difference.	1,937	1,942	0,271	0,000	0,000	0,000	0,000
# SC cabinets required.	28,039	19,741	11,911	###########	##############	##############	##############
# SC > # SC lim.? [1=Yes, 0=No]	0,000	0,000	0,000	1,000	1,000	1,000	1,000
AVG SC converter efficiency. [%]	98,6	98,6	98,6	100	100	100	100
AVG SC temp. in Cabinet [°C]	39,938	39,938	40,702	35,000	35,000	35,000	35,000
AVG SC cooling power required. [W]	917,934	917,938	1022,824	0,000	0,000	0,000	0,000
Lifetime SC left. [year]	20,000	20,000	20,000	1,666	1,666	1,666	1,666
DG rated power no SC. [W]	6451200,000	5203200,000	8601600,000	902400,000	8601600,000	6451200,000	4300800,000
DG rated power with SC. [W]	4300800,000	3052800,000	8601600,000	902400,000	8601600,000	6451200,000	4300800,000

Table 8: Case 1's peak power shaving results for SC

Op. Mode:	DP High	DP Low	Anchor Handling	Harbor	BP	Transit Towing	Transit Supply
Peak Shaving with HPB							
FFOC without HPB [gram]	845721027,445	1272110870,090	539387651,276	14935901,618	128731355,617	1309149139,420	1601463420,410
FFOC with HPB [gram]	776602638,233	1138791129,366	535156151,071	14935901,618	128731355,617	1309149139,420	1601463420,410
%FFOC difference.	8,173	10,480	0,785	0,000	0,000	0,000	0,000
VFOC without HPB [gram]	688664797,550	1015016366,360	477197419,549	8228537,383	114448295,428	1167289372,333	1423793522,086
VFOC with HPB [gram]	683305819,763	1006686940,006	476218711,922	8228537,383	114448295,428	1167289372,333	1423793522,086
% VFOC difference.	0,778	0,821	0,205	0,000	0,000	0,000	0,000
# HPB cabinets required.	32,516	22,893	14,638	1,398	1,000	10,331	95,454
# HPB > # HPB lim.? [1=Yes, 0=No]	0,000	0,000	0,000	0,000	0,000	0,000	0,000
AVG HPB converter efficiency. [%]	98,5	98,5	98,5	100	100	100	100
AVG HPB temp. in Cabinet [°C]	40,062	40,062	40,065	35,000	35,000	35,000	35,000
AVG HPB cooling power required. [W]	1180,344	1180,399	1197,884	0,000	0,000	0,000	0,000
Lifetime HPB left. [cycles]	8307,965	7624,965	7581,965	0,000	0,000	0,000	0,000
DG rated power no HPB. [W]	6451200,000	5203200,000	8601600,000	902400,000	8601600,000	6451200,000	4300800,000
DG rated power with HPB. [W]	4300800,000	3052800,000	8601600,000	902400,000	8601600,000	6451200,000	4300800,000

Table 9: Case 1's peak power shaving results for HPB

The results in Table 10 and Table 11 which are taken from the peak shaving strategy in case 2, shows the same trend as the results in case 1. The case 2 results show a smaller reduction in fuel consumption with VDG's and FDG's when compared to the case 1 results. In case2, the DP high, DP low, harbor and transit towing has a variable load data input. It is seen that none of these operation modes requires any larger ES cabinet amount then the maximum limit. Since the BP and transit supply operation mode only contain a constant load data input, these results are neglected.

Op. Mode:	DP High	DP Low	Anchor Handling	Harbor	BP	Transit Towing	Transit Supply
Peak Shaving with SC							
FFOC without SC [gram]	1020999460,975	1384742803,810	505530570,129	53317272,230	128731355,617	1416686891,341	1627792890,342
FFOC with SC [gram]	952751915,097	1298398619,478	503596645,484	52335428,064	128731355,617	1415434833,269	1627792890,342
%FFOC difference.	6,684	6,235	0,383	1,842	0,000	0,088	0,000
VFOC without SC [gram]	802632435,320	1103411844,358	446299658,272	44540913,112	114448295,428	1240656929,325	1445945416,752
VFOC with SC [gram]	789457804,723	1086452697,821	445827056,339	44210895,471	114448295,428	1240497743,736	1445945416,752
% VFOC difference.	1,641	1,537	0,106	0,741	0,000	0,013	0,000
# SC cabinets required.	29,683	16,021	7,885	2,313	50,000	4,026	50,000
# SC > # SC lim.? [1=Yes, 0=No]	0,000	0,000	0,000	0,000	1,000	0,000	1,000
AVG SC converter efficiency. [%]	98,6	98,6	98,6	98,6	100	98,6	1 00
AVG SC temp. in Cabinet [°C]	39,938	39,938	40,702	39,938	35,000	40,702	35,000
AVG SC cooling power required. [W]	917,934	917,967	1022,824	917,991	0,000	1022,897	0,000
Lifetime SC left. [year]	20,000	20,000	20,000	20,000	1,666	20,000	1,666
DG rated power no SC. [W]	8601600,000	5203200,000	8601600,000	902400,000	8601600,000	8601600,000	4300800,000
DG rated power with SC. [W]	6451200,000	4300800,000	8601600,000	902400,000	8601600,000	8601600,000	4300800,000

Table 10: Case 2's peak power shaving results for SC

Op. Mode:	DP High	DP Low	Anchor Handling	Harbor	BP	Transit Towing	Transit Supply
Peak Shaving with HPB							
FFOC without HPB [gram]	1020999460,975	1384742803,810	505530570,129	53317272,230	128731355,617	1416686891,341	1627792890,342
FFOC with HPB [gram]	959477652,719	1305717471,851	503804706,002	52534569,754	128731355,617	1415726376,531	1627792890,342
%FFOC difference.	6,026	5,707	0,341	1,468	0,000	0,068	0,000
VFOC without HPB [gram]	802632435,320	1103411844,358	446299658,272	44540913,112	114448295,428	1240656929,325	1445945416,752
VFOC with HPB [gram]	797156536,695	1094780741,503	446029511,931	44436695,389	114448295,428	1240800715,922	1445945416,752
% VFOC difference.	0,682	0,782	0,061	0,234	0,000	-0,012	0,000
# HPB cabinets required.	34,422	18,580	9,690	2,683	1,000	4,948	50,000
# HPB > # HPB lim.? [1=Yes, 0=No]	0,000	0,000	0,000	0,000	0,000	0,000	1,000
AVG HPB converter efficiency. [%]	98,5	98,5	98,5	98,5	100	98,5	100
AVG HPB temp. in Cabinet [°C]	40,062	40,062	40,065	40,062	35,000	40,066	35,000
AVG HPB cooling power required. [W]	1180,344	1180,399	1197,899	1180,273	0,000	1197,927	0,000
Lifetime HPB left. [cycles]	8307,965	7624,965	7581,965	7453,965	0,000	7324,965	0,000
DG rated power no HPB. [W]	8601600,000	5203200,000	8601600,000	902400,000	8601600,000	8601600,000	4300800,000
DG rated power with HPB. [W]	6451200,000	4300800,000	8601600,000	902400,000	8601600,000	8601600,000	4300800,000

Table 11: Case 2's peak power shaving results for HPB

Table 12 shows the case 1 results for the load sharing strategy when one DG is removed. The results show a relative large decrease in FOC for both VDG's and FDG's with this strategy. Here, the VDG's gives a lower decrease in FOC when compared to the FDG's in most cases, except for BP and transit towing. Since this simulation was carried out without a maximum limit for the ES cabinets, the number of HEB cabinets needed is quite large for all the load operation modes. The number of SC cabinets required is in the vicinity of what was required for the peak shaving strategy. As explained above, the harbor, BP, transit towing and transit supply operation mode only contain constant load data. Therefore, the number of SC cabinets required in these operation modes, are shown obscured in the results. Due to this, all the SC results with these load operation modes are neglected.

The DC-DC converters efficiency for the HEB's is somewhat low for all the load operation modes. The reason for this is not quite known, but it may be related to the large number of cabinets since each of them would only need to discharge a small current. This small current could then give rise to problems in the DC-DC converters loss calculations. The DC–DC converter efficiency for the SC cabinets shows a value similar to the peak shaving strategy. The assumption of a low HEB current is further enhanced, due to the low temperature increase in the HEB cabinet and the low cooling power required. The lifetime calculations of the HEB's are not used since no charging process has been included in this strategy. The SC's temperature, cooling and lifetime follow a similar trend as for the peak shaving strategy.

Op. Mode:	DP High	DP Low	Anchor Handling	Harbor	BP	Transit Towing	Transit Supply
Replace a Gen. with HEB+SC							
FFOC without HEB+SC [gram]	845721027,445	1272110870,090	539387651,276	14935901,618	128731355,617	1309149139,420	1601463420,410
FFOC with HEB+SC [gram]	709117361,383	1128508466,163	436899542,740	4512045,816	98918121,029	1158660130,508	1287853425,793
%FOFC difference	16,152	11,289	19,001	69,791	23,159	11,495	19,583
VFOC without HEB+SC [gram]	688664797,550	1015016366,360	477197419,549	8228537,383	114448295,428	1167289372,333	1423793522,086
VFOC with HEB+SC [gram]	589153291,344	951769331,948	387648587,125	2314927,968	87826692,207	1017351237,811	1297230642,151
% VFOC difference	14,450	6,231	18,766	71,867	23,261	12,845	8,889
# HEB Cabinets required.	147141,585	351492,686	57388,421	3460,477	12266,330	245484,097	597502,325
# HEB > # HEB lim.? [1=Yes, 0=No]	0,000	0,000	0,000	0,000	0,000	0,000	0,000
# SC Cabinets required.	9,346	6,580	2,978	###########	##############	###############	##############
# SC > # SC Cabinets lim.? [1=Yes, 0=No]	0,000	0,000	0,000	1,000	1,000	1,000	1,000
AVG HEB converter efficiency. [%]	44,3	19,8	76,9	73,1	93,8	46,6	28,2
AVG SC Converter efficiency. [%]	98,6	98,6	98,6	100	100	100	100
AVG HEB Temp. in cabinet [°C]	35,000	35,000	35,000	35,000	35,001	35,000	35,000
AVG SC Temp. in cabinet [°C]	39,938	39,938	40,702	35,000	35,000	35,000	35,000
AVG HEB Cooling Power req. [W]	0,000	0,000	0,000	0,000	0,000	0,000	0,000
AVG SC Cooling Power req. [W]	918,004	918,007	1022,876	0,000	0,000	0,000	0,000
Lifetime HEB left. (Not used)	0,000	0,000	0,000	0,000	0,000	0,000	0,000
Lifetime SC left. [years]	20,000	20,000	20,000	1,666	1,666	1,666	1,666

Table 12: Case 1, HEB and SC's load sharing results.

The case 2 results for the load sharing strategy are shown in Table 13, where an ES cabinet limit was applied in the simulations. This limit would also be the cause for the increased FOC by bot VDG's and FDG's in the load operation modes, except DP high and transit supply. The ES cabinet limit may also have led to overloading of the DG's, but this is not possible to assess from the information given in Table 13. Since the BP and transit supply contains only a constant load, the results from the SC's can be neglected in these load operation modes. The results show that the required amount of HEB cabinets is larger than the maximum limit set. The required SC cabinet on the other hand, is well within the limits. The DC-DC converter efficiency with the HEB's is quite high. This could again be related to the low currents from the HEB modules. The low currents would also account for the temperature and cooling power results from the HEB cabinet. The SC's DC-DC converters efficiency, cabinet temperature, cooling power and lifetime is similar to the results from the load sharing strategy in case 1.

Op. Mode:	DP High	DP Low	Anchor Handling	Harbor	BP	Transit Towing	Transit Supply
Replace a Gen. with HEB+SC							
FFOC without HEB+SC [gram]	1020999460,975	1384742803,810	505530570,129	53317272,230	128731355,617	1416686891,341	1627792890,342
FFOC with HEB+SC [gram]	973672130,863	1318807146,009	518238535,410	53181428,640	136622843,692	1421388050,063	737513525,197
%FOFC difference	4,635	4,762	-2,514	0,255	-6,130	-0,332	54,692
VFOC without HEB+SC [gram]	802632435,320	1103411844,358	446299658,272	44540913,112	114448295,428	1240656929,325	1445945416,752
VFOC with HEB+SC [gram]	802471114,614	1123492891,635	458085737,868	44425880,072	119482691,256	1263674955,944	1430512244,806
% VFOC difference	0,020	-1,820	-2,641	0,258	-4,399	-1,855	1,067
# HEB Cabinets required.	50,000	50,000	50,000	50,000	50,000	50,000	50,000
# HEB > # HEB lim.? [1=Yes, 0=No]	1,000	1,000	1,000	1,000	1,000	1,000	1,000
# SC Cabinets required.	7,420	5,340	1,971	2,313	50,000	1,007	50,000
# SC > # SC Cabinets lim.? [1=Yes, 0=No]	0,000	0,000	0,000	0,000	1,000	0,000	1,000
AVG HEB converter efficiency. [%]	100	100	100	100	100	100	100
AVG SC Converter efficiency. [%]	98,6	98,6	98,6	98,6	100	98,6	100
AVG HEB Temp. in cabinet [°C]	35,004	35,002	35,017	35,007	35,085	35,006	35,003
AVG SC Temp. in cabinet [°C]	39,938	39,938	40,702	39,938	35,000	40,702	35,000
AVG HEB Cooling Power req. [W]	0,000	0,000	0,071	0,000	0,356	0,024	0,014
AVG SC Cooling Power req. [W]	918,004	918,007	1022,876	917,991	0,000	1022,897	0,000
Lifetime HEB left. (Not used)	0,000	0,000	0,000	0,000	0,000	0,000	0,000
Lifetime SC left. [years]	20,000	20,000	20,000	20,000	1,666	20,000	1,666

Table 13: Case 2, HEB and SC's load sharing results.

From the given component parameters, assumptions and load input data, the peak shaving results in case 1 and case 2 shows that SC's reduces the FOC slightly more than HPB's. Both of these two ES technologies does achieve relative good FOC reduction when used with FDG's, especially during DP operations. But when using VDG's, there is only a small reduction.

The peak shaving results shows that the number of SC cabinets required is less than for the HPB cabinets. But the SC and Li-ion battery cabinet datasheets in Appendix A shows that the volume of the SC cabinet is close to $1\ m^3$, while the Li-ion battery cabinet is close to $0{,}6\ m^3$. This should even out the total cabinet volume required from the SC's and HPB, when the results in Table 8 and Table 9 for case 1 and the results in Table 10 and Table 11 for case 2

are compared. The cooling power needed by the HPB's are according to the results generally higher than for SC's. But there is an uncertainty in these results due to lack of real component parameters, especially for the ones used in the HPB's. The lifetime results indicated that SC's should last longer than HPB's. This is based in the amount of battery cycles used after a year of operation, and the number of cycles left. But lifetime calculations are a delicate process. Therefore these results should be used with caution since they are calculated with a simplified lifetime model based on the available data.

The cost of Li-ion batteries and SC's were discussed in earlier chapters, where the SC's were described with the highest direct cost. As seen from the results and the discussion above, there are a lot of involving factors for estimating the total investment costs of either SC's or HPB's. The involving SC and HPB factors may also be difficult to compare, as these are two different ES technologies.

The load sharing results from case 1 shows a relative good reduction in FOC, especially for harbor operation mode using VDG's. As this simulation was done without any maximum limit on the number of ES cabinets, the results show that a large number of HEB cabinets are needed. Since this this strategy is thought to be applied on OSV's where footprint and weight should be kept at a minimum, this number of cabinets would seem impractical. The load sharing results from case 2, where the number of cabinets has a limit, shows the best result in transit supply mode with FDG's.

As previously mentioned, the results of case 2 does not show if the DG's are overloaded without the adequate number of cabinets. But since the numbers of HEB cabinets needed are dimensioned with respect to their stored energy, it is most likely that the DG's are overloaded once the HEB's SOC reaches the lower SOC limit. This assumption gets stronger when looking at the FOC which shows an increase for some load operation modes in case 2. The case 2 results of the load sharing strategy are therefore not completely consistent with the expected results. The SC's with a load sharing strategy in case 1 behaves in a similar manner as with the peaks shaving strategy. The number of SC cabinets are also well within the limits in case 2.

The HEB's DC-DC converter efficiency does show some unclear results in load sharing results from case 1, and a rather high value in case 2. These results would perhaps have been more

clear if the DC-DC converter was modeled for lower currents or if several HEB cabinets were connected to a common converter. The size of the discharging current for the HPB's during charging mode could also have been optimized for increasing the efficiency of this charging strategy. The optimization would then be dependent on the system efficiency during charging and discharging of the HPB's.

The MATLAB program itself should also have been made more robust and user-friendly. An optimization process should also have been included in the program, as this would have made it easier to assess the total costs from the ES cost dependent factors. But before an optimization is included, more real and precise ES parameters should have been obtained. The program could also have contained other SC or Li-ion battery technologies, as there are many different variations and suppliers.

15- Conclusion and future work

15.1- Conclusion

The motivation for this thesis was to investigate the effect of applying ES in a ships DC distribution. Two PMS's known as peak shaving and load sharing strategies were applied with the use of Li-ion batteries and SC's. The operations of these PMS's were to be simulated for seven different load operation modes with the duration of one year. Each of the involving components such as loads , ES, FDG's or VDG's and bidirectional DC-DC converters were then modeled in MATLAB by using equations found in the literature, manufactures datasheet's, information from previous work and *ABB marine*. The component models were then combined in a MATLAB program, which simulated two cases with a different loading and limits for the amount of ES.

In the load sharing strategy where there were no limits on the number of ES cabinets, showed the best reduction in FOC. But the practical possibility of implementing such a large ES quantity would be unlikely for this kind of vessel. The peak shaving strategy showed the best FOC reduction for FDG's while the VDG's gave a relative weak reduction. A comparison between the usage of SC and HPB for the peak shaving strategy was also done. It was observed from the results that the SC's gave the best reduction in FOC for this strategy. But from an economical point of view where the total costs such as cooling, lifetime, ES size and costs are assessed, more research is needed. The results do however indicate that the amount of ES needed in a peak shaving strategy may be within an acceptable range.

This work has shown a method for analyzing ES, such as Li-ion batteries and SC's for annual vessel operations with known load data. From the simulation results and the assumptions made, it would be possible to reduce the FOC in ships application by applying ES. The results do however indicate that this ability is dependent on the system setup. This is because the reduction in FOC is influenced by the DG's operation mode, vessel's load power, ES operation strategy and requirements.

15.2- Future work

Obtaining real and accurate parameters from the ES suppliers and manufactures proved to be difficult. A description of the test and measurement methods used in the suppliers and manufacturers datasheets is not always described either. Therefore, physical tests and measurements should be done on Li-ion batteries and SC's for obtaining accurate parameters.

Real vessel load data should also be obtained, preferably measured on a reference vessel for different load operation modes and weather conditions.

For making an easier assessment of the SC's and HPB in the peak shaving strategy, an optimization should be done. The optimization should considers the amount of ES, cooling required, size of the discharge current during charging mode of the HPB's.

The use of HEB's and SC's in the load sharing strategy could be considered in other vessels with different load operation modes, e.g. battery powered ferries.

16- References

1. Rose, R.S.K., *Future characteristics of offshore support vessels* in *Naval architecture and marine engineering webb institute* 2011, Massaschusetts Institute of technology: Massaschusetts Institute of technology

2. Jan Fredrik Hansen*, J.O.L., Ulf U. Ødegaard**, and Tor Arne Myklebust, *Increased operational performance of OSVs by Onboard DC Grid.* 2011.

3. Massimo Ceraolo, A.d.D., and Giulia Franceschi, *General Approach to Energy Optimization of Hybrid Electric Vehicles.* IEEE TRANSACTIONS ON VEHICULAR TECHNOLOGY, 2008.

4. Mamadou Baïlo Camara, H.G., Frederic Gustin, and a.B.D. Alain Berthon, *DC/DC Converter Design for Supercapacitor and Battery Power Management in Hybrid Vehicle Applications.* IEEE TRANSACTIONS ON INDUSTRIAL ELECTRONICS, 2010.

5. A. Della Valle, G.P., A. Coccia, E.Sciubba *Thermo-economic analysis of Dual-Mode Hybrid Trains: concept development and possible applications.* 2007.

6. Stefano Barsali, M.C., and Andrea Possenti, *Techniques to Control the Electricity Generation in a Series Hybrid Electrical Vehicle.* IEEE TRANSACTIONS ON ENERGY CONVERSION, 2002.

7. Ned Mohan, T.M.U., William P. Robbins, *Power Electronics:Converters, Application, Design* 2003: Wiley.

8. Solberg, M.B., *Fuel efficiency operation of DP thruster Drives by use of super capacitors*, in *Department of Electric Power Engineering* 2010, Norwegian University of Science and Technology.

9. Nebb, O.C., *LVDC distribution in ships application with batteries and super capacitors for increased fuel efficiency* in *Department Of Electrical Engineering* 2011, Norwegian University of Science and Technology.

10. Ole Christian Nebb, B.Z., John Olav Lindtjorn, Lars Norum, *Increased Fuel Efficiency in Ship LVDC Power Distribution Systems.* VPPC 2012 conference, 2012.

11. Bijan Zahedi, O.C.N., Lars Einar Norum, *An Isolated Bidirectional Converter Modeling for Hybrid Electric Ship Simulations.* iTec 2012 conference, 2012.

12. Kisacikoglu, M.C., M. Uzunoglu, and M.S. Alam, *Load sharing using fuzzy logic control in a fuel cell/ultracapacitor hybrid vehicle.* International Journal of Hydrogen Energy, 2009. **34**(3): p. 1497-1507.

13. Chen, J.-W., *Super Capacitors Energy Storage System: Marine Application*, in *Business Unit Marine* 2009, ABB AS.

14. HydroComp. *Bollard Pull: A HydroComp Technical Report*. 2007 [cited 2012 29.04]; Available from: http://www.hydrocompinc.com/knowledge/whitepapers/HC110-BollardPull.pdf.

15. Institute, U.S.N. *Chapter 2: Ship Resistance*. Marine Fouling and Its Prevention 1952 [cited 2012 29.04]; Available from: https://darchive.mblwhoilibrary.org/bitstream/handle/1912/191/chapter%202.pdf?sequence=9.

16. Sørfonn, I., *Power Management Control of Electrical Propulsion Systems*, in *DYNAMIC POSITIONING CONFERENCE* 2007, Wärtsilä N.A. Inc.

17. Radan, D., *Intergrated control of marine electrical power systems*, in *Department of Marine Technology* 2008: Norwegian University of Science and Technology.

18. Constantine D. Rakopoulos, E.G.G., *Diesel Engine Transient Operation: Principles of Operation and Simulation Analysis* 2009: Springer-Verlag London Limited.

19. jan Machowski, J.W.B., James R. Bumby, *Power System Dynamics: Stability and Control*. second ed2009: Wiley.

20. *Lithium-ion (Li-ion) - Large VLP cell range*. 2007 [cited 2012 28.02]; Available from: http://www.saftbatteries.com/MarketSegments/Marinecivil/tabid/155/Language/en-US/tabid/301/TypeControl/Produit/ProduitId/63/Default.aspx.

21. Buchmann, I. *Lithium-based Batteries*. 2012 [cited 2012 28.02]; Available from: http://batteryuniversity.com/learn/article/lithium_based_batteries.

22. Chris Mi, M.A.M., David Wenzhong Gao, *HYBRID ELECTRIC VEHICLES: PRINCIPLES AND APPLICATIONS WITH PRACTICAL PERSPECTIVES* 2011: A John Wiley & Sons, Ltd., Publication.

23. Cuenca, L.G.a.R., *Costs of Lithium-Ion Batteries for Vehicles*, 2000, Center for Transportation Research, Energy Systems Division, Argonne National Laboratory, 9700 South Cass Avenue, Argonne, Illinois 60439.

24. Brown, N. *Cheaper Ultracapacitors for Electric Vehicles*. 2011 [cited 2012 9.05]; Available from: http://cleantechnica.com/2011/05/11/cheaper-ultracapacitors-for-electric-vehicles/.

25. Marano, V., et al. *Lithium-ion batteries life estimation for plug-in hybrid electric vehicles*. in *Vehicle Power and Propulsion Conference, 2009. VPPC '09. IEEE*. 2009.

26. Lam, L., *A Practical Circui-based Model For State of Healt Estimation of Li-ion Battery Cells in Vehicles*, 2011, University of Technology Delft.

27. Park, S., *A Comprehensive Thermal Management System Model for Hybrid Electric Vehicles*, in *Mechanical Engineering* 2011, The University of Michigan.

28. Lino Guzzella, A.S., *Vehicle Propulsion Systems: Introduction to Modeling and Optimization*, ed. edition2005: Springer.

29. Sadoun, R., et al. *Optimal sizing of hybrid supply for electric vehicle using Li-ion battery and supercapacitor*. in *Vehicle Power and Propulsion Conference (VPPC), 2011 IEEE*. 2011.

30. Buchmann, I. *Types of Lithium-ion*. 2012 [cited 2012 30.3]; Available from: http://batteryuniversity.com/learn/article/types_of_lithium_ion.

31. Ingersoll, T.D.H.a.D., *Selected Test Results from the LiFeBatt Iron Phosphate Li-ion Battery.* Sandia National Laboratories, Albuquerque, New Mexico 87185 and Livermore, California 94550, 2008.

32. Pesaran, V.H.J.A.A., *Temperature-Dependent Battery Models for High-Power Lithium-Ion Batteries.* Presented at the 17th Annual Electric Vehicle Symposium, 2001.

33. Keyser, A.A.P.a.M., *Thermal Characteristics of Selected EV and HEV Batteries.* Annual Battery Conference: Advances and Applications, 2001.

34. Ledger, J. *Saft Li-ion battery technology provides the energy storage at the heart of ABB's new SVC Light concept for the Smart Grid* 2010; Available from: http://www.saftbatteries.com/SAFT/UploadedFiles/PressOffice/2010/CP_16-10_eng.pdf.

35. Buchmann, I. *super capacitors*. 2012 [cited 2012 30.3]; Available from: http://batteryuniversity.com/learn/article/whats_the_role_of_the_supercapacitor.

36. Christian Tallner, S.L., *Batteries or supercapacitors as energy storage in HEVs?*, in *Dept. of Industrial Electrical Engineering and Automation* 2005, Lund University.

37. Inc., I.C. *Supercapacitors*. [cited 2012 30.3]; Available from: http://www.illinoiscapacitor.com/pdf/papers/supercapacitors.pdf.

38. Zhang, J., *Bidirectional DC-DC Power Converter Design Optimization, Modeling and Control*, in *Electrical Engineering* 2008, Virginia Polytechnic Institute and State University: Blacksburg, Virginia.

39. Erickson, R.W., *Fundamentals of power electronics*: 1997 by Chapman & Hall Fifth printing 1999 by Kluwer Achademic Publisher.

40. DNV, *ELECTRICAL INSTALLATIONS OFFSHORE STANDARD*, in *DNV-OS-D201* 2011.

41. Dr. Dušan Graovac, M.P., *IGBT Power Losses Calculation Using the Data-Sheet Parameters* Infineon, 2009.

42. Zhao, Y., *SINGLE PHASE POWER FACTOR CORRECTION CIRCUIT WITH WIDE OUTPUT VOLTAGE RANGE*, in *Faculty of the Virginia Polytechnic Institute and State University* 1998, Virginia Polytechnic State University

17- Appendix

A- Datasheets

A.1 High Power Li-ion battery cell

Rechargeable $LiFePO_4$ lithium-ion battery
Super-Phosphate™ VL 10V Fe
Very high power cell

Saft's VL 10V Fe cell is ideally suited for applications requiring high discharge, continuous or pulse power; fast re-charge; low temperature performance; long cycle life; low heat generation; and/or higher levels of safety.

Saft always supplies cells as complete energy storage systems customized as need to meet customer specifications.

Saft's battery systems

Individual lithium-ion cells need to be mechanically and electrically integrated into battery systems to operate properly. The battery system includes electronic devices for performance, thermal and safety management specific to each application.

Benefits

- Non-toxic, extremely stable cathode material
- Excellent power density and specific power
- Hermetically sealed cells
- Maintenance free battery
- Operates in any orientation
- No memory effect
- State of charge identifiable by voltage
- Electrochemistry stable under most abuse conditions

Features

- Industry standard iron phosphate nano technology
- High discharge, pulse and continuous power
- Fast re-charge
- Excellent low temperature performance
- Long cycle and calendar life
- Low heat generation
- Exceptionally high efficiency

Applications

- Military hybrid electric vehicles
- Pulse power for unmanned applications
- Naval power for torpedoes, actuators and launchers
- Airborne power

Cell electrical characteristics	
Nominal capacity at C rate at 3.6 V/2.0 V & 25°C	10 Ah
Nominal voltage	3.3 V
Energy	33 Wh
Recommended maximum discharge current at 25°C:	
Continuous	1,750 A
2 s pulse	2,000 A
200 ms pulse	2,600 A
Power (25°C/100% SOC)	
Continuous	3,000 W
2 s pulse	3,300 W
200 ms pulse	4,300 W
Impedance (25°C/50% SOC at 500 A)	
2 s pulse	0.8 mΩ
200 ms pulse	0.66 mΩ
Low temperature performance*	see chart on p.2
Cell mechanical characteristics	
Diameter	47 mm
Height**	173 mm
Mass	0.60 kg
Volume**	0.27 L
Cell operating conditions	
Lower voltage limit for discharge:	
Continuous (- 60°C to + 60°C)	2/1.5 V
Pulse	1.5 V
Charging method	Constant current/constant voltage (CCCV)
Charging voltage	3.6 V
Recommended continuous charge current at 25°C	C/1
Fast charging is acceptable, depending on conditions of use	
6 minutes (at 150 A rate)***	
15 minutes (at 50 A rate)***	
Operating temperature	
Discharge	- 60°C to + 60°C
Charge**	
Storage and transportation temperature	- 50°C to + 65°C

**Consult Saft for system performance*

***Includes terminals*

****Fast charging may impact life - contact Saft for higher current or temperature*

April 2010

Super-Phosphate™ VL 10V Fe

Battery-level features

- Incorporation of several levels of redundant safety features to prevent abuse conditions such as overcharge, over-discharge, and short circuit
- Incorporating electronics for performance efficiency:
  - Charge/floating/discharge management
  - Cell balancing
- Battery protection controller
- CanProbe® at module level
- Safety vent and shutdown separator at cell level
- Consult Saft for complete battery system design

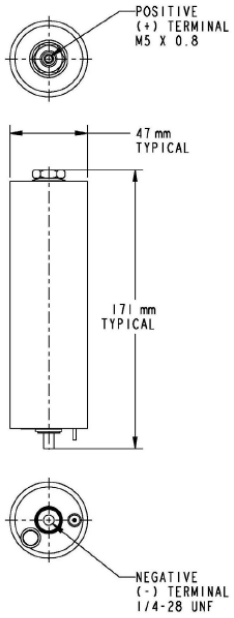

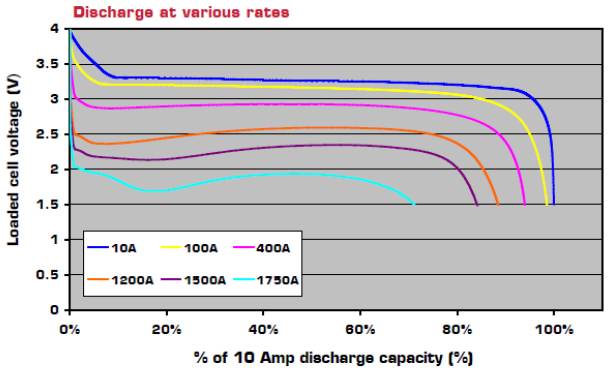

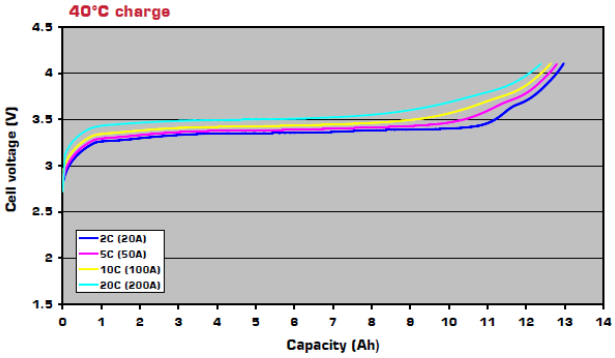

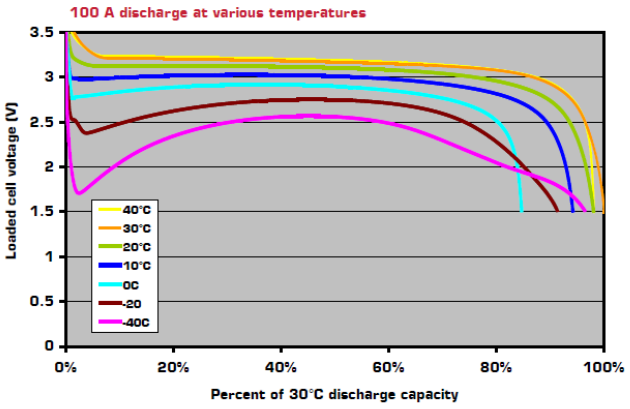

Saft America, Inc.
Space & Defense Division
107 Beaver Court
Cockeysville, MD 21030 - USA
Tel +1 410 771 3200
Fax +1 410 771 1144
SaftDefenseUS@saftbatteries.com

www.saftbatteries.com

Doc N° 54077-2-0410
Edition: April 2010

A.2 High energy Li-ion battery cell

Rechargeable $LiFePO_4$ lithium-ion battery

Super-Phosphate™ VL 45E Fe

Very high energy cell

Saft's VL 45E Fe cell is ideally suited for applications requiring high energy density; continuous discharge; moderate re-charge; and long cycle and calendar life.

Saft always supplies cells as complete energy storage systems customized as needed to meet customer specifications.

Saft's battery systems

Individual lithium-ion cells need to be mechanically and electrically integrated into battery systems to operate properly. The battery system includes electronic devices for performance, thermal and safety management specific to each application.

Benefits

- Excellent energy density and specific energy combined with proven long life
- Hermetically sealed cells
- Maintenance free battery
- Operates in any orientation
- No memory effect

Features

- Very long run time
- Fast re-charge capability
- Excellent low temperature performance
- Very long cycle life
- Low heat generation
- Exceptionally high efficiency

Applications

- Underwater vehicles
- Silent watch
- Long duration missions

Cell electrical characteristics		
Nominal capacity at C rate at 4.1 V/2.5 V & 25°C		44 Ah
Nominal voltage		3.3 V
Energy		140 Wh
Recommended maximum discharge current at 25°C		
	Continuous	50 A
	2 s pulse	100 A
Low temperature performance*		See chart on p. 2
Cell mechanical characteristics		
Diameter		54 mm
Height**		208 mm
Mass		0.9 kg
Volume**		0.48 L
Cell operating conditions		
Lower voltage limit for discharge		
	Continuous (- 60°C to + 60°C)	2.0 V
	Pulse	1.5 V
Charging method	Constant current/constant voltage (CCCV)	
Charging voltage		3.6 ± 0.04 V
Recommended continuous charge current at 25°C		C/7
Operating temperature		
	Discharge	- 40°C to + 55°C
	Charge***	- 0°C to + 55°C
Storage and transportation temperature		- 40°C to + 55°C

**Consult Saft for system performance*

***Includes terminals*

****Fast charging may impact life - contact Saft for higher current or temperature*

June 2010

Super-Phosphate™ VL 45E Fe

Battery-level features

- Saft provides complete battery system design
- Incorporation of several levels of redundant safety features to prevent abuse conditions such as overcharge, over-discharge, and short circuit
- Incorporating electronics for performance efficiency:
  - Charge/floating/discharge management
  - Cell balancing
- Battery protection controller at system level
- CanProbe® at module level

9 Amp discharge at various temperatures

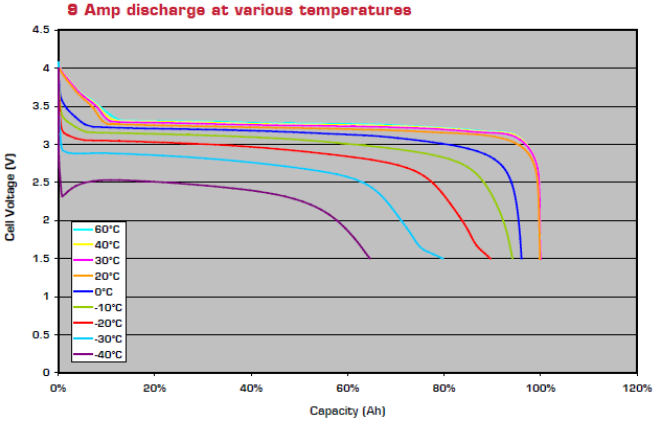

Discharge at 30°C at various rates

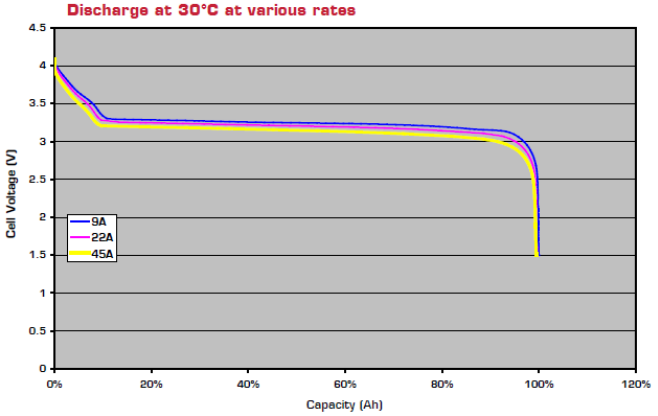

Saft America, Inc.
Space & Defense Division
107 Beaver Court
Cockeysville, MD 21030 - USA
Tel +1 410 771 3200
Fax +1 410 771 1144
SaftDefenseUS@saftbatteries.com

www.saftbatteries.com

Doc N° 54078-2-0610
Edition: June 2010

A.3 Super capacitor

DATASHEET 125V HEAVY TRANSPORTATION MODULES

FEATURES AND BENEFITS

- CAN bus digital monitoring and communications
- Highest power performance available
- Over 1,000,000 duty cycles
- Temperature and voltage monitoring
- Ultra-low resistance

TYPICAL APPLICATIONS

- Buses
- Electric trains and trolleys
- Heavy duty transportation
- Cranes, RTGS
- Utility vehicles
- Mining equipment

PRODUCT SPECIFICATIONS

ELECTRICAL	BMOD0063 P125 B04/B08
Rated Capacitance[1]	63 F
Minimum Capacitance, initial[1]	63 F
Maximum ESR_{DC}, initial[1]	18 mΩ
Rated Voltage	125 V
Absolute Maximum Voltage[15]	136 V
Maximum Continuous Current (ΔT = 15°C)[2]	140 A_{RMS}
Maximum Continuous Current (ΔT = 40°C)[2]	240 A_{RMS}
Maximum Peak Current, 1 second (non repetitive)[3]	1,800 A
Leakage Current, maximum (VMS 2.0)[4]	10 mA
Maximum Series Voltage	1,500 V
TEMPERATURE	
Operating Temperature (Ambient temperature)	
Minimum	-40°C
Maximum	65°C
Storage Temperature (Stored uncharged)	
Minimum	-40°C
Maximum	70°C

Maxwell TECHNOLOGIES
Enabling Energy's Future™

PRODUCT SPECIFICATIONS (Cont'd)

BMOD0063 P125 B04/B08

SAFETY

Short Circuit Current, typical (Current possible with short circuit from rated voltage. Do not use as an operating current.)	6,900 A
Factory High-Pot Test[14]	4,000 V DC
Certifications	RoHS eMark 72/245/EEC (B08 only) UN10.03 (B08 only)

TYPICAL CHARACTERISTICS

THERMAL CHARACTERISTICS

Thermal Resistance ($R_{ma,}$ Modulel Case to Ambient), typical	0.01°C/W
Thermal Resistance ($R_{ca,}$ All Cell Cases to Ambient), typical	0.04°C/W
Thermal Capacitance (C_{th}), typical [2]	33,370 J/°C

ESR AND CAPACITANCE VS TEMPERATURE

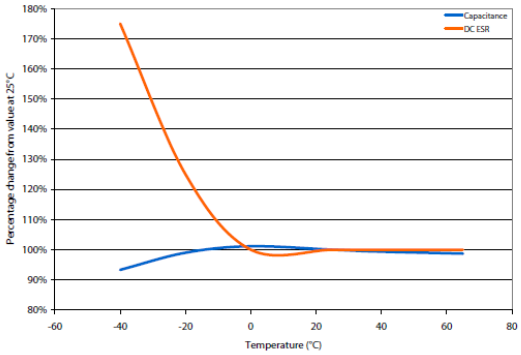

Maxwell TECHNOLOGIES
Enabling Energy's Future™

Marine integrated battery system

High Energy/Medium Power/High Power rack-mount lithium-ion battery system

Marine integrated battery system has been designed to suit the various power and energy requirements of a large variety of marine applications.

Its modular design allows to adapt the battery configuration:

- **to any system voltage from 24 V to 1000 V,**
- **to float or cycling applications,**
- **to any discharge pattern from high energy: energy requirements (hours or days of discharge) to very high power demands of seconds or minutes**

Applications

- Passenger vessels (cruise liners, ferries, Ro-Pax, urban transports)
- Workboats (tugs, offshore vessels, administration ships, fishing vessels)
- Inland shippings (river-sea shuttles, pushers/tugs, freight)
- Leisure vessels (mega yachts, medium size yachts)

Integrated system

The marine battery system integrates power, safety, management and communication. It is a stand-alone rackable battery system, which offers the benefits of Saft Li-ion technology in a qualified industrial design.

The marine integrated battery system provides maintenance-free energy storage in a reduced volume, combining safety and high operational reliability with outstanding lifetime under the most difficult environmental conditions.

March 2011

Features

Unprecedented design flexibility through:

- 24 or 48 V base modules in three versions: High Energy, Medium Power and High Power
- Series connection of base modules to suit system voltages of up to 1000 V maximum
- One unique control module per string, containing battery management and communication
- Parallel operation

Highest energy/power density

- The marine energy module uses battery cells VL 45 E 313 Wh/liter, surpassing most advanced battery designs
- The marine medium power module provides a well balanced compromise of power and energy, suitable for discharges of 10 min and above
- The high power module provides 18 kW of power (1100 W/liter), i.e. three times higher than most advanced battery designs. Suitable for discharges inferior to 10 min

Stand-alone system

- Integrating power, controls, communication and safety into a standard rack-assembly

Smart operation

- State of charge and state of health indication
- Built-in battery control for efficient operation
- Redundant safety
- Comprehensive communication
- Compatible with standard rectifiers

	High Energy	Medium Power	High Power
Nominal characteristics			
Nominal voltage (V) (with 13 modules max)	624	312	624
Capacity* (C/3) (Ah)	45 *	82 * *	30 *
Energy* (C/3) (Wh)	28 000 *	25 580 * *	18 720 *
Mechanical characteristics			
Width max (mm)		600	
Height max (mm)		2204	
Depth (mm)		450	
Weight (kg)		360	
Electrical characteristics			
Voltage window (V)	546 to 728	273 to 364	546 to 728
Maximum charge voltage (V)	728	364	728
Nominal discharge current (A)	30	150	300
Nominal charge current (A)	14	38	30 to 40
Peak power (30 sec; 20°C/68°F) (W)	18,500	37,000	164,000
Recharge time (h) at nominal current		3	
Faradic charge efficiency (20°C/68°F)		99%	
Energy charge efficiency (20°C/68°F)		96%	
Operating conditions			
Lifetime at +20°C perm (+68°F)		20 years	
Lifetime at +40°C (+104°F)		>10 years	
Cycle life (depending on delta DoD%; +20°C/+68°F)		from 3000 to 1 million cycles	
Operating temperature		-25°C/+60°C (-13°F/+140°F)	
Storage temperature		-40°C/+65°C (-40°F/+149°F)	
Compliance to standards			
Cell safety		UL 1642	
Module safety		EN 50178, cCSAus 60950, IEC 60950	
United Nation Class		UN 3480	
Hazard classification		Class 9	
Transport regulation compliance		UN recommendations for dangerous goods transportation, model regulations and manual tests and criteria 38.3	
EMC		EN 61000-4-2 Class B EN 61000-4-3 Class A EN 614000-4-4 Class B EN 614000-4-6 Class A EN 55022 Class B	
Protection class		IP 40	

* Ufloat 728 V Ucutoff 546 V, +20°C/+68°F
* * Ufloat 364 V Ucutoff 273 V, +20°C/+68°F

A.5 Super capacitor cabinet

Data sheet

TS 8005.500

Main data:

Model No.:	TS 8005.500
Designation:	Top enclosure system, painted RAL 7035, with mounting plate, double-door
Variant:	mit Montageplatte, lackiert
Packs of:	1 ST
W x H x D:	1.000 mm x 2.000 mm x 500 mm
Mounting surface:	n/a
Volume:	1144,00 dm³
Net weight:	149,25 kg
EAN:	4028177250826
Customs number:	85381000
Protection categories:	IP 55, NEMA 12

You can find the product in Catalogue 32, page 144

A.6 IGBT module

Powerex, Inc., 173 Pavilion Lane, Youngwood, Pennsylvania 15697 (724) 925-7272

CM300DU-24NFH

Dual IGBTMOD™ NFH-Series Module
300 Amperes/1200 Volts

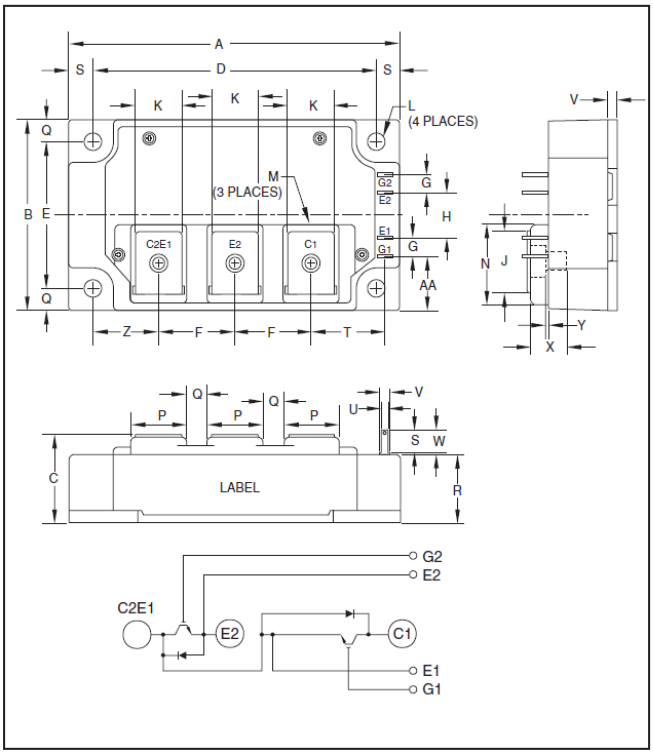

Outline Drawing and Circuit Diagram

Dimensions	Inches	Millimeters
A	4.25	108.0
B	2.44	62.0
C	1.14+0.04/-0.02	29.0+1.0/-0.5
D	3.66±0.01	93.0±0.25
E	1.89±0.01	48.0±0.25
F	0.98	25.0
G	0.24	6.0
H	0.59	15.0
J	0.7854	19.95
K	0.55	14.0
L	0.26 Dia.	6.5 Dia.
M	M6 Metric	M6
N	1.022	25.95

Dimensions	Inches	Millimeters
P	0.71	18.0
Q	0.28	7.0
R	0.874	22.2
S	0.30	7.5
T	0.94	24.0
U	0.11	2.8
V	0.16	4.0
W	0.33	8.5
X	0.46	11.75
Y	0.012 ~ 0	0.3 ~ 0
Z	0.85	21.5
AA	0.69	17.5

Description:
Powerex IGBTMOD™ Modules are designed for use in high frequency applications; 30 kHz for hard switching applications and 60 to 70 kHz for soft switching applications. Each module consists of two IGBT Transistors in a half-bridge configuration with each transistor having a reverse-connected super-fast recovery free-wheel diode. All components and interconnects are isolated from the heat sinking baseplate, offering simplified system assembly and thermal management.

Features:
- ☐ Low $E_{SW(off)}$
- ☐ Discrete Super-Fast Recovery Free-Wheel Diode
- ☐ Isolated Baseplate for Easy Heat Sinking

Applications:
- ☐ Power Supplies
- ☐ Induction Heating
- ☐ Welders

Ordering Information:
Example: Select the complete part module number you desire from the table below -i.e. CM300DU-24NFH is a 1200V (V_{CES}), 300 Ampere Dual IGBTMOD™ Power Module.

Type	Current Rating Amperes	V_{CES} Volts (x 50)
CM	300	24

X

CM300DU-24NFH
Dual IGBTMOD™ NFH-Series Module
3 00 Amperes/1200 Volts

Absolute Maximum Ratings, T_j = 25 °C unless otherwise specified

Ratings	Symbol	CM300DU-24NF	Units
Junction Temperature	T_j	–40 to 150	°C
Storage Temperature	T_{stg}	–40 to 125	°C
Collector-Emitter Voltage (G-E Short)	V_{CES}	1200	Volts
Gate-Emitter Voltage (C-E Short)	V_{GES}	±20	Volts
Collector Current (T_C = 25°C)	I_C	300*	Amperes
Peak Collector Current	I_{CM}	600*	Amperes
Emitter Current** (T_C = 25°C)	I_E	300*	Amperes
Peak Emitter Current**	I_{EM}	600*	Amperes
Maximum Collector Dissipation (T_C = 25°C, T_j ≤ 150°C)	P_C	1130	Watts
Maximum Collector Dissipation ($T_{C'}$ = 25°C, $T_{j'}$ ≤ 150°C)	P_C	1900	Watts
Mounting Torque, M6 Main Terminal	—	40	in-lb
Mounting Torque, M6 Mounting	—	40	in-lb
Weight	—	400	Grams
Isolation Voltage (Main Terminal to Baseplate, AC 1 min.)	V_{ISO}	2500	Volts

Static Electrical Characteristics, T_j = 25 °C unless otherwise specified

Characteristics	Symbol	Test Conditions	Min.	Typ.	Max.	Units
Collector-Cutoff Current	I_{CES}	V_{CE} = V_{CES}, V_{GE} = 0V	—	—	1.0	mA
Gate Leakage Current	I_{GES}	V_{GE} = V_{GES}, V_{CE} = 0V	—	—	1.0	µA
Gate-Emitter Threshold Voltage	$V_{GE(th)}$	I_C = 30mA, V_{CE} = 10V	4.5	6.0	7.5	Volts
Collector-Emitter Saturation Voltage	$V_{CE(sat)}$	I_C = 300A, V_{GE} = 15V, T_j = 25°C	—	5.0	6.5	Volts
		I_C = 300A, V_{GE} = 15V, T_j = 125°C	—	5.0	—	Volts
Total Gate Charge	Q_G	V_{CC} = 600V, I_C = 300A, V_{GE} = 15V	—	1360	—	nC
Emitter-Collector Voltage**	V_{EC}	I_E = 300A, V_{GE} = 0V	—	—	3.5	Volts

Dynamic Electrical Characteristics, T_j = 25 °C unless otherwise specified

Characteristics		Symbol	Test Conditions	Min.	Typ.	Max.	Units
Input Capacitance		C_{ies}	V_{CE} = 10V, V_{GE} = 0V	—	—	47	nf
Output Capacitance		C_{oes}		—	—	4.0	nf
Reverse Transfer Capacitance		C_{res}		—	—	0.9	nf
Inductive	Turn-on Delay Time	$t_{d(on)}$	V_{CC} = 600V, I_C = 300A, V_{GE1} = V_{GE2} = 15V, R_G = 1.0Ω, Inductive Load Switching Operation, I_E = 300A	—	—	300	ns
Load	Rise Time	t_r		—	—	80	ns
Switch	Turn-off Delay Time	$t_{d(off)}$		—	—	500	ns
Time	Fall Time	t_f		—	—	150	ns
Diode Reverse Recovery Time**		t_{rr}		—	—	250	ns
Diode Reverse Recovery Charge**		Q_{rr}		—	13	—	µC

* Pulse width and repetition rate should be such that device junction temperature (T_j) does not exceed $T_{j(max)}$ rating.
**Represents characteristics of the anti-parallel, emitter-to-collector free-wheel diode (FWDi).

Absolute Maximum Ratings, T_j = 25 °C unless otherwise specified

Ratings	Symbol	CM300DU-24NF	Units
Junction Temperature	T_j	–40 to 150	°C
Storage Temperature	T_{stg}	–40 to 125	°C
Collector-Emitter Voltage (G-E Short)	V_{CES}	1200	Volts
Gate-Emitter Voltage (C-E Short)	V_{GES}	±20	Volts
Collector Current (T_C = 25°C)	I_C	300*	Amperes
Peak Collector Current	I_{CM}	600*	Amperes
Emitter Current** (T_C = 25°C)	I_E	300*	Amperes
Peak Emitter Current**	I_{EM}	600*	Amperes

Powerex, Inc., 173 Pavilion Lane, Youngwood, Pennsylvania 15697 (724) 925-7272

CM300DU-24NFH
Dual IGBTMOD™ NFH-Series Module
300 Amperes/1200 Volts

Thermal and Mechanical Characteristics, T_j = 25 °C unless otherwise specified

Characteristics	Symbol	Test Conditions	Min.	Typ.	Max.	Units
Thermal Resistance, Junction to Case	$R_{th(j-c)}Q$	Per IGBT 1/2 Module, T_C Reference Point per Outline Drawing	—	—	0.11	°C/W
Thermal Resistance, Junction to Case	$R_{th(j-c)}D$	Per FWDi 1/2 Module, T_C Reference Point per Outline Drawing	—	—	0.18	°C/W
Thermal Resistance, Junction to Case	$R_{th(j-c)}'Q$	Per IGBT 1/2 Module, T_C Reference Point Under Chips	—	—	0.066	°C/W
Thermal Resistance, Junction to Case	$R_{th(j-c)}'D$	Per FWDi 1/2 Module, T_C Reference Point Under Chips	—	—	0.1	°C/W
Contact Thermal Resistance	$R_{th(c-f)}$	Per 1/2 Module, Thermal Grease Applied	—	0.04	—	°C/W
External Gate Resistance	R_G		1.0	—	10	Ω

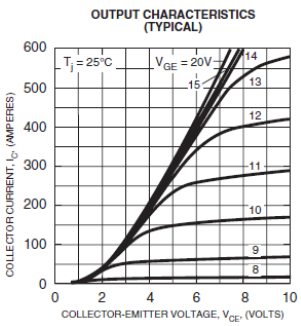

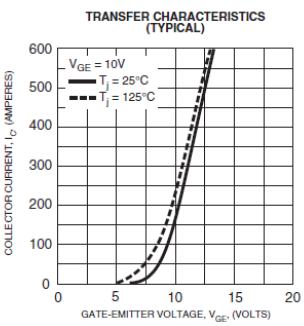

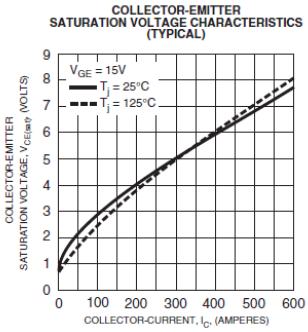

Absolute Maximum Ratings, T_j = 25 °C unless otherwise specified

Ratings	Symbol	CM300DU-24NF	Units
Junction Temperature	T_j	–40 to 150	°C
Storage Temperature	T_{stg}	–40 to 125	°C
Collector-Emitter Voltage (G-E Short)	V_{CES}	1200	Volts
Gate-Emitter Voltage (C-E Short)	V_{GES}	±20	Volts
Collector Current (T_C = 25°C)	I_C	300*	Amperes
Peak Collector Current	I_{CM}	600*	Amperes
Emitter Current** (T_C = 25°C)	I_E	300*	Amperes
Peak Emitter Current**	I_{EM}	600*	Amperes

Powerex, Inc., 173 Pavilion Lane, Youngwood, Pennsylvania 15697 (724) 925-7272

CM300DU-24NFH
Dual IGBTMOD™ NFH-Series Module
300 Amperes/1200 Volts

Thermal and Mechanical Characteristics, T_j = 25 °C unless otherwise specified

Characteristics	Symbol	Test Conditions	Min.	Typ.	Max.	Units
Thermal Resistance, Junction to Case	$R_{th(j-c)}Q$	Per IGBT 1/2 Module, T_C Reference Point per Outline Drawing	—	—	0.11	°C/W
Thermal Resistance, Junction to Case	$R_{th(j-c)}D$	Per FWDi 1/2 Module, T_C Reference Point per Outline Drawing	—	—	0.18	°C/W

Powerex, Inc., 173 Pavilion Lane, Youngwood, Pennsylvania 15697 (724) 925-7272

CM300DU-24NFH
Dual IGBTMOD™ NFH-Series Module
3 00 Amperes/1200 Volts

HALF-BRIDGE SWITCHING CHARACTERISTICS (TYPICAL)

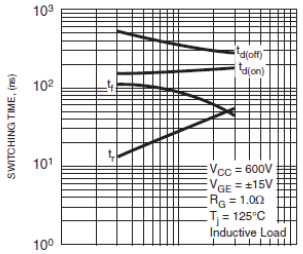

REVERSE RECOVERY CHARACTERISTICS (TYPICAL)

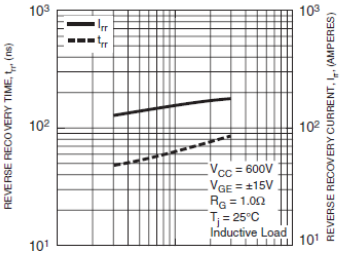

GATE CHARGE VS. V_{GE}

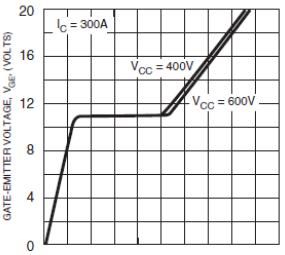

B- Case data input

B.1 Case 1: DP High

Case 1: DP High								
Component	**On [1 0]**	**Rated Power (kW)**	**Electric eff.**	**Hours**	**Amplitude (kW)**	**Frequency (kW)**	**Offset (kW)**	**Load Shape (kW)**
Generator1	1	2240	0,96	1402				
Generator2	1	2240	0,96	1402				
Generator3	1	2240	0,96	1402				
Generator4		2240	0,96	1402				
Generator5		940	0,96	1402				
Thruster1	1	950	0,96	1402	630	0,033333	630	sin
Thruster2	1	950	0,96	1402	630	0,033333	630	sin
Thruster3	1	880	0,94	1402	394	0,033333	394	sin
Thruster4		2200	0,96	1402				
Thruster5	1	2200	0,96	1402	712	0,033333	712	sin
Consumer1		1600	0,98	1402				
Consumer2	1	1250	0,98	1402			150	constant
Consumer3		1600	0,98	1402				
Consumer4	1	1250	0,98	1402			150	constant

B.2 Case 1: DP Low

Case 1: DP Low								
Component	**On [1 0]**	**Rated Power (kW)**	**Electric eff.**	**Hours**	**Amplitude (kW)**	**Frequency (kW)**	**Offset (kW)**	**Load Shape (kW)**
Generator1	1	2240	0,96	2803				
Generator2	1	2240	0,96	2803				
Generator3		2240	0,96	2803				
Generator4		2240	0,96	2803				
Generator5	1	940	0,96	2803				
Thruster1	1	950	0,96	2803	315	0,033333	315	sin
Thruster2	1	950	0,96	2803	315	0,033333	315	sin
Thruster3	1	880	0,94	2803	315	0,033333	315	sin
Thruster4		2200	0,96	2803				
Thruster5	1	2200	0,96	2803	720	0,033333	720	sin
Consumer1		1600	0,98	2803				
Consumer2	1	1250	0,98	2803			150	constant
Consumer3		1600	0,98	2803				
Consumer4	1	1250	0,98	2803			150	constant

B.3 Case 1: Anchor Handling

Case 1: Anchor Handling								
Component	**On [1 0]**	**Rated Power (kW)**	**Electric eff.**	**Hours**	**Amplitude (kW)**	**Frequency (kW)**	**Offset (kW)**	**Load Shape (kW)**
Generator1	1	2240	0,96	438				
Generator2	1	2240	0,96	438				
Generator3	1	2240	0,96	438				
Generator4	1	2240	0,96	438				
Generator5		940	0,96	438				
Thruster1	1	950	0,96	438	354	0,01	354	sin
Thruster2	1	950	0,96	438	354	0,01	354	sin
Thruster3	1	880	0,94	438	354	0,01	354	sin
Thruster4	1	2200	0,96	438			2250	constant
Thruster5	1	2200	0,96	438			2250	constant
Consumer1	1	1600	0,98	438			150	constant
Consumer2	1	1250	0,98	438			150	constant
Consumer3	1	1600	0,98	438			150	constant
Consumer4		1250	0,98	438				

B.4 Case 1: Harbor

Case 1: Harbor								
Component	**On [1 0]**	**Rated Power (kW)**	**Electric eff.**	**Hours**	**Amplitude (kW)**	**Frequency (kW)**	**Offset (kW)**	**Load Shape (kW)**
Generator1		2240	0,96	526				
Generator2		2240	0,96	526				
Generator3		2240	0,96	526				
Generator4		2240	0,96	526				
Generator5	1	940	0,96	526				
Thruster1		950	0,96	526				
Thruster2		950	0,96	526				
Thruster3		880	0,94	526				
Thruster4		2200	0,96	526				
Thruster5		2200	0,96	526				
Consumer1		1600	0,98	526				
Consumer2		1250	0,98	526				
Consumer3		1600	0,98	526				
Consumer4	1	1250	0,98	526			75	constant

B.5 Case 1: BP

Case 1: BP								
Component	**On [1 0]**	**Rated Power (kW)**	**Electric eff.**	**Hours**	**Amplitude (kW)**	**Frequency (kW)**	**Offset (kW)**	**Load Shape (kW)**
Generator1	1	2240	0,96	88				
Generator2	1	2240	0,96	88				
Generator3	1	2240	0,96	88				
Generator4	1	2240	0,96	88				
Generator5		940	0,96	88				
Thruster1	1	950	0,96	88			730	constant
Thruster2	1	950	0,96	88			730	constant
Thruster3	1	880	0,94	88			630	constant
Thruster4	1	2200	0,96	88			2200	constant
Thruster5	1	2200	0,96	88			2200	constant
Consumer1	1	1600	0,98	88			150	constant
Consumer2	1	1250	0,98	88			150	constant
Consumer3	1	1600	0,98	88			150	constant
Consumer4	1	1250	0,98	88			150	constant

B.6 Case 1: Transit towing

Case 1: Transit towing								
Component	**On [1 0]**	**Rated Power (kW)**	**Electric eff.**	**Hours**	**Amplitude (kW)**	**Frequency (kW)**	**Offset (kW)**	**Load Shape (kW)**
Generator1	1	2240	0,96	1314				
Generator2	1	2240	0,96	1314				
Generator3	1	2240	0,96	1314				
Generator4		2240	0,96	1314				
Generator5		940	0,96	1314				
Thruster1		950	0,96	1314				
Thruster2		950	0,96	1314				
Thruster3		880	0,94	1314				
Thruster4	1	2200	0,96	1314			2200	constant
Thruster5	1	2200	0,96	1314			2200	constant
Consumer1	1	1600	0,98	1314			99	constant
Consumer2	1	1250	0,98	1314			150	constant
Consumer3	1	1600	0,98	1314			99	constant
Consumer4	1	1250	0,98	1314			150	constant

B.7 Case 1: Transit supply

Case 1: Transit supply								
Component	**On [1 0]**	**Rated Power (kW)**	**Electric eff.**	**Hours**	**Amplitude (kW)**	**Frequency (kW)**	**Offset (kW)**	**Load Shape (kW)**
Generator1	1	2240	0,96	2190				
Generator2		2240	0,96	2190				
Generator3	1	2240	0,96	2190				
Generator4		2240	0,96	2190				
Generator5		940	0,96	2190				
Thruster1		950	0,96	2190				
Thruster2		950	0,96	2190				
Thruster3		880	0,94	2190				
Thruster4	1	2200	0,96	2190			1650	constant
Thruster5	1	2200	0,96	2190			1650	constant
Consumer1		1600	0,98	2190				
Consumer2	1	1250	0,98	2190			100	constant
Consumer3		1600	0,98	2190				
Consumer4	1	1250	0,98	2190			150	constant

B.8 Case 2: DP High

Case 2: DP High								
Component	**On [1 0]**	**Rated Power (kW)**	**Electric eff.**	**Hours**	**Amplitude (kW)**	**Frequency (kW)**	**Offset (kW)**	**Load Shape (kW)**
Generator1	1	2240	0,96	1402				
Generator2	1	2240	0,96	1402				
Generator3	1	2240	0,96	1402				
Generator4	1	2240	0,96	1402				
Generator5		940	0,96	1402				
Thruster1	1	950	0,96	1402	315	0,033333	315	sin
Thruster2	1	950	0,96	1402	315	0,033333	315	sin
Thruster3	1	880	0,94	1402	450	0,033333	450	sin
Thruster4	1	2200	0,96	1402	712	0,033333	712	sin
Thruster5	1	2200	0,96	1402	712	0,033333	712	sin
Consumer1		1600	0,98	1402				
Consumer2	1	1250	0,98	1402			300	constant
Consumer3		1600	0,98	1402				
Consumer4	1	1250	0,98	1402			300	constant

B.9 Case 2: DP Low

Case 2: DP Low								
Component	**On [1 0]**	**Rated Power (kW)**	**Electric eff.**	**Hours**	**Amplitude (kW)**	**Frequency (kW)**	**Offset (kW)**	**Load Shape (kW)**
Generator1	1	2240	0,96	2803				
Generator2	1	2240	0,96	2803				
Generator3		2240	0,96	2803				
Generator4		2240	0,96	2803				
Generator5	1	940	0,96	2803				
Thruster1		950	0,96	2803				
Thruster2	1	950	0,96	2803	315	0,033333	315	sin
Thruster3	1	880	0,94	2803	315	0,033333	315	sin
Thruster4		2200	0,96	2803				
Thruster5	1	2200	0,96	2803	720	0,033333	720	sin
Consumer1		1600	0,98	2803				
Consumer2	1	1250	0,98	2803			100	constant
Consumer3	1	1600	0,98	2803			400	constant
Consumer4	1	1250	0,98	2803			300	constant

B.10 Case 2: Anchor Handling

Case 2: Anchor Handling								
Component	**On [1 0]**	**Rated Power (kW)**	**Electric eff.**	**Hours**	**Amplitude (kW)**	**Frequency (kW)**	**Offset (kW)**	**Load Shape (kW)**
Generator1	1	2240	0,96	438				
Generator2	1	2240	0,96	438				
Generator3	1	2240	0,96	438				
Generator4	1	2240	0,96	438				
Generator5		940	0,96	438				
Thruster1	1	950	0,96	438	354	0,01	354	sin
Thruster2	1	950	0,96	438	354	0,01	354	sin
Thruster3		880	0,94	438				
Thruster4	1	2200	0,96	438			2250	constant
Thruster5	1	2200	0,96	438			2250	constant
Consumer1		1600	0,98	438				
Consumer2	1	1250	0,98	438			100	constant
Consumer3	1	1600	0,98	438			400	constant
Consumer4	1	1250	0,98	438			300	constant

B.11 Case 2: Harbor

Case 2: Harbor								
Component	**On [1 0]**	**Rated Power (kW)**	**Electric eff.**	**Hours**	**Amplitude (kW)**	**Frequency (kW)**	**Offset (kW)**	**Load Shape (kW)**
Generator1		2240	0,96	526				
Generator2		2240	0,96	526				
Generator3		2240	0,96	526				
Generator4		2240	0,96	526				
Generator5	1	940	0,96	526				
Thruster1		950	0,96	526				
Thruster2		950	0,96	526				
Thruster3		880	0,94	526				
Thruster4		2200	0,96	526				
Thruster5		2200	0,96	526				
Consumer1		1600	0,98	526				
Consumer2	1	1250	0,98	526	150	0,033333	300	sin
Consumer3	1	1600	0,98	526			75	constant
Consumer4	1	1250	0,98	526	50	0,033333	100	sin

B.12 Case 2: BP

Case 2: BP								
Component	**On [1 0]**	**Rated Power (kW)**	**Electric eff.**	**Hours**	**Amplitude (kW)**	**Frequency (kW)**	**Offset (kW)**	**Load Shape (kW)**
Generator1	1	2240	0,96	88				
Generator2	1	2240	0,96	88				
Generator3	1	2240	0,96	88				
Generator4	1	2240	0,96	88				
Generator5		940	0,96	88				
Thruster1	1	950	0,96	88			730	constant
Thruster2	1	950	0,96	88			730	constant
Thruster3	1	880	0,94	88			630	constant
Thruster4	1	2200	0,96	88			2200	constant
Thruster5	1	2200	0,96	88			2200	constant
Consumer1	1	1600	0,98	88			150	constant
Consumer2	1	1250	0,98	88			150	constant
Consumer3	1	1600	0,98	88			150	constant
Consumer4	1	1250	0,98	88			150	constant

B.13 Case 2: Transit towing

Case 2: Transit towing								
Component	**On [1 0]**	**Rated Power (kW)**	**Electric eff.**	**Hours**	**Amplitude (kW)**	**Frequency (kW)**	**Offset (kW)**	**Load Shape (kW)**
Generator1	1	2240	0,96	1314				
Generator2	1	2240	0,96	1314				
Generator3	1	2240	0,96	1314				
Generator4	1	2240	0,96	1314				
Generator5		940	0,96	1314				
Thruster1		950	0,96	1314				
Thruster2		950	0,96	1314				
Thruster3	1	880	0,94	1314	354	0,01	354	sin
Thruster4	1	2200	0,96	1314			2200	constant
Thruster5	1	2200	0,96	1314			2200	constant
Consumer1	1	1600	0,98	1314			99	constant
Consumer2	1	1250	0,98	1314			150	constant
Consumer3	1	1600	0,98	1314			99	constant
Consumer4	1	1250	0,98	1314			150	constant

B.13 Case 2: Transit supply

Case 2: Transit supply								
Component	**On [1 0]**	**Rated Power (kW)**	**Electric eff.**	**Hours**	**Amplitude (kW)**	**Frequency (kW)**	**Offset (kW)**	**Load Shape (kW)**
Generator1	1	2240	0,96	2190				
Generator2		2240	0,96	2190				
Generator3	1	2240	0,96	2190				
Generator4		2240	0,96	2190				
Generator5		940	0,96	2190				
Thruster1		950	0,96	2190				
Thruster2		950	0,96	2190				
Thruster3	1	880	0,94	2190				
Thruster4	1	2200	0,96	2190			1650	constant
Thruster5	1	2200	0,96	2190			1650	constant
Consumer1		1600	0,98	2190				
Consumer2	1	1250	0,98	2190			150	constant
Consumer3		1600	0,98	2190				
Consumer4	1	1250	0,98	2190			150	constant

C- Lifetime calculations

a, b, C and D are known values.

I: $\text{Cycles}_0 \cdot e^{\lambda \cdot a} = C$

II: $\text{Cycles}_0 \cdot e^{\lambda \cdot b} = D$

Solving I for Cycles_0

I: $\text{Cycles}_0 = \frac{C}{e^{\lambda \cdot a}}$

Inserting I ⇒ II

$$\text{II: } \frac{C}{e^{\lambda \cdot a}} \cdot e^{\lambda \cdot b} = D \quad \Rightarrow \quad e^{\lambda \cdot b - \lambda \cdot a} = \left(\frac{D}{C}\right) \quad \Rightarrow \quad \lambda \cdot (b-a) = l\,n\left(\frac{D}{C}\right) \quad \Rightarrow \quad \lambda = \frac{l\,n\left(\frac{D}{C}\right)}{(b-a)}$$

To summaries, a solution for the unknown Cycles_0 and λ yealds:

$$\text{Cycles}_0 = \frac{C}{e^{\lambda \cdot a}} \quad , \quad \lambda = \frac{l\,n\left(\frac{D}{C}\right)}{(b-a)}$$

D- Single line diagram of the reference vessel

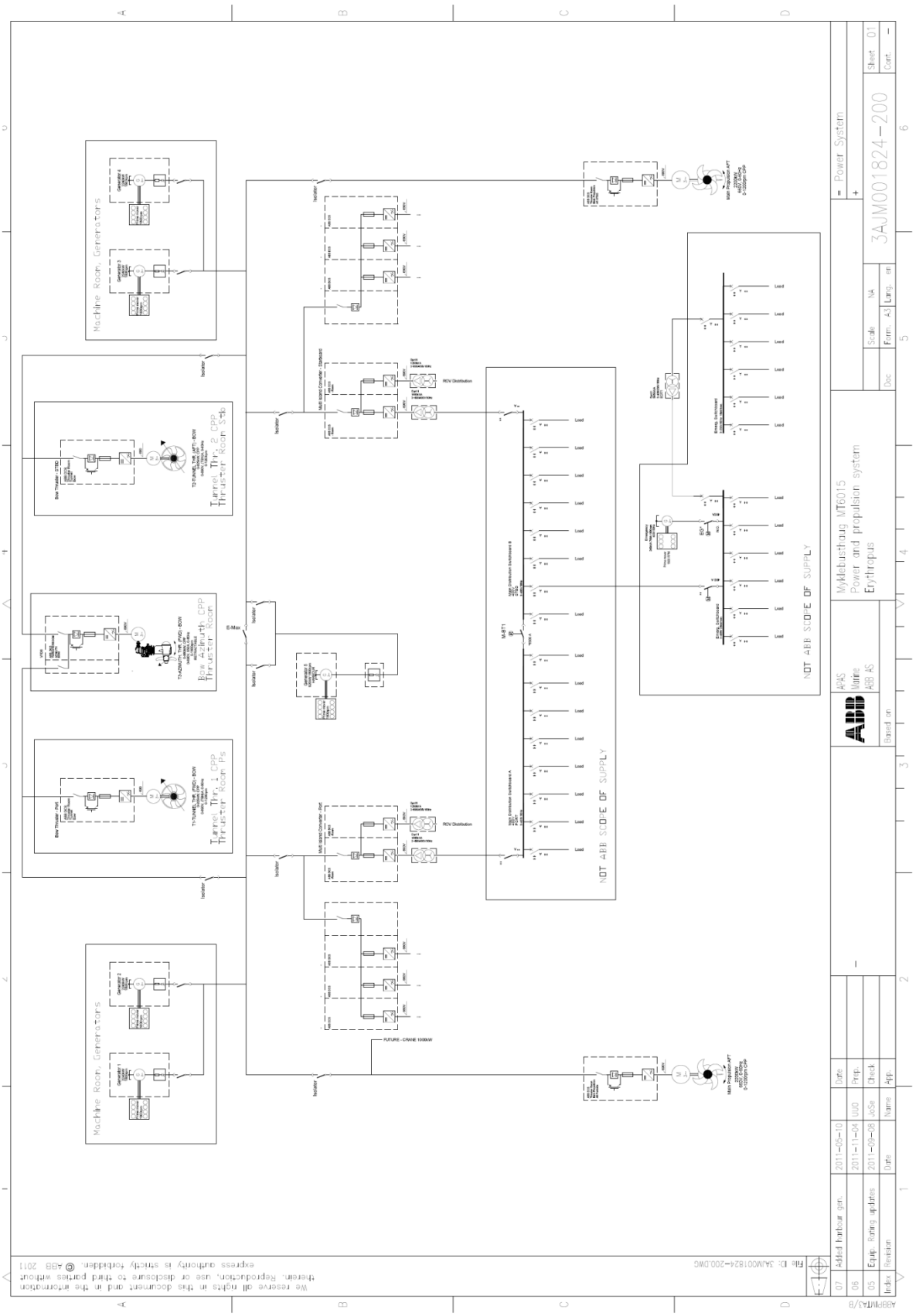

E- MATLAB program

E.1 Input function

```
%%                        INPUT FUNCTION
%*************************************************************************
%*************************************************************************
%-------------------------------------------------------------------------
%    Function:       Load_input.m
%    Description:    Subroutine for sorting and retrieving the information
%                    given in input.xls file.
%                    Some of the sorting procedures are dependent on
%                    the power management strategy selected.
%                    The information is to be used in the DC_BUS_FLOW.m
%                    calculations.
%                    The load-frequency, operation time, fuel graph and
%                    control limits are equal for all components, during
%                    each load operation mode.
%                    Transient fuel consumption is not accounted for and
%                    all bus ties are assumed closed.
%    Version:        2.0
%    Target:         Input.xls,DC_BUS_FLOW.m
%    Type:           Input and sorting script
%    Copyright       ABB
%    Date:           April 2012



function [t_end,totthrusoffset,totconsumeroffset,totthrusamplitude,...
        totconsumeramlitude,frequency,totgenpower,load_amplitude_comb,...
        load_offset_comb,totgenpower_NO_ES]=Load_input(alpha,...
        bravo,generator,thruster,consumer,gen,thrus,cons,frequency,...
        opmodes,charlie,ES_Combined,load_amplitude_comb,load_offset_comb)







%%   Gets data from Exel and sorts numbers and strings in matrixes
%*************************************************************************
%*************************************************************************


% Gets data and string information from Excel.
[data textmatr] = xlsread('Input');



%***********************Generators*****************************************


     for g = 1:8
          on=str2num (char(textmatr(g+3, 8+7*opmodes)));
```

```
        if ~isempty(on) %If a generators is on

         alpha=1+alpha;% Matrix count.
        gen(alpha,1)=data(g,1); % Bus.
        gen(alpha,2)=data(g,2); % Power.
        gen(alpha,3)=data(g,4); % Efficiency.
        gen(alpha,4)=data(g,5); % Transient fuel consumption.
        gen(alpha,5)=data(g,12+7*(-1+opmodes));% Hours.
        gen(alpha,9)=on(1,1);% Connection value for bus 1.
        gen(alpha,10)=on(1,2);% Connection value for bus 2.
        t_end=gen(alpha,5);% Operation time for calculations when assuming
                           % same time for all loads.

        %Creates generator matrix.
        eval(['generator' ' = gen']);

        end

    end


%*************Thrusters*****************************************************


    for th = 9:16
          on=str2num (char(textmatr(th+3, 8+7*opmodes)));


        if ~isempty(on) %If a thruster is on.

        bravo=1+bravo;% Matrix count.

        % Type of load.
        loadshape=textmatr(th+3, 9+7*opmodes);

        thrus(bravo,1)=data(th,1); % Bus.
        thrus(bravo,2)=data(th,2); % Power.
        thrus(bravo,3)=data(th,4); % Efficiency.
        thrus(bravo,4)=data(th,12+7*(-1+opmodes));% Hours.
        thrus(bravo,9)=on(1,1);% Connection value for bus 1.
        thrus(bravo,10)=on(1,2);% Connection value for bus 2.


        if strcmp(loadshape,'sin')==1
            thrus(bravo,5)=data(th,9+7*(-1+opmodes));% Amplitude.
            thrus(bravo,6)=data(th,10+7*(-1+opmodes));% Frequency.
            thrus(bravo,7)=data(th,11+7*(-1+opmodes));% Offset.
            frequency=thrus(bravo,6);% Frequency for calculations when
                                     % assuming same frequency for all
                                     % loads.

         elseif strcmp(loadshape,'constant')==1
        thrus(bravo,5)=0;% Amplitude.
        thrus(bravo,6)=0;% Frequency.
        thrus(bravo,7)=data(th,11+7*(-1+opmodes)); Offset.
```

```
        else
            thrus(bravo,5)=0; Amplitude.
            thrus(bravo,6)=0; Frequency.
            thrus(bravo,7)=0; Offset.

        end

        eval(['thruster'  ' = thrus']);

        end
    end


%*********Consumers*************************************************************

    for c = 17:20

      on=str2num (char(textmatr(c+3, 8+7*opmodes)));

        if ~isempty(on) %If a consumer is on.

           charlie=1+charlie;% Matrix counter.

           % Type of load.
           loadshape=textmatr(c+3, 9+7*opmodes);
           cons(charlie,1)=data(c,1); % Bus.
           cons(charlie,2)=data(c,2); % Power.
           cons(charlie,3)=data(c,4); % Efficiency.
           cons(charlie,4)=data(c,12+7*(-1+opmodes));% Hours.
           cons(charlie,9)=on(1,1);% Connection value for bus 1.
           cons(charlie,10)=on(1,2);% Connection value for bus 2.


           if strcmp(loadshape,'sin')==1
               cons(charlie,5)=data(c,9+7*(-1+opmodes));% Amplitude.
               cons(charlie,6)=data(c,10+7*(-1+opmodes));% Frequency.
               cons(charlie,7)=data(c,11+7*(-1+opmodes));% Offset.
               frequency=cons(charlie,6);% Frequency for calculations when
                                         % assuming same frequency for all
                                         % loads.

           elseif strcmp(loadshape,'constant')==1
               cons(charlie,5)=0;% Amplitude.
               cons(charlie,6)=0;% Frequency.
               cons(charlie,7)=data(c,11+7*(-1+opmodes));% Offset.

           else
               cons(charlie,7)=0;% Offset.
               cons(charlie,5)=0;% Amplitude.
               cons(charlie,6)=0;% Frequency.

           end

           eval(['consumer'  ' = cons']);

        end

    end
```

```
%%        Combining loads and DG's from the EXCEL configuration
%*****************************************************************
%*****************************************************************


     totgenpower=0;% Total DG with ES power.
     totthrusoffset=0;% Total thruster offset variable.
     totthrusamplitude=0;% Total thruster amplitude variable.
     totconsumeroffset=0;% Total consumer offset variable.
     totconsumeramlitude=0;% Total consumer amplitude variable.
     totgenpower_NO_ES=0;


%****Summing_power_deliverd_from_generators_and_subtrackt_the_efficienc****

          for sum_g=1:alpha

               % Summing total generators and subtracts efficiency.
            if ((generator(sum_g,9)==1) && (generator(sum_g,10)==1));

                 genpower_NO_ES= (generator(sum_g,2)...
                     *generator(sum_g,3))*1e3;

                %Total gen power
                totgenpower_NO_ES=genpower_NO_ES+totgenpower_NO_ES;

             end

            end


%*************Summing_thruster_loads_and_adds_the_efficiency**************

            for sum_t=1:bravo

                if ((thruster(sum_t,9)==1) && (thruster(sum_t,10)==1));

              % Summing total thruster offset and adds efficiency.
                     thrusoffset=(thruster(sum_t,7)/thruster(sum_t,3))*1e3;
                      totthrusoffset=thrusoffset+totthrusoffset;

              % Summing total thruster amplitude and adds efficiency.
                   thrusamplitude=(thruster(sum_t,5)/thruster(sum_t,3))*1e3;
                     totthrusamplitude=thrusamplitude+totthrusamplitude;

                end

            end


%********summing_consumers_and_subtrackts_the_efficiency******************

            for sum_c=1:charlie
```

```
            if ((consumer(sum_c,9)==1) && (consumer(sum_c,10)==1));

              % Summing total consumer offset and adds efficiency.
              consoffset=((consumer(sum_c,7))/(consumer(sum_c,3)))*1e3;
              totconsumeroffset=consoffset+totconsumeroffset;

              % Summing total consumer amplitude and adds efficiency
              consamplitude=((consumer(sum_c,5)/consumer(sum_c,3)))*1e3;
              totconsumeramlitude=consamplitude+ totconsumeramlitude;

            end

        end

%****Summing_power_deliverd_from_generators_and_subtrackt_the_efficienc****

        for sum_ges=1:alpha

            % Summing total generators and subtracts efficiency.
          if ((generator(sum_ges,9)==1) && (generator(sum_ges,10)==1));
              genpower= (generator(sum_ges,2)*generator(sum_ges,3))*1e3;

               % Removes the first DG in the Excel sheet
               % since the combined ES is replacing one during load
               % sharing.

               if ES_Combined==1 && sum_ges==1
                 genpower= 0;

               end

               load_ratio=((totconsumeroffset+totthrusoffset)/...
                          (genpower+totgenpower));

               % Removes all the excess DG's which deviates from an 0.8
               % loading ratio, during peak shaving.

               if ES_Combined==0
                   % If the DG loading ratio gets too low, the DG stays
                   % on.

                   if load_ratio<= 0.5 && sum_ges>1

                   genpower=0;

                   end

               end

             totgenpower=genpower+totgenpower;  % Total generator power.

          end

        end
```

```
            % If there is only one DG available.
            if sum_ges==1

                totgenpower=totgenpower_NO_ES;

            end



%***the_load_amplitude_and_offset_the_ES_needs_to_supply_in_load_sharing***

             if ES_Combined==1

                    load_amplitude_comb=...
                        (totconsumeramlitude+totthrusamplitude)/alpha ;
                    load_offset_comb=...
                        (totconsumeroffset+totthrusoffset)/alpha;

             end

             if ES_Combined==0

                 load_amplitude_comb=0;
                 load_offset_comb=0;

             end



%**********************Clears_the_variables_not_needed**********************


            clearvars -except t_end totthrusoffset ...
                totconsumeroffset totthrusamplitude totconsumeramlitude...
                frequency totgenpower load_amplitude_comb...
                load_offset_comb totgenpower_NO_ES
```

E.2 Dimension function

```
%%                        DIMENSION FUNCTION
%*************************************************************************
%*************************************************************************
%-------------------------------------------------------------------------
--------
%   Function:       Dimensioning.m
%   Description:    Sums the load requirements from the input function
%                   while calculating and adding converter losses.
%                   Then the function calculates the required number of
%                   energy storage cabinets for a given load operation
%                   mode. The calculations are dependent on the maximum
%                   value of energy storage cabinets allowed.
%   Version:        1.0
%   Target:         DC_BUS_FLOW.m
%   Type:           Dimensioning script
%   Copyright       ABB
%   Date:           April 2012


function [NR_BattCab_MAX,NR_SCCab_MAX,Batt_MAX_t,SC_MAX_t] =
Dimensioning...
    (t_start,sample,t_end,totthrusoffset,totconsumeroffset,...
    totthrusamplitude,totconsumeramlitude,ES_Combined,PBload_dis,...
    IbussB,ESCload_dis,NrBcellseries,NrBcellparallell,VBatMod,Vbuss,...
    NrSCcellparallell,VSCMod,SOCB_car,SOCB_MAX_CONSTR,SOCB_MIN_CONSTR,...
    IBmodule_MAX_Dis,IBmodule_MAX_Cha,SOCSC_car,SOCSC_MAX_CONSTR,...
    SOCSC_MIN_CONSTR,ISCmodule_MAX_Dis,ISCmodule_MAX_Cha,ResrB,ResrSC,...
    PollyEswo,PollyEswf,
PollyEswd,Vtest,Induct_ripple,Induct_loss,SOC_B,...
    SOCmodB,CBcell,PollyBatV,CSC,Vcabinet,SOCmodC,PBload_MAX_dis,...
    EBload_MAX_dis,PBload_MAX_cha,PBload_cha,fsw,...
    PBmodule_dis,EBmodule_dis,PBmodule_cha,NR_BattCab_MAX,MAX_BCab,...
    EBload_dis,ESCcounter,ESCload_MAX_dis,NR_SCCab_MAX,VSCMod_MAX,...
    MAX_SCCab,Dummy_var_Batt_MAX,Dummy_var_SC_MAX,SOCmodB_COMBINED_ES,...
    frequency,load_amplitude_comb,load_offset_comb,...
    ISCmodule_MAX_Dis_when_cha,IBmodule_MAX_Dis_when_cha,PSCmodule_dis,...
    Batt_coloumb_eff,PSCload_MAX_dis,ChargeVBatMod)


%%             CALCULATION FOR DIMENSIONING BATTERY OR SC.
%*************************************************************************
%*************************************************************************

klo=0;
tic

for t=t_start:sample:t_end;

klo=klo+1; % Counter for various operations:

%*************************setup_of_ES_current_request*********************


% Peak shaving.
if ES_Combined==0
```

```
    % Total load power.
    load=((totthrusoffset+totconsumeroffset)+...
    (totthrusamplitude+totconsumeramlitude)...
    *sin(2*pi*frequency*(t)*60*60));
    I=(load-(totthrusoffset+totconsumeroffset))/Vbuss;% Current variation
    IB=I;                                          % determined by the power.
    ISC=I;

end

 % Load sharing.
if ES_Combined==1

    I=(load_offset_comb+((load_amplitude_comb)*sin(2*pi*frequency*...
        (t)*60*60)))/Vbuss;
    IB=(load_offset_comb/Vbuss);
    ISC=((load_amplitude_comb)*sin(2*pi*frequency*(t)*60*60))/Vbuss;

end


%**********************Duty_cycle_batteries*******************************

DBbu=VBatMod/Vbuss; % Duty cycle on.
DBbo=1-DBbu; % Duty cycle off.

%**********************Duty_cycle_SC**************************************

DSCbu=VSCMod/Vbuss; % Duty cycle on.
DSCbo=1-DSCbu; % Duty cycle off.

%**********************currents_Battery***********************************

NBcab=NR_BattCab_MAX;

% Total current request from each module on the bus side.
IBmodule=IB/NBcab;

% Activates dummy variable if the battery is full.
if SOCmodB>=SOCB_MAX_CONSTR

        SOCB_car=0;

end

% Deactivates dummy variable if the battery is empty.
if SOCmodB<SOCB_MIN_CONSTR

    SOCB_car=1;

end



% Current request from a cabinet when the battery is not empty:
if SOCB_car<1;
```

```
    if IBmodule<=0 % During charge
        IESB=IBmodule*(1/DBbu);

        if IESB<-IBmodule_MAX_Cha*NrBcellparallell
            IESB=-IBmodule_MAX_Cha*NrBcellparallell;

        end

        IbussB=IESB*DBbu; % Output from DC-DC converter.

    end

    if IBmodule>0% For batteries during discharge.

        IESB=IBmodule*(1/DBbu);
        if IESB>IBmodule_MAX_Dis*NrBcellparallell

            IESB=IBmodule_MAX_Dis*NrBcellparallell;

        end

        IbussB=IESB*DBbu; % Output from DC-DC converter.

    end

end


% Peak shaving
if ES_Combined==0

% Current request from a cabinet when the battery is empty.
    if SOCB_car>0;

        if IBmodule>0 % Discharge modus.

            IESB=IBmodule*(1/DBbu);

            if IESB>IBmodule_MAX_Dis_when_cha*NrBcellparallell

            IESB=IBmodule_MAX_Dis_when_cha*NrBcellparallell;

            end

            IbussB=IESB*DBbu;% Output from converter.
        end

        if IBmodule<=0 % Only charge modus.

            IESB=IBmodule*(1/DBbu);
            if IESB<-IBmodule_MAX_Cha*NrBcellparallell

                IESB=-IBmodule_MAX_Cha*NrBcellparallell;

            end
```

```
            IbussB=IESB*DBbu; % Output from DC-DC converter.
        end

    end

end


% If battery and SC is combined.
if ES_Combined==1

% Current request from a cabinet when the battery is empty.
    if SOCB_car>0;

      IESB=0;
      IbussB=0;
      SOCmodB=SOCmodB_COMBINED_ES;
      SOCB_car=0;

    end

end


%**********************currents_SC*****************************************

% NSCcab gets new value.
NSCcab=NR_SCCab_MAX;
% Total current request from each module on the bus side.
ISCmodule=ISC/NSCcab;


% Activates dummy variable if the SC is full:
if SOCmodC>=SOCSC_MAX_CONSTR

        SOCSC_car=0;

end

% Deactivates dummy variable if the SC is empty.
if SOCmodC<SOCSC_MIN_CONSTR

    SOCSC_car=1;

end


% Current request from a cabinet when the SC is not empty.
if SOCSC_car<1;

    % For SC charging.
    if ISCmodule<=0

        IESSC=ISCmodule*(1/DSCbu);

        if IESSC<-ISCmodule_MAX_Cha*NrSCcellparallell
```

```
            IESSC=-ISCmodule_MAX_Cha*NrSCcellparallell;

        end

        IbussSC=IESSC*DSCbu; % Output from DC-DC converter.

    end

    % For SC discharge.
    if ISCmodule>0% For SC discharge.

        IESSC=ISCmodule*(1/DSCbu);

        if IESSC>ISCmodule_MAX_Dis*NrSCcellparallell

            IESSC=ISCmodule_MAX_Dis*NrSCcellparallell;

        end

        IbussSC=IESSC*DSCbu; % Output from converter.

    end

end




% Current request from a cabinet when the SC is empty.
if SOCSC_car>0;

    if ISCmodule>0% For SC discharge.

        IESSC=ISCmodule*(1/DSCbu);

        if IESSC>ISCmodule_MAX_Dis_when_cha*NrSCcellparallell

             % The maximum charging current when in charging mode.
            IESSC=ISCmodule_MAX_Dis_when_cha*NrSCcellparallell;

        end

       IbussSC=IESSC*DSCbu; % Output from converter.

    end

    if ISCmodule<=0 % Only charge.
        IESSC=ISCmodule*(1/DSCbu);

        if IESSC<-ISCmodule_MAX_Cha*NrSCcellparallell
            IESSC=-ISCmodule_MAX_Cha*NrSCcellparallell;

        end

        IbussSC=IESSC*DSCbu; % Output from converter.
```

```
    end

end



%**********************DC_DC_Converter+ES_efficiency**********************


% RMS Currents.
IESB_RMS=sqrt(IESB^2+(((IESB*Induct_ripple)^2)/3));
IESSC_RMS=sqrt(IESSC^2+(((IESSC*Induct_ripple)^2)/3));


% Inductor battery currents buck.
IonBbu_max=(((1+(Induct_ripple/2))*abs(IbussB))*sqrt(DBbu/3));% IGBT
Current.
IonBbu_min=(((1-(Induct_ripple/2))*abs(IbussB))*sqrt(DBbo/3));% IGBT
Current.
IdBbu_max=(((1-(Induct_ripple/2))*abs(IESB))*sqrt(DBbo/3)); % Diode
current.
IdBbu_min=(((1+(Induct_ripple/2))*abs(IESB))*sqrt(DBbu/3)); % Diode
current.

% Inductor battery currents boost.

IonBbo_max=(((1+(Induct_ripple/2))*abs(IbussB))*sqrt(DBbo/3));% IGBT
Current.
IonBbo_min=(((1-(Induct_ripple/2))*abs(IbussB))*sqrt(DBbu/3));% IGBT
Current.
IdBbo_max=(((1-(Induct_ripple/2))*abs(IESB))*sqrt(DBbu/3)); % Diode
current.
IdBbo_min=(((1+(Induct_ripple/2))*abs(IESB))*sqrt(DBbo/3)); % Diode
current.


% Inductor battery RMS currents buck.
if IESB<0

    IonB_RMS=IonBbu_max+IonBbu_min;
    IdB_RMS=IdBbu_max+IdBbu_min;

else

    % Inductor battery RMS currents boost.
    IonB_RMS=IonBbo_max+IonBbo_min;
    IdB_RMS=IdBbo_max+IdBbo_min;

end


% Inductor SC currents buck.
IonSCbu_max=(((1+(Induct_ripple/2))*abs(IbussSC))*sqrt(DSCbu/3));%IGBT
                                                                  %Current.
IonSCbu_min=(((1-(Induct_ripple/2))*abs(IbussSC))*sqrt(DSCbo/3));%IGBT
                                                                  %Current.
IdSCbu_max=(((1-(Induct_ripple/2))*abs(IESSC))*sqrt(DSCbo/3)); %Diode
                                                               %Current.
```

```
IdSCbu_min=(((1+(Induct_ripple/2))*abs(IESSC))*sqrt(DSCbu/3)); %Diode
                                                               %Current.


% Inductor SC currents boost.
IonSCbo_max=(((1+(Induct_ripple/2))*abs(IbussSC))*sqrt(DSCbo/3)); %IGBT
                                                                  %Current.
IonSCbo_min=(((1-(Induct_ripple/2))*abs(IbussSC))*sqrt(DSCbu/3)); %IGBT
                                                                  %Current.
IdSCbo_max=(((1-(Induct_ripple/2))*abs(IESSC))*sqrt(DSCbu/3)); %Diode
                                                               %Current.
IdSCbo_min=(((1+(Induct_ripple/2))*abs(IESSC))*sqrt(DSCbo/3)); %Diode
                                                               %Current.


% Inductor SC RMS currents buck.
if IESSC<0

    IonSC_RMS=IonSCbu_max+IonSCbu_min;
    IdSC_RMS=IdSCbu_max+IdSCbu_min;

else

    % Inductor SC RMS currents boost.
    IonSC_RMS=IonSCbo_max+IonSCbo_min;
    IdSC_RMS=IdSCbo_max+IdSCbo_min;

end


% Look up table for switch losses in each ES module:

% Battery switch loss with a voltage correction.
EswoB=polyval(PollyEswo,abs(IbussB))*(Vbuss/Vtest);
EswfB=polyval(PollyEswf,abs(IbussB))*(Vbuss/Vtest);
EswdB=polyval(PollyEswd,abs(IESB))*(Vbuss/Vtest);
% SC switch loss with a voltage correction.
EswoSC=polyval(PollyEswo,abs(IbussSC))*(Vbuss/Vtest);
EswfSC=polyval(PollyEswf,abs(IbussSC))*(Vbuss/Vtest);
EswdSC=polyval(PollyEswd,abs(IESSC))*(Vbuss/Vtest);


% Battery conduction loss.
VonB=(1+(0.01167)*IonB_RMS);
VdB=(1+(4.827*1e-3)*IdB_RMS);

% SC conduction loss.
VonSC=(1+(0.01167)*IonSC_RMS);
VdSC=(1+(4.827*1e-3)*IdSC_RMS);

% Power loss in inductor.
Pind_lossB=(Vbuss)*abs(IbussB)*Induct_loss;
Pind_lossSC=(Vbuss)*abs(IbussSC)*Induct_loss;

% Total Efficiency for Batteries.
PBloss=(VonB*IonB_RMS)+(VdB*IdB_RMS)+ Pind_lossB +...
    ((EswoB+EswfB+EswdB)*fsw);
NefB=(VBatMod*abs(IESB)/((VBatMod*abs(IESB)+PBloss)));
```

```
% Total Efficiency for SC's.
PSCloss=(VonSC*IonSC_RMS)+(VdSC*IdSC_RMS) + Pind_lossSC +...
    ((EswoSC+EswfSC+EswdSC)*fsw);
NefSC=(VSCMod*abs(IESSC)/((VSCMod*abs(IESSC)+PSCloss)));



%**********************Voltages_and_soc_battery*****************************

% Battery SOC.
if IESB<=0 % Efficiency is added and.

        SOC_B=(((-IESB*sample*NefB*Batt_coloumb_eff)/...
            (CBcell*NrBcellparallell))+SOC_B);

else

        SOC_B=(((-IESB*sample)/(CBcell*NrBcellparallell))+SOC_B);

end

SOCmodB=SOC_B;


% Limits if there are no SOC MAX_MIN Interval(can be ignored).

if SOCmodB<=0 % Min. SOC.

    SOCmodB=0;

end

if SOCmodB>1 % Max. SOC.

    SOCmodB=1;

end


% Battery cabinet voltage where the voltage drop of the
% internal resistance is subtracted.

if IESB<=0

    VBatMod= ChargeVBatMod;

    else

    VBatMod=(polyval(PollyBatV,SOCmodB))*NrBcellseries -(ResrB*abs(IESB));

end
```

```
%**********************Voltages_and_soc_SC*********************************

%New voltage

if IESSC<=0 % While in buck, efficiency is added and the voltage drop

            % of the internal resistance is subtracted.
        VSCMod=sqrt((VSCMod)^2-
((2*VSCMod_MAX*IESSC*sample*(NefSC)*60*60)...
            /CSC*NrSCcellparallell))+(IESSC*ResrSC);


else % While in boost, voltage drop

     % of the internal resistance is subtracted.
    VSCMod=sqrt((VSCMod)^2-((2*VSCMod*IESSC*sample*60*60)...
        /CSC*NrSCcellparallell))-(IESSC*ResrSC);
end


% Limits if there are no SOC MAX/MIN Interval(can be ignored).
if imag(VSCMod)~=0% Complex voltage.

    VSCMod=0;

end

if VSCMod>Vcabinet % Overcharged

    VSCMod=Vcabinet;

end

% SC SOC.
SOCmodC=VSCMod/Vcabinet;




%******************Sizing_number_of_Battery_modules**********************

% Peak shaving.
if ES_Combined==0

% Finding new values from load discharge power/energy.
    if IESB>=0

    PBload_dis=(IB*Vbuss+(PBloss*NR_BattCab_MAX));

EBload_dis=((IB*Vbuss+(PBloss*NR_BattCab_MAX))*sample*60*60)+EBload_dis;

    end


    % Finding new values from load charge energy.
    if IESB<0
```

```
    PBload_cha=abs(IB*Vbuss)+(PBloss*NR_BattCab_MAX);
    EBload_dis=0;

    end

end


% Load sharing.
if ES_Combined==1

        EBload_dis=((IB*Vbuss+(PBloss*NR_BattCab_MAX))...
        *sample*60*60)+EBload_dis;

end


% Finding new max values from load discharge power.

if PBload_dis>PBload_MAX_dis

    PBload_MAX_dis=PBload_dis;

end

% Finding new max values from load discharge energy.

if EBload_dis>EBload_MAX_dis

    EBload_MAX_dis=EBload_dis;

end

% Finding new max values from load charge power.

if PBload_cha>PBload_MAX_cha

    PBload_MAX_cha=PBload_cha;

end


% Peak shaving.
if ES_Combined==0

    % Maximum Nr modules with respect to discharging power.
    Nrbatmod(1)=PBload_MAX_dis/(PBmodule_dis);

    % Maximum Nr modules with respect to discharging energy.
    Nrbatmod(2)=EBload_MAX_dis/(EBmodule_dis...
        *(SOCB_MAX_CONSTR-SOCB_MIN_CONSTR));

    % Maximum Nr modules with respect to charging power.
    Nrbatmod(3)=PBload_MAX_cha/(PBmodule_cha);
```

```
    % Finding MAX Nr of battery modules.
    NR_BattCab=max(Nrbatmod);


% Stores max number of cabinets.
    if NR_BattCab>NR_BattCab_MAX

      NR_BattCab_MAX=NR_BattCab;

    end

end


% Load sharing.
if ES_Combined==1

    % Maximum Nr modules with respect to discharging energy.
    NR_BattCab=EBload_MAX_dis/(EBmodule_dis*...
        (SOCB_MAX_CONSTR-SOCB_MIN_CONSTR));

        if NR_BattCab>NR_BattCab_MAX

            NR_BattCab_MAX=NR_BattCab;

        end

end



% Exceeding maximum allowed cabinets.
if NR_BattCab_MAX>=MAX_BCab

    NR_BattCab_MAX=MAX_BCab; % Assigning max value.

end



% Assigning a value to Batt_MAX_t for preventing error when the
% limit is not exceeded.
if NR_BattCab_MAX<MAX_BCab

    Batt_MAX_t=0;

end

% Stores the time when the battery exceeds its limits.
if NR_BattCab_MAX>=MAX_BCab && Dummy_var_Batt_MAX<=0

    Batt_MAX_t=klo*sample;% Time of max value.
    Dummy_var_Batt_MAX=1;% Dummy variable for preventing the
                         % value to be changed.

end
```

```
%******************Sizing_number_of_SC_modules*****************************


% Peak shaving and load sharing.
if ES_Combined==0 || ES_Combined==1

    if IESSC>=0

    ESCcounter=ESCcounter+1;
    ESCload_dis=((ISC*Vbuss+(PSCloss*NR_SCCab_MAX))*...% Energy.
        sample*60*60*ESCcounter);
    PSCload_dis=(ISC*Vbuss+(PSCloss*NR_SCCab_MAX)); % Power.

    end

    if IESSC<0

    ESCcounter=0;
    PSCload_dis=0;

    end

    % Storing max value.
    if ESCload_dis>ESCload_MAX_dis

        ESCload_MAX_dis=ESCload_dis;

    end

    if PSCload_dis>PSCload_MAX_dis

        PSCload_MAX_dis=PSCload_dis;

    end

end

% Nr modules with respect to discharging energy and power.
NR_SCCabb(1)=((8*ESCload_MAX_dis)/...
    (3*(VSCMod_MAX^2)*CSC*(SOCSC_MAX_CONSTR-SOCSC_MIN_CONSTR)));
NR_SCCabb(2)=PSCload_MAX_dis/PSCmodule_dis;


% Nr modules with respect to discharging energy or power.
NR_SCCab=max(NR_SCCabb);


% Stores max number of cabinets.
if NR_SCCab>NR_SCCab_MAX

    NR_SCCab_MAX=NR_SCCab;

end


% Exceeding maximum allowed cabinets.
```

```
if NR_SCCab_MAX>=MAX_SCCab

    NR_SCCab_MAX=MAX_SCCab; % Assigning max value.

end

% Stores the time when the SC exceeds its limits.

if NR_SCCab_MAX>=MAX_SCCab && Dummy_var_SC_MAX<=0

    SC_MAX_t=klo*sample;% Time of max value.
    Dummy_var_SC_MAX=1;% Dummy variable for preventing the value to be
                       % changed.

end


% Assigning a value to SC_MAX_t for preventing error, when limit is not
% exceeded.

if NR_SCCab_MAX<MAX_SCCab

    SC_MAX_t=0;

end


end


%*******************Clears_the_variables_not_needed************************

% Clearing all variables except the function output.
clearvars -except NR_BattCab_MAX NR_SCCab_MAX Batt_MAX_t SC_MAX_t

toc
```

E.3 Main function for the DC bus power flow

```
%%                  MAIN FUNCTION FOR THE DC BUS POWER FLOW
%**************************************************************************
%**************************************************************************
%--------------------------------------------------------------------------
%
%   File:            DC_BUS_FLOW.m
%   Description:     This file is used for calculating the fuel and power
%                    for high energy Li-ion batteries, high power Li-ion
%                    batteries and super capacitors. this done for two power
%                    management strategies such as peak shaving and load
%                    sharing. The file first sums the load given by the
%                    input functions requirements.
%                    The then it calculates the DC-DC converter losses,
%                    temperature, cooling requirements, lifetime, power and
%                    fuel. The results are then written to the Input.xls
%                    file
%
%   Version:         1.0
%   Target:          Input.xls
%   Type:            Power management strategy script
%   Copyright        ABB
%   Date:            April 2012




% Initial processes when program start.
clear all;
results=[];% defines results matrix
resul=[];%defined elements in results matrix



%%                  NUMBER OF LOAD OPERATION MODES
%**************************************************************************
%**************************************************************************


for opmodes=1:7

% Resets most of the variables when a new load operation mode is used

if opmodes>1

clearvars -except resul results opmodes NDODB

end
```

```
%%                  INITILA VALUES FOR ALL CALCULATIONS
%*************************************************************************
%*************************************************************************


%*************************INIT_Setup_of_ES_system************************

ES_Combined=0; % Peak shaving =0, load sharing= 1.
sample=0.002; % Sample time for simulations:
t_start=1e-4; % Start time.


%*************************INIT--Setup_of_Load_input_function**************
% Matrix sorting variables:
alpha=0; % Counts elements in generator matrix.
bravo=0; % Counts elements in thrusters matrix
charlie=0; % Counts elements in consumer matrix.
generator=[];% Generator matrix.
thruster=[];% Thruster matrix.
consumer=[];% Consumer matrix.
gen=[];% Generator matrix elements.
thrus=[];% Thruster matrix elements.
cons=[];% Consumer matrix elements.
frequency=0;% Initial frequency.
t_end=0;% Initial simulation end time.
totthrusoffset=0; % Thruster offset load power request.
totconsumeroffset=0;% Consumer offset load power request.
totthrusamplitude=0; % Thruster amplitude load power request.
totconsumeramlitude=0; % Consumer amplitude load power request.
load_amplitude_comb=0;% Equivalent amplitude load power request for one DG.
load_offset_comb=0;% Equivalent offset load power request for one DG.

%***********************INIT--Duty_cycle_batteries**************************
NrBcellseries=12*13;% Cells timed modules.
NrBcellparallell=1;% Number of cells in parallel, 1 means none.
VBatMod=3.3*NrBcellseries;% Cabinet battery voltage rating from datasheet.
ChargeVBatMod=3.6*NrBcellseries;% Nominal cabinet battery voltage.
Vbuss=1000;% Fixed bus voltage.

%***********************INIT--Duty_cycle_SC*********************************
NrSCcellseries=7*48;% Cells timed modules.
NrSCmodules=7;% Number of modules in a cabinet.
NrSCcellparallell=1; % Number of cells in parallell,1 means none.
VSCMod=2.6*NrSCcellseries;% Cabinet SC voltage rating.

%***********************INIT--Currents_Battery******************************
SOCB_car=0; % Dummy variable for empty battery.
SOCB_MAX_CONSTR=0.90; % Maximum allowed SOC level.
SOCB_MIN_CONSTR=0.30; % Minimum allowed SOC level.
IbussB=0;% Init. of output battery current.

if ES_Combined==1 % High energy cell.

    IBmodule_MAX_Dis=50;
    IBmodule_MAX_Cha=6.3;
    IBmodule_MAX_Dis_when_cha=0;

else % High power cell.
```

```
    IBmodule_MAX_Dis=150;
    IBmodule_MAX_Cha=150;
    IBmodule_MAX_Dis_when_cha=100; % Maximum discharge when in
                                   % charging mode.

end

%**********************INIT--Currents_SC*********************************
SOCSC_car=0;% Dummy variable for empty SC.
SOCSC_MAX_CONSTR=1; % Maximum allowed SOC level.
SOCSC_MIN_CONSTR=0.5;% Minimum allowed SOC level.
ISCmodule_MAX_Dis=150; % Maximum discharge current.
ISCmodule_MAX_Cha=150; % Maximum charge current.
ISCmodule_MAX_Dis_when_cha=50; % Maximum discharge when in charging mode.

%**********************INIT--DC_DC_Converter*****************************
ResrB=(0.8e-3)*NrBcellseries;% Battery cabinet resistance.
ResrSC=(3.75e-4)*NrSCcellseries;%S C cabinet resistance:
fsw=2000;% Switch frequency:
%Look up table for switch losses in each ES module:
Isw=[0 30 60 80 200 300];
Eswo_ref=[0 0.003 0.004 0.005 0.009 0.0105]; % On.
Eswf_ref=[0 0.003 0.004 0.0045 0.0075 0.0095]; % Off.
Eswd_ref=[0 0.0101 0.0101 0.0104 0.025 0.03]; % Diode reverse recovery.
PollyEswo=polyfit(Isw,Eswo_ref,3);
PollyEswf=polyfit(Isw,Eswf_ref,3);
PollyEswd=polyfit(Isw,Eswd_ref,3);
Vtest=600; % IGBT voltage used for test.
Induct_ripple=0.10;% Inductor ripple in decimals.
Induct_loss=0.01;% Inductor loss in decimal of output power.
AVG_Coneff_SC_sum=0; % Init. efficiency summer when calculating
                     % AVG efficiency for SC.
AVG_Coneff_batt_sum=0;% Init. efficiency summer when calculating
                      % AVG efficiency for batteries.
AVG_Coneff_SC=0;% Init. AVG efficiency for SC.
AVG_Coneff_batt=0;% Init. AVG efficiency for batteries.


%**********************INIT--Voltages_and_soc_battery*********************
SOCmodB=0.9;% Init. SOC in battery.
SOC_B=SOCmodB; % Init. SOC summer.

if ES_Combined==1 % High energy cell.

    % High-energy look up table voltage VS SOC.
VBat_ref=[4 3.42 3.3 3.26 3.26 3.26 3.26 3.23 3.2 3.15 1.5];
SOCBatV_ref=[1 0.9 0.8 0.7 0.6 0.5 0.4 0.3 0.2 0.1 0];

CBcell=44;% Battery capacitance.

else % High power cell.

     % High-power look up table voltage VS SOC.
VBat_ref=[4 3.26 3.26 3.26 3.26 3.14 3.14 3.14 3.02 2.96 1.15];
SOCBatV_ref=[1 0.9 0.8 0.7 0.6 0.5 0.4 0.3 0.2 0.1 0];

CBcell=10;% Battery capacitance.

end
```

```
Batt_coloumb_eff=0.98; % Columbic charge efficiency.
PollyBatV=polyfit(SOCBatV_ref,VBat_ref,8); % Makes cell voltage polynomial.

%**********************INIT-- Voltages_and_soc_SC**************************
CSC=1/((1/63)*NrSCmodules);% Capacitance.
Vcabinet=VSCMod;% Starting voltage of a cabinet.
SOCmodC=1;% Init. soc in SC.

%**********************INIT--Battery_Cabinet_cooling***********************
ToB=35; % Ambient temperature.
CspesB=795; % Specific heat capacitance per cell.
cellWhg=0.6; % Weight of one cell in kg.
TBlim=40; % Max temp. before cooling is needed.
PBcool=0; % Init. cool power.
HTCB=5; % Heat transfer coefficient battery.
AB=3.576; % Area of battery cabinet.
Tbatt_instant=ToB; % Start value for temp. battery.
Tbatt_tot=0;% Init. Temp summer average.
Tbattsum=0;% Init. Temp summer for increase.
TBcount=0; % Init. Battery counter variable.
PBcooltot=0; % Init. sum of cooling power.
PBcoolMax=0; % Init. max. of cooling power.

%**********************INIT--SC_Cabinet_cooling****************************
ToSC=35; % Ambient temperature.
CsC=33.370; % Heat capacitance per module.
TSClim=40; % Max temp. before cooling is needed.
PSCcool=0; % Init. cool power.
HTCSC=5; % Heat transfer coefficient SC.
ASC=4.5; % Area of SC cabinet.
TSC_instant=ToSC; % Start value for temp. SC.
TSC_tot=0; % Init. temp summer average.
TSCsum=0; % Init. Temp summer for increase.
TSCcount=0; % Init. SC counter variable.
PSCcooltot=0;% Init. sum of cooling power.
PSCcoolMax=0;% Init. max. of cooling power.

%************************INIT--Batt_lifetime*******************************
% Ensures the battery cycle counter starts at zero and
% is not reset in next load operation mode.

if opmodes==1

NDODB=0;% Init. number of delta DOD.

end

DODB_cons=0; % Intit value for dummy cycle var.
% Cycle DelatDOD curve, Cycle= X*exp(-K*DeltaDOD)constants.
KB=-0.0754;
XB=797558.574;
CyclesB=0;% Intit. value cycle counter.

%************************INIT--SC_lifetime*********************************
NSCL=0; % Init. counter for samples lifetime averaging.
SOCSCL=0; % Init. Sum SOC level after each sample.
%Lifetime years SC curve, year= X*exp(-K*DeltaDOD)constants
KSC=-0.1345;
```

```
XSC=1155923.812;
SOCSCL_lim=0.815;

%******************INIT_Sizing_number_of_Battery_modules*****************
PBload_MAX_dis=0; % Init. max discharge power.
EBload_MAX_dis=0; % Init. max discharge energy.
PBload_MAX_cha=0; % Init. max charge power.
PBload_cha=0; % Init. of required charging load.
PBload_dis=1; % Init. of required discharging load.
PBmodule_dis=VBatMod*IBmodule_MAX_Dis; % Nominal cell discharge power.
EBmodule_dis=VBatMod*CBcell*60*60; % Nominal cell energy.
PBmodule_cha=VBatMod*IBmodule_MAX_Cha; % Nominal charge power.
NR_BattCab=1;% Init. number of battery cabinets.
NR_BattCab_MAX=1;% Init. larges number of battery cabinets.
MAX_BCab=50; % Max allowed battery cabinets.
EBload_dis=0;% Init. load energy.
Batt_MAX_t=0; % Time battery achieves max cabinets.
Dummy_var_Batt_MAX=0; % Variable used for storing Batt_MAX_T.
SOCmodB_COMBINED_ES=0.6; % Fixed SOC battery status used for calculating
                         % losses when dimensioning high Energy batteries.

%*****************INIT_Sizing_number_of_SC_modules************************
ESCcounter=0;% Counter for energy calculations.
ESCload_MAX_dis=0;% Init. max discharge energy.
PSCload_MAX_dis=0;% Init. max discharge power.
ESCload_dis=0;% Init. load energy SC:
PSCmodule_dis=ISCmodule_MAX_Dis*VSCMod;% Nominal cell discharge power.
NR_SCCab=0;% Init. number of SC cabinets.
NR_SCCab_MAX=1;% Init. larges number of SC cabinets.
VSCMod_MAX=VSCMod; % Init. module voltage.
MAX_SCCab=50;% Max allowed SC cabinets.
SC_MAX_t=0; % Time SC achieves max cabinets.
Dummy_var_SC_MAX=0; % Variable used for storing SC_MAX_T.

%*********************INIT_Fuel_Calculations*****************************
totgenpower=0; % Sum of all generators rated power.
totgenpower_NO_ES=0; % DG power no ES.
% Fixed speed generator look up table.
sFOC_Fixed_ref=[205 195 210 280];
Loading_Fixed_ref=[1 0.75 0.5 0.25];
PollysFOC_F=polyfit(Loading_Fixed_ref,sFOC_Fixed_ref,3);
% Variable speed generator look up table.
sFOC_Variable_ref=[180 173.75 173.75 186.25];
Loading_Variable_ref=[1 0.75 0.5 0.25];
PollysFOC_V=polyfit(Loading_Variable_ref,sFOC_Variable_ref,3);
TFC_NoES_F=0;% Total consumption variable for no ES with FDG.
TFC_NoES_V=0;% Total consumption variable for no ES with VDG.
TFC_Batt_F=0;% Total consumption variable for batteries with FDG.
TFC_Batt_V=0;% Total consumption variable for batteries with VDG.
TFC_SC_F=0;% Total consumption variable for SC with FDG.
TFC_SC_V=0;% Total consumption variable for SC with VDG.
TFC_Comb_F=0;% Total consumption variable for combined batt. and SC with
FDG.
TFC_Comb_V=0;% Total consumption variable for combined batt. and SC with
VDG.



%%                          SUBROUTINES
%*********************************************************************
```

```
%************************************************************************


tic


% Gets input load data using a function called: Load_input.
  [t_end,totthrusoffset,totconsumeroffset,totthrusamplitude,...
        totconsumeramlitude,frequency,totgenpower,load_amplitude_comb,...
        load_offset_comb,totgenpower_NO_ES]=Load_input(alpha,...
        bravo,generator,thruster,consumer,gen,thrus,cons,frequency,...
        charlie,ES_Combined,load_amplitude_comb,load_offset_comb,opmodes);


% Calculates nr of ES cabinets using a function called: Dimensioning.
[NR_BattCab_MAX,NR_SCCab_MAX,Batt_MAX_t,SC_MAX_t]=Dimensioning...
    (t_start,sample,t_end,totthrusoffset,totconsumeroffset,...
    totthrusamplitude,totconsumeramlitude,ES_Combined,PBload_dis,...
    IbussB,ESCload_dis,NrBcellseries,NrBcellparallell,VBatMod,Vbuss,...
    NrSCcellparallell,VSCMod,SOCB_car,SOCB_MAX_CONSTR,SOCB_MIN_CONSTR,...
    IBmodule_MAX_Dis,IBmodule_MAX_Cha,SOCSC_car,SOCSC_MAX_CONSTR,...
    ISCmodule_MAX_Dis,ISCmodule_MAX_Cha,ResrB,ResrSC,fsw,PollyEswo,...
    PollyEswd,Vtest,Induct_ripple,Induct_loss,SOC_B,SOCmodB,CBcell,...
    CSC,Vcabinet,SOCmodC,PBload_MAX_dis,EBload_MAX_dis,PBload_MAX_cha,...
    PBmodule_dis,EBmodule_dis,PBmodule_cha,NR_BattCab_MAX,MAX_BCab,...
    EBload_dis,ESCcounter,ESCload_MAX_dis,NR_SCCab_MAX,VSCMod_MAX,...
    MAX_SCCab,Dummy_var_Batt_MAX,Dummy_var_SC_MAX,SOCmodB_COMBINED_ES,...
    load_amplitude_comb,load_offset_comb,ISCmodule_MAX_Dis_when_cha,...
    IBmodule_MAX_Dis_when_cha,PSCmodule_dis,Batt_coloumb_eff,...
    PSCload_MAX_dis,ChargeVBatMod,SOCSC_MIN_CONSTR,PBload_cha,...
    frequency,PollyBatV,PollyEswf);



%%                          CALCULATIONS
%************************************************************************
%************************************************************************

klo=0;% Counter for miscellaneous operations.

for t=t_start:sample:t_end;

klo=klo+1;


%************************Setup_of_ES_current_request*********************

% Total load power.
load=((totthrusoffset+totconsumeroffset)+...
    (totthrusamplitude+totconsumeramlitude)...
    *sin(2*pi*frequency*(t)*60*60));

% If peak shaving.
if ES_Combined==0

I=(load-(totthrusoffset+totconsumeroffset))/Vbuss;
IB=I;% Determined by the energy.
ISC=I;
```

```
end

 % If load sharing.
if ES_Combined==1

I=load_offset_comb+((load_amplitude_comb)*sin(2*pi*frequency*(t)*60*60));
    IB=load_offset_comb/Vbuss;
    ISC=(load_amplitude_comb*sin(2*pi*frequency*(t)*60*60))/Vbuss;

end


%**********************Duty_cycle_batteries*******************************

DBbu=VBatMod/Vbuss; % Duty cycle buck.
DBbo=1-DBbu; % Duty cycle boost.

%**********************Duty_cycle_SC**************************************

DSCbu=VSCMod/Vbuss; % Duty cycle buck.
DSCbo=1-DSCbu; % Duty cycle boost.

%**********************Currents_Battery***********************************

% NBcab gets new value.
NBcab=NR_BattCab_MAX;
% Total current request from each module on the bus side.
IBmodule=IB/NBcab;



% Activates dummy variable if the battery is full.
if SOCmodB>=SOCB_MAX_CONSTR

        SOCB_car=0;

end

% Deactivates dummy variable if the battery is empty.
if SOCmodB<SOCB_MIN_CONSTR

    SOCB_car=1;

end



% Current request from a cabinet when the battery is not empty.

if SOCB_car<1;

     if IBmodule<=0 % For batteries during charge.

         IESB=IBmodule*(1/DBbu);
```

```
            if IESB<-IBmodule_MAX_Cha*NrBcellparallell

                IESB=-IBmodule_MAX_Cha*NrBcellparallell;

            end

            IbussB=IESB*DBbu; % Output from DC-DC converter.

        end

        if IBmodule>0% For batteries during discharge.

            IESB=IBmodule*(1/DBbu);

            if IESB>IBmodule_MAX_Dis*NrBcellparallell

                IESB=IBmodule_MAX_Dis*NrBcellparallell;

            end

            IbussB=IESB*DBbu; % Output from DC-DC converter.

        end

end


% Peak shaving.
if ES_Combined==0

% Current request from a cabinet when the battery is empty.

    if SOCB_car>0;

        if IBmodule>0 % Discharge modus.

            IESB=IBmodule*(1/DBbu);
            if IESB>IBmodule_MAX_Dis_when_cha*NrBcellparallell

            IESB=IBmodule_MAX_Dis_when_cha*NrBcellparallell;

            end

            IbussB=IESB*DBbu;% Output from DC-DC converter.

        end

        if IBmodule<=0 % Only charge mode.

            IESB=IBmodule*(1/DBbu);

            if IESB<-IBmodule_MAX_Cha*NrBcellparallell

                IESB=-IBmodule_MAX_Cha*NrBcellparallell;

            end
```

```
            IbussB=IESB*DBbu; % Output from DC-DC converter.

        end

    end

end


% If battery and SC is combined.
if ES_Combined==1

% Current request from a cabinet when the battery is empty.

    if SOCB_car>0;

      IESB=0;
      IbussB=0;

    end

end

%**********************Currents_SC*****************************************

% NSCcab gets new value.
NSCcab=NR_SCCab_MAX;
% Total current request from each module on the bus side.
ISCmodule=ISC/NSCcab;


% Activates dummy varable if the SC is full.
if SOCmodC>=SOCSC_MAX_CONSTR

        SOCSC_car=0;

end

% Deactivates dummy varable if the SC is empty.
if SOCmodC<SOCSC_MIN_CONSTR

    SOCSC_car=1;

end



% Current request from a cabinet when the SC is not empty.
if SOCSC_car<1;

    % For SC charge.
    if ISCmodule<=0

        IESSC=ISCmodule*(1/DSCbu);
        if IESSC<-ISCmodule_MAX_Cha*NrSCcellparallell
```

```
            IESSC=-ISCmodule_MAX_Cha*NrSCcellparallell;

        end

        IbussSC=IESSC*DSCbu; % Output from converter.

    end

    % For SC discharge.
    if ISCmodule>0% For SC discharge.

        IESSC=ISCmodule*(1/DSCbu);

        if IESSC>ISCmodule_MAX_Dis*NrSCcellparallell

            IESSC=ISCmodule_MAX_Dis*NrSCcellparallell;

        end

        IbussSC=IESSC*DSCbu; % Output from DC-DC converter.

    end

end



% Current request from a cabinet when the SC is empty.
if SOCSC_car>0;


    if ISCmodule>0% For SC discharge.

        IESSC=ISCmodule*(1/DSCbu);
        if IESSC>ISCmodule_MAX_Dis_when_cha*NrSCcellparallell

            % The maximum charging current, when in charging mode.
            IESSC=ISCmodule_MAX_Dis_when_cha*NrSCcellparallell;

        end

       IbussSC=IESSC*DSCbu; % Output from converter.

    end

    if ISCmodule<=0 % Only charge.

        IESSC=ISCmodule*(1/DSCbu);

        if IESSC<-ISCmodule_MAX_Cha*NrSCcellparallell
            IESSC=-ISCmodule_MAX_Cha*NrSCcellparallell;

        end

        IbussSC=IESSC*DSCbu; % Output from converter.
```

```
    end

end



%**********************DC_DC_Converter************************************


% RMS Currents.
IESB_RMS=sqrt(IESB^2+(((IESB*Induct_ripple)^2)/3));
IESSC_RMS=sqrt(IESSC^2+(((IESSC*Induct_ripple)^2)/3));


% Inductor battery currents buck.
IonBbu_max=(((1+(Induct_ripple/2))*abs(IbussB))*sqrt(DBbu/3));% IGBT
Current.
IonBbu_min=(((1-(Induct_ripple/2))*abs(IbussB))*sqrt(DBbo/3));% IGBT
Current.
IdBbu_max=(((1-(Induct_ripple/2))*abs(IESB))*sqrt(DBbo/3));% Diode current.
IdBbu_min=(((1+(Induct_ripple/2))*abs(IESB))*sqrt(DBbu/3));% Diode current.
% Inductor battery currents boost.
IonBbo_max=(((1+(Induct_ripple/2))*abs(IbussB))*sqrt(DBbo/3));% IGBT
Current.
IonBbo_min=(((1-(Induct_ripple/2))*abs(IbussB))*sqrt(DBbu/3));% IGBT
Current.
IdBbo_max=(((1-(Induct_ripple/2))*abs(IESB))*sqrt(DBbu/3));% Diode current.
IdBbo_min=(((1+(Induct_ripple/2))*abs(IESB))*sqrt(DBbo/3));% Diode current.


% Inductor battery RMS currents buck.

if IESB<0

    IonB_RMS=IonBbu_max+IonBbu_min;
    IdB_RMS=IdBbu_max+IdBbu_min;

else

% Inductor battery RMS currents boost.
    IonB_RMS=IonBbo_max+IonBbo_min;
    IdB_RMS=IdBbo_max+IdBbo_min;

end


% Inductor SC currents buck.
IonSCbu_max=(((1+(Induct_ripple/2))*abs(IbussSC))*sqrt(DSCbu/3)); % IGBT
                                                                  % Current.
IonSCbu_min=(((1-(Induct_ripple/2))*abs(IbussSC))*sqrt(DSCbo/3)); % IGBT
                                                                  % Current.
IdSCbu_max=(((1-(Induct_ripple/2))*abs(IESSC))*sqrt(DSCbo/3)); % Diode
                                                               % Current.
IdSCbu_min=(((1+(Induct_ripple/2))*abs(IESSC))*sqrt(DSCbu/3)); % Diode
                                                               % Current.

% Inductor SC currents boost.
```

```
IonSCbo_max=(((1+(Induct_ripple/2))*abs(IbussSC))*sqrt(DSCbo/3)); % IGBT
                                                                  % Current.
IonSCbo_min=(((1-(Induct_ripple/2))*abs(IbussSC))*sqrt(DSCbu/3)); % IGBT
                                                                  % Current.
IdSCbo_max=(((1-(Induct_ripple/2))*abs(IESSC))*sqrt(DSCbu/3)); %Diode
                                                                  % Current.
IdSCbo_min=(((1+(Induct_ripple/2))*abs(IESSC))*sqrt(DSCbo/3)); %Diode
                                                                  % Current.

% Inductor SC RMS currents buck

if IESSC<0
    IonSC_RMS=IonSCbu_max+IonSCbu_min;
    IdSC_RMS=IdSCbu_max+IdSCbu_min;

else

    % Inductor SC RMS currents boost.
    IonSC_RMS=IonSCbo_max+IonSCbo_min;
    IdSC_RMS=IdSCbo_max+IdSCbo_min;

end


% Look up table for switch losses in each ES module:

% Battery switch loss with a voltage correction.
EswoB=polyval(PollyEswo,abs(IonB_RMS))*(Vbuss/Vtest);
EswfB=polyval(PollyEswf,abs(IonB_RMS))*(Vbuss/Vtest);
EswdB=polyval(PollyEswd,abs(IdB_RMS))*(Vbuss/Vtest);
% SC switch loss with a voltage correction.
EswoSC=polyval(PollyEswo,abs(IonSC_RMS))*(Vbuss/Vtest);
EswfSC=polyval(PollyEswf,abs(IonSC_RMS))*(Vbuss/Vtest);
EswdSC=polyval(PollyEswd,abs(IdSC_RMS))*(Vbuss/Vtest);


% Battery conduction loss.
VonB=(1+(0.01167)*IonB_RMS);
VdB=(1+(4.827*1e-3)*IdB_RMS);

% SC conduction loss.
VonSC=(1+(0.01167)*IonSC_RMS);
VdSC=(1+(4.827*1e-3)*IdSC_RMS);


% Power loss in inductor.
Pind_lossB=(Vbuss)*abs(IbussB)*Induct_loss;
Pind_lossSC=(Vbuss)*abs(IbussSC)*Induct_loss;




 % Efficiency used for calculating discharged power as the internal
 % impedance effect of the ES has been withdrawn during voltage
 % calculations:

 % Efficiency Battery.
PBloss_PCalc=(VonB*IonB_RMS)+(VdB*IdB_RMS) + Pind_lossB +...
```

```
    ((EswoB+EswfB+EswdB)*fsw);
NefB_PCalc=(Vbuss*abs(IbussB)/((VBatMod*abs(IESB)+PBloss_PCalc)));

 % Efficiency Super capacitor.
PSCloss_PCalc=(VonSC*IonSC_RMS)+(VdSC*IdSC_RMS) + Pind_lossSC +...
    ((EswoSC+EswfSC+EswdSC)*fsw);
NefSC_PCalc=(Vbuss*abs(IbussSC)/((VSCMod*abs(IESSC)+PSCloss_PCalc)));


% To avoiding infinity in later calculations when VonSC*IonSC_RMS=0.
if abs(IESSC)==0

    NefSC=1;
    NefSC_PCalc=1;

end

if abs(IESB)==0

    NefB=1;
    NefB_PCalc=1;

end


% Average converter efficiency for batteries.
if NefB_PCalc>0

    AVG_Coneff_batt_sum=AVG_Coneff_batt_sum+NefB_PCalc;
    AVG_Coneff_batt=AVG_Coneff_batt_sum/klo; % Average battery efficiency.

end


% Average converter efficiency for SC.

if NefSC_PCalc>0

    AVG_Coneff_SC_sum= AVG_Coneff_SC_sum+NefSC_PCalc;
    AVG_Coneff_SC=AVG_Coneff_SC_sum/klo;% Average SC efficiency.

end


%**********************Voltages_and_soc_battery*****************************


% Battery SOC.
if IESB<=0 % While charging, efficiency is added.

        SOC_B=(((-IESB*sample*NefB_PCalc*Batt_coloumb_eff)/...
            (CBcell*NrBcellparallell))+SOC_B);

else

        SOC_B=(((-IESB*sample)/(CBcell*NrBcellparallell))+SOC_B);
```

```
end

SOCmodB=SOC_B;


% Limits if there are no SOC MAX_MIN interval(can be ignored).
if SOCmodB<=0 % Min. SOC.

    SOCmodB=0;

end

if SOCmodB>1 % Max. SOC.

    SOCmodB=1;

end


% Battery cabinet voltage where the voltage drop of the
% internal resistance is subtracted.
if IESB<=0

    VBatMod= ChargeVBatMod;

    else

    VBatMod=(polyval(PollyBatV,SOCmodB))*NrBcellseries -(ResrB*abs(IESB));

end

%**********************Voltages_and_soc_SC*********************************


% New voltage.
if IESSC<=0 % While charging, efficiency is added and the voltage drop

            % of the internal resistance is subtracted.
        VSCMod=sqrt((VSCMod)^2-
((2*VSCMod_MAX*IESSC*sample*(NefSC_PCalc)*60*60)...
            /CSC*NrSCcellparallell))+(IESSC*ResrSC);


else % While discharging, voltage drop
     % of the internal resistance is subtracted.
    VSCMod=sqrt((VSCMod)^2-((2*VSCMod*IESSC*sample*60*60)...
        /CSC*NrSCcellparallell))-(IESSC*ResrSC);

end


% Limits if there are no SOC MAX/MIN Interval(can be ignored).
if imag(VSCMod)~=0 % Complex voltage.

    VSCMod=0;
```

```
end

if VSCMod>Vcabinet% Overcharged.
    VSCMod=Vcabinet;

end


% SC SOC.
SOCmodC=VSCMod/Vcabinet;


%**********************Battery_Cabinet_cooling*****************************

% Heat transfer.
PBtrans=AB*HTCB*((Tbatt_instant)-ToB);
% Power disipadet in cabinet.
PBq=(((IESB_RMS*NrBcellparallell)^2)*(ResrB));


% New instantaneus Cabinet Cell temperature.
TBatt=(((PBq-PBcool-PBtrans)*sample*60*60)/...
    (CspesB*cellWhg*(NrBcellseries)));


% Sum temp. in battery.
Tbattsum=TBatt+Tbattsum;


% Instantaneus temp. in battery.
Tbatt_instant=Tbattsum+ToB;


% Average Temp.
Tbatt_tot=Tbatt_instant+Tbatt_tot;% Adding ambient temp.
TBcount=TBcount+1;
TBatt_avg=Tbatt_tot/TBcount; % Average temperature.


% Finding maximum cooling power.

if (Tbatt_instant)>=TBlim

    PBcool=PBq;

end

if (Tbatt_instant)<TBlim

    PBcool=0;

end


% Average cooling power.
```

```
PBcooltot=PBcool+PBcooltot;
PBcool_avg=PBcooltot/TBcount;



%**********************SC_Cabinet_cooling*********************************



% Heat transfer.
PSCtrans=ASC*HTCSC*((TSC_instant)-ToSC);
% Power dissipated in cabinet.
PSCq=(((IESSC_RMS*NrSCcellparallell)^2)*(ResrSC));


% New instantaneous Cabinet module temperature.
TSC=(((PSCq-PSCcool-PSCtrans)*sample*60*60)/...
    (CsC*NrSCmodules));


% Sum temp. in SC.
TSCsum=TSC+TSCsum;


% Instantaneous temp. in SC
TSC_instant=TSCsum+ToSC;


% Average Temp.
TSC_tot=TSC_instant+TSC_tot;
TSCcount=TSCcount+1;
TSC_avg=TSC_tot/TSCcount;%average temperature


% Finding maximum cooling power.
if TSC_instant>TSClim

   PSCcool=1.07*PSCq;

end

if TSC_instant<TSClim

    PSCcool=0;

end


% Average cooling power.
PSCcooltot=PSCcool+PSCcooltot;
PSCcool_avg=PSCcooltot/TSCcount;



%************************Batt_lifetime*********************************
```

```
if ES_Combined==0

% Battery delta-DOD cycle and lifetime calculated.
if SOCB_car >0
    if DODB_cons>0

        NDODB=1+NDODB;% Cycle counter.
        Delta_DODB=(SOCB_MAX_CONSTR-SOCB_MIN_CONSTR)*100; % Delta DOD in
                                                          % percent.
        CyclesB=XB*exp(KB*Delta_DODB)-NDODB; % Average cycles left.
        DODB_cons=0;% Deactivates DOD dummy variable during charging.

    end

end


% Activates DOD dummy variable during discharging.

if SOCB_car <1

DODB_cons=1;

end

end

%**************************SC_lifetime***********************************

% SOC average.
NSCL=NSCL+1; % Counter.
SOCSCL=SOCSCL+SOCmodC;
SOCSCL_avg=SOCSCL/NSCL;


% Findig average lifetime in years.
if SOCSCL_avg>=SOCSCL_lim % SOC status when SC starts to degrade.

    SCYear=XSC*exp(KSC*(SOCSCL_avg*100));

else

    SCYear=20;
end




%**************************Power_Calculations*****************************



if ES_Combined==0

% Total power with batteries in peak shaving.
```

```
if IESB>0 % Discharge.

    PlWB=load-(IbussB*Vbuss*NefB_PCalc*NR_BattCab_MAX);

else % Charge.
    PlWB=load-(IbussB*Vbuss*NR_BattCab_MAX);

end


% Total power with SC in peak shaving.
if IESSC>0 %Discharge.

    PlWSC=load-(IbussSC*Vbuss*NefSC_PCalc*NR_SCCab_MAX);

else % Charge.

    PlWSC=load-(IbussSC*Vbuss*NR_SCCab_MAX);

end

end




% Total power with load sharing.
if ES_Combined==1

    % Only SC charges and discharges.
    if IESSC >0  % SC efficiency on, battery efficiency on.

         PlWCOMB= load-(IbussSC*Vbuss*NefSC_PCalc*NR_SCCab_MAX)...
         -(IbussB*Vbuss*NefB_PCalc*NR_BattCab_MAX);

    else % SC efficiency off, battery efficiency on.
         PlWCOMB=load-(IbussSC*Vbuss*NR_SCCab_MAX)-...
         (IbussB*Vbuss*NR_BattCab_MAX*NefB_PCalc);

    end


    % SC is removed from the calculations when battery is empty.
    if IbussB==0

        PlWCOMB=load;

    end

end
%*************************Fuel_Calculations*****************************



% Fuel calculations with no ES.
NoES_rat=(load/totgenpower_NO_ES);% DG's loading ratio.
```

```
% FDG.
sFOC_NoES_F=(polyval(PollysFOC_F,NoES_rat)*(totgenpower_NO_ES/1e3))...
    *sample*NoES_rat;% Instantaneous consumption.
TFC_NoES_F=(sFOC_NoES_F)+TFC_NoES_F; % Total consumption.
% VDG.
sFOC_NoES_V=(polyval(PollysFOC_V,NoES_rat)*(totgenpower_NO_ES/1e3))...
    *sample*NoES_rat;% Instantaneous consumption.
TFC_NoES_V=(sFOC_NoES_V)+TFC_NoES_V;% Total consumption.


% Fuel calculations for peak shaving.

if ES_Combined==0

    % Fuel calculations with batteries.
    Batt_rat=(PlWB/totgenpower);% % DG's loading ratio.
    % FDG.
    sFOC_Batt_F=(polyval(PollysFOC_F,Batt_rat)*(totgenpower/1e3))...
        *sample*Batt_rat; % Instantaneous consumption.
    TFC_Batt_F=(sFOC_Batt_F)+TFC_Batt_F; % Total consumption.
    % VDG.
    sFOC_Batt_V=(polyval(PollysFOC_V,Batt_rat)*(totgenpower/1e3))...
        *sample*Batt_rat;% Instantaneous consumption.
    TFC_Batt_V=(sFOC_Batt_V)+TFC_Batt_V;% Total consumption.

    % Fuel calculations with SC's.
    SC_rat=(PlWSC/totgenpower);% DG's loading ratio.
    % FDG.
    sFOC_SC_F=(polyval(PollysFOC_F,SC_rat)*(totgenpower/1e3))...
        *sample*SC_rat; % Instantaneous consumption.
    TFC_SC_F=(sFOC_SC_F)+TFC_SC_F; % Total consumption.
    % VDG.
    sFOC_SC_V=(polyval(PollysFOC_V,SC_rat)*(totgenpower/1e3))...
        *sample*SC_rat;% Instantaneous consumption.
    TFC_SC_V=(sFOC_SC_V)+TFC_SC_V;% Total consumption.

end

% Fuel calculations for load sharing.

if ES_Combined==1

    % Fuel calculations with Batteries and SC combined.
    Comb_rat=(PlWCOMB/totgenpower);%  DG's loading ratio.
    % FDG.
    sFOC_Comb_F=(polyval(PollysFOC_F,Comb_rat)*(totgenpower/1e3))...
        *sample*Comb_rat; % Instantaneous consumption.
    TFC_Comb_F=(sFOC_Comb_F)+TFC_Comb_F; % Total consumption.
    % VDG.
    sFOC_Comb_V=(polyval(PollysFOC_V,Comb_rat)*(totgenpower/1e3))...
        *sample*Comb_rat;% Instantaneous consumption.
    TFC_Comb_V=(sFOC_Comb_V)+TFC_Comb_V;% Total consumption.

end



%**************************Plot_variables*********************************
```

```
%if ES_Combined==0
% SC.
%POWERC(klo)=PlWSC; % Power minus SC.
%currentSC(klo)=IESSC;% SC current.
%currentSCout(klo)=IbussSC;% SC current out from DC-DC converter.
%BoostSC(klo)=DSCbo; % Duty boost SC.
%BuckSC(klo)=DSCbu;% Duty buck SC.
%Il(klo)=I;% Load current.
%PSCo(klo)=(-PlWSC+load); % Power delivered by SC.
%SCloss(klo)=NefSC_PCalc; % Instantaneous efficiency from DC-DC converter.
%SOCSC(klo)=SOCmodC*100; % SOC SC.
%VOLTSC(klo)=VSCMod/(48*7); % Voltage SC.
%TEMPSCAVG(klo)=TSC_avg; % Average temperature.
%TEMPSCINST(klo)=TSC_instant; % Instantaneous temperature.
%IRMSSC(klo)=PSCcool_avg; % Average cooling power.
%SCCOOL(klo)=PSCcool;% Instantaneous cooling power.
%SCLIFE(klo)= SCYear;% Lifetime


% Battery.
%POWERB(klo)=PlWB;% Power minus battery
%PBo(klo)=-PlWB+load;% Power delivered by battery.
%currentB(klo)=IESB;% Battery current.
%currentBout(klo)=IbussB;% Battery current out from DC-DC converter.
%Bloss(klo)=NefB_PCalc;% Instantaneous efficiency from DC-DC converter.
%SOCB(klo)=SOCmodB;% SOC battery.
%VOLTB(klo)=VBatMod;% Voltage battery
%TEMPBAVG(klo)=TBatt_avg;% Average battery temperature.
%TEMPBINST(klo)=Tbatt_instant;% Instantaneous battery temperature.
%BCOOL(klo)=PBcool; % Instantaneous cooling power battery.
%IRMSB(klo)=PBcool_avg; % Average cooling power battery.
%BCYCL(klo)=AVG_Coneff_batt;% Average efficiency from DC-DC converter.
%end

% Power.
%PBo(klo)=-PlWB+load; % Power delivered by battery.
%PSCo(klo)=-PlWSC+load; % Power delivered by SC.

% Fuel.
%POWER(klo)=load; % Power without ES.
%FUELF(klo)=TFC_NoES_F; % No ES fuel consumption FDG.
%FUELV(klo)=TFC_NoES_V;% % No ES fuel consumption VDG
%FUELBV(klo)=TFC_Batt_V; % Battery fuel consumption VDG
%FUELBF(klo)=TFC_Batt_F;% Battery fuel consumption FDG
%FUELSCV(klo)=TFC_SC_V;% SC fuel consumption VDG.
%FUELSCF(klo)=TFC_SC_F;% SC fuel consumption FDG.


% Load sharing.
%if ES_Combined==1
%POWERCOMB(klo)=PlWCOMB; % DG power with combined ES .
%FUELCOMBF(klo)=TFC_Comb_F; % Combined ES fuel consumption FDG.
%FUELCOMBV(klo)=TFC_Comb_V;% Combined ES fuel consumption VDG.
%end

%kobb(klo)=(klo*sample); % Plot variable counter.

end
```

```
%**************************Results*****************************************

% Peak shaving.
if ES_Combined==0

% SC out.
resul(1,opmodes)= TFC_NoES_F; % No ES fuel consumption FDG.
resul(2,opmodes)= TFC_SC_F; % With ES fuel consumption FDG.
resul(3,opmodes)= (1-(TFC_SC_F/TFC_NoES_F))*100; % Percent difference FDG.
resul(4,opmodes)= TFC_NoES_V; % No ES fuel consumption VDG.
resul(5,opmodes)= TFC_SC_V; % With ES fuel consumption VDG.
resul(6,opmodes)= (1-(TFC_SC_V/TFC_NoES_V))*100; % Percent difference VDG.
resul(7,opmodes)= NR_SCCab_MAX; % Number of SC cabinets.

if SC_MAX_t>0% Logic signal if number of cabinets has reached a max value.

resul(8,opmodes)= 1;

else

resul(8,opmodes)= 0;

end

resul(9,opmodes)= AVG_Coneff_SC;% Average efficiency from DC-DC converter.
resul(10,opmodes)= TSC_avg; % Average temperature.
resul(11,opmodes)= PSCcool_avg; % Average cooling power.
resul(12,opmodes)= SCYear; % Lifetime.
resul(13,opmodes)= totgenpower_NO_ES; % Total DG power without ES.
resul(14,opmodes)= totgenpower; % Total DG power with ES.

% Battery out.
resul(17,opmodes)= TFC_NoES_F;% No ES fuel consumption FDG.
resul(18,opmodes)= TFC_Batt_F;% With ES fuel consumption FDG.
resul(19,opmodes)= (1-(TFC_Batt_F/TFC_NoES_F))*100;%Percent difference FDG.
resul(20,opmodes)= TFC_NoES_V;% No ES fuel consumption VDG.
resul(21,opmodes)= TFC_Batt_V;% With ES fuel consumption VDG.
resul(22,opmodes)= (1-(TFC_Batt_V/TFC_NoES_V))*100;%Percent difference VDG.
resul(23,opmodes)= NR_BattCab_MAX; % Number of battery cabinets.

if Batt_MAX_t>0%Logic signal if number of cabinets has reached a max value.

resul(24,opmodes)= 1;

else

resul(24,opmodes)= 0;

end

resul(25,opmodes)= AVG_Coneff_batt;%Average efficiency DC-DC converter.
resul(26,opmodes)= TBatt_avg;% Average temperature.
resul(27,opmodes)= PBcool_avg;% Average cooling power.
resul(28,opmodes)= CyclesB; % Lifetime.
resul(29,opmodes)= totgenpower_NO_ES;% Total DG power without ES.
resul(30,opmodes)= totgenpower;% Total DG power with ES.
```

```
end


% Load sharing.
if ES_Combined==1

resul(33,opmodes)= TFC_NoES_F;% No ES fuel consumption FDG.
resul(34,opmodes)= TFC_Comb_F;% With ES fuel consumption FDG.
resul(35,opmodes)= (1-(TFC_Comb_F/TFC_NoES_F))*100;% Percent difference FDG
resul(36,opmodes)= TFC_NoES_V;% No ES fuel consumption VDG.
resul(37,opmodes)= TFC_Comb_V;% With ES fuel consumption VDG.
resul(38,opmodes)= (1-(TFC_Comb_V/TFC_NoES_V))*100;% Percent difference VDG
resul(39,opmodes)= NR_BattCab_MAX; % Number of battery cabinets.

if Batt_MAX_t>0%Logic signal if number of cabinets has reached max value.

resul(40,opmodes)= 1;

else

resul(40,opmodes)= 0;

end

resul(41,opmodes)= NR_SCCab_MAX;   % Number of SC cabinets.

if SC_MAX_t>0% Logic signal if number of cabinets has reached a max value.

resul(42,opmodes)= 1;

else

resul(42,opmodes)= 0;

end

resul(43,opmodes)= AVG_Coneff_batt;% Average battery efficiency
                                   % from DC-DC converter.
resul(44,opmodes)= AVG_Coneff_SC;  % Average SC efficiency
                                   % from DC-DC converter.
resul(45,opmodes)= TBatt_avg; % Average battery temp.
resul(46,opmodes)= TSC_avg;    % Average SC temp.
resul(47,opmodes)= PBcool_avg;  % Average battery cooling power.
resul(48,opmodes)= PSCcool_avg; % Average SC cooling power.
resul(49,opmodes)= CyclesB;    % Battery lifetime (NOT USED).
resul(50,opmodes)= SCYear;     % SC lifetime.

end

eval(['results' ' = resul']);

end
```

```
%*******************************Plot*****************************************

%----SC
%plot(kobb,POWERC,'b')
%plot(kobb,POWER,'r')
%plot(kobb,SCloss,'r')
%plot(kobb,PSCo,'r')
%plot(kobb,currentSC,'r')
%plot(kobb,BoostSC)
%plot(kobb,BuckSC,'r')
%plot(kobb,Il)
%plot(kobb,currentSCout,'g')
%plot(kobb,SOCSC,'y')
%plot(kobb,TEMPSCAVG,'m')
%plot(kobb,TEMPSCINST,'g')
%plot(kobb,SCCOOL,'g')
%plot(kobb,IRMSSC,'m')
%plot(kobb,SCLIFE)
%plot(kobb,VOLTSC, 'b')
%plot(kobb,PSClosss)

%----Battery
%plot(kobb,POWERB,'b')
%plot(kobb,currentB,'r')
%plot(kobb,currentBout,'g')
%plot(kobb,Il)
%plot(kobb,Bloss,'y')
%plot(kobb,SOCB, 'y')
%plot(kobb,VOLTB, 'b')
%plot(kobb,TEMPBAVG, 'm')
%plot(kobb,TEMPBINST, 'g')
%plot(kobb,BCOOL,'g')
%plot(kobb,IRMSB,'m')
%plot(kobb,BCYCL,'g')
%plot(kobb,PBo)
%plot(kobb,POWERCOMB,'b')

%----Fuel
%plot(kobb,FUELBV,'c')
%plot(kobb,FUELBF,'g')
%plot(kobb,FUELSCV,'b')
%plot(kobb,FUELSCF,'m')
%plot(kobb,FUELCOMBV,'r')
%plot(kobb,FUELCOMBF,'k')
%plot(kobb,FUELF,'k')
%plot(kobb,FUELV,'r')



%**************************Send_Results_to_Excel*************************

% Write results to excel.
xlswrite('Input',results,'Results','B6:I55');

toc
```